

**Role of metabolism and epigenetics
in forced and endogenous neurogenesis
*in vivo***



**Dissertation der Graduate School of Systemic
Neurosciences der Ludwig-Maximilians-Universität
München**

Elisa Murenu

10.06.2016

Role of metabolism and epigenetics in forced and endogenous neurogenesis *in vivo*

Performed at the Institute of Physiology
of the Ludwig-Maximilians-Universität München
Work group: Prof. Dr. Magdalena Götz



Elisa Murenu
from Pisa (Italy)

Date of submission: 10.06.2016

Supervisor: Prof. Dr. Magdalena Götz

2nd reviewer: Prof. Dr. Gunnar Schotta

3rd reviewer: Prof. Dr. Martin Kerschensteiner

Date of oral defense: 24.11.2016

*To every person
I hold dear*

*"I tell young people: do not think of
yourself, think of the others.
Think of the future that awaits you,
think about what you can do and do
not fear anything [...] Above all, do
not fear difficult moments. The best
comes out of them."*

Rita Levi-Montalcini

Abstract	5
1. Introduction	9
1.1. The central nervous system in Mammals: an overview.....	11
1.2. Neurogenesis in the developing brain.....	12
1.2.1. Shaping the cortex: the dorsal telencephalon	14
1.2.2. Shaping the cortex: the contribution of the ganglionic eminence	14
1.3. Development of the main olfactory bulb.....	16
1.4. Neurogenic niches in the adult brain.....	17
1.4.1. The sub-granular zone (SGZ) niche	17
1.4.2. The sub-ependymal zone (SEZ) niche	19
1.5. The rostral migratory stream (RMS).....	20
1.6. The adult main olfactory bulb	22
1.6.1. Granule cells.....	23
1.6.2. Periglomerular cells.....	25
1.7. Neuronal direct reprogramming <i>in vivo</i>: why and how?	26
1.8. Epigenetic hurdles in neuronal reprogramming: Polycomb Repressive Complex 1 (PRC1) and Ring1B.....	28
1.8.1. PRC1 and Ring1B in neurogenesis and reprogramming.....	29
1.9. Metabolic hurdles in neuronal reprogramming: oxidative stress	30
2. Results.....	33
2.1. Role of metabolism in forced neurogenesis: the starting point.....	35
2.2. Proliferating cells in the lesion site do not include neuronal progenitors.....	35
2.3. <i>Neurog2</i> over-expression in reactive glia cells does not trigger neuronal conversion	38
2.4. Calcitriol improves neuronal reprogramming initiated by <i>Neurog2</i>	38
2.5. The simultaneous over-expression of <i>Neurog2</i> and <i>Bcl-2</i> results in large numbers of reprogrammed neurons.....	39
2.6. <i>Bcl-2</i> and Calcitriol bring neuronal reprogramming <i>in vivo</i> to unprecedented levels	40
2.7. Reprogrammed neurons dramatically decrease in number over time	43
2.8. Several administrations of Calcitriol are required to promote long-term survival and further maturation of reprogrammed neurons.....	45
2.9. α-Tocotrienol potently enhances neuronal maturation	46
2.10. Reprogrammed neurons express deep layer markers	49
2.11. α-Tocotrienol and Calcitriol co-administration might further improve efficiency of conversion and neuronal maturation after <i>Neurog2</i> over-expression.....	51
2.12. Role of epigenetics in forced and endogenous neurogenesis: the starting point	53

Table of Contents

2.13. Ring1B knockdown in neural stem cells impairs forced neuronal differentiation triggered by Dlx2	53
2.14. Ring1B protein is expressed in a generalised manner in the adult brain	56
2.15. Ring1B protein is not detected 7 days after inducing the knockout of the gene	56
2.16. Ring1B knockout does not affect cell identity or proliferation in the SEZ and the RMS	58
2.17. Ring1B knockout leads to an increase in the proportion of superficial granule cells.....	59
2.18. Ring1B-deficient superficial granule neurons do not change OB subtype identity	61
2.19. Initial phenotype characterisation in the olfactory bulbs.....	63
2.20. Ring1B loss results in accumulation of neuroblasts in the core of the OB	65
2.21. Wild type neuroblasts can differentiate in the deep granule cell layer of Ring1B knockout mice.....	68
2.22. Initial phenotype characterisation in the dentate gyrus of the hippocampus	69
3. Discussion	71
3.1. Bcl-2 shows a new role beyond the known anti-apoptotic effect.....	73
3.2. Oxidative stress and metabolism influence reprogramming.....	74
3.3. Reprogrammed neurons in vivo adopt a deep layer identity	75
3.4. Ring1B is necessary for neuronal differentiation into the GABAergic lineage.....	76
3.5. Ring1B regulates specific neurogenic determinants	77
3.6. Migration or subtype specification?	78
4. Materials and Methods.....	81
4.1. Experimental animals	83
4.2. Genotyping.....	83
4.3. Dissection of the embryonic cerebral cortex and primary culture in adherent conditions	85
4.4. Passaging of NSCs from the embryonic cerebral cortex	86
4.5. Dissection of the adult sub-ependymal zone (SEZ)	87
4.6. Primary SEZ culture in adherent conditions	88
4.7. Passaging of NSCs from the adult SEZ.....	89
4.8. Transfection	90
4.9. Retroviral constructs used.....	92
4.10. Animal Surgery	92
4.10.1. Stab-wound injury	93
4.10.2. Injection of retroviral suspension in the lesion.....	93
4.10.3. Injection of retroviral suspension into the SEZ and RMS.....	94
4.11. Compound administration to animals.....	94

4.11.1. Vitamins	94
4.11.2. Tamoxifen	95
4.12. Perfusion	95
4.13. Vibrating microtome (free-floating sections).....	97
4.14. Immunocytochemistry	98
4.15. Immunohistochemistry	99
4.16. Heat-mediated antigen retrieval: Citrate Buffer	100
4.17. MicroRNA (miRNA) design and cloning	101
4.18. Image acquisition and elaboration	102
4.19. Quantifications and statistics	102
5. References.....	103

Since the characterisation of the very first methods to perform direct reprogramming into neurons, much work has been published on the topic describing new combinations of genes to improve the conversion efficiency or to obtain subtype-specific neurons (Arlotta and Berninger, 2014; Tsunemoto et al., 2015). However, while the ultimate goal of neuronal reprogramming is being actively explored and ameliorated, key questions revolving around the underlying mechanisms of conversion remain largely unanswered. Particularly, identifying the molecular roadblocks during direct neuronal conversion not only would bring a deeper knowledge of the overall procedure, but it would also represent a necessary prerequisite to improved conversion strategies *in vivo*, where direct reprogramming into neurons is often inefficient (Dametti et al., 2016; Grande et al., 2013; Guo et al., 2014a; Heinrich et al., 2014).

In the projects discussed here I tackled this scientific question from two diverse perspectives, one metabolic and one epigenetic. We recently described how oxidative stress is produced during direct reprogramming into neurons triggered by *Ascl1* or *Neurog2* and how ultimately it affects the outcome of the procedure (Gascón, Murenu et al., 2016). Reactive oxygen species would result from an unsuccessful conversion of the metabolism of the starting cell population into the typical neuronal metabolism and indeed this critical check-point was overcome when molecules alleviating oxidative stress (*Bcl-2*, vitamin D or E) were provided (Gascón, Murenu et al., 2016). In my first project I extended this concept *in vivo* in a model of cortical grey matter stab-wound injury (Buffo et al., 2005). By using a retroviral approach to over-express *Neurog2* and *Bcl-2* in proliferating cells within the lesion area, I was able to successfully reprogram a high proportion of these cells into neurons, as compared to the over-expression of *Neurog2* only (Gascón, Murenu et al., 2016; Grande et al., 2013). Combining this method with the administration of vitamin D or vitamin E further increased the efficiency of direct neuronal conversion *in vivo* to previously unprecedented levels. Moreover, I could show that the reprogrammed neurons acquire a deep layer identity, but also that they can develop mature structures and survive until late time points (Gascón, Murenu et al., 2016).

Additionally to the effects of metabolism in direct neuronal reprogramming, I also addressed the implications of epigenetics by investigating the role of Ring1B, the catalytic protein of the Polycomb Repressive Complex 1 (PRC1). As Ring1B was previously described as a repressor of pro-neuronal genes in the glutamatergic lineage at the onset of the gliogenic phase during corticogenesis (Hirabayashi and Gotoh, 2010a; Hirabayashi et al., 2009), we speculated that it could also act as a major roadblock in direct neuronal reprogramming. To explore this

hypothesis, I chose to use the neurogenic determinant *Dlx2*, which is important for the generation of GABAergic neurons during embryonic and adult neurogenesis but is only moderately effective in direct neuronal reprogramming (Brill et al., 2008; Heinrich et al., 2010; Petryniak et al., 2007). By simultaneously over-expressing *Dlx2* and a miRNA against *Ring1B* in cortical cultures from the embryonic cortex as well as in cultures from the adult sub-ependymal zone (SEZ) I could show that less differentiated neurons are obtained, thus suggesting a different role for *Ring1B* during neuronal differentiation in the GABAergic lineage. Following these observations, I used a genetic approach to conditionally induce the knockout of *Ring1B* in adult neural stem cells and address the role of this gene in adult neurogenesis. The deletion of *Ring1B* resulted in the accumulation of neuroblasts migrating from the SEZ in the core of the olfactory bulb. Moreover, differentiating neurons were mainly found in the superficial region of the granule cell layer but did not express markers found in other cell populations within the olfactory bulb (Calbindin, Calretinin, Tyrosine Hydroxylase, Parvalbumin), suggesting that they still maintain their granule cell identity and have switched fate from deep to superficial granule cells. Interestingly, differentiating neurons originating from the sub-granular zone (SGZ) of the hippocampus showed longer and more branched dendrites after *Ring1B* deletion, indicating a function of this gene also in this neurogenic niche.

Thus, *Ring1B* plays a key role in the specification of neuronal subtypes in adult neurogenesis. Taken together, my work has unravelled mechanisms inducing neuronal subtype specification in endogenous or forced neurogenesis.

1. Introduction

1.1. The central nervous system in Mammals: an overview

The mechanisms and the events that take place during embryogenesis are largely shared among all Vertebrates and the same applies to the nervous system, although with some exception (Harrington et al., 2009; Tam and Quinlan, 1996). During neurulation in Mammals, the presumptive nervous system (neural plate) originates from specific areas within the ectodermal region of the gastrula. This area gradually invaginates and detaches from the surrounding tissue, eventually forming a hollow neural tube along the rostro-caudal axis of the embryo (Harrington et al., 2009).

Under the influence of various morphogens acting on all axes – in particular BMP, FGFs, Wnt and Shh molecules and their antagonists (Figure 1 and Tole and Hébert, 2013) – the neural tube re-shapes and expands. In a first phase, three vesicles are formed: the prosencephalon at the very rostral end, the mesencephalon in the middle and the rhombencephalon at the caudal end. In a second phase, prosencephalon and rhombencephalon further re-model into two vesicles each: telencephalon and diencephalon in the former case, metencephalon and myelencephalon in the latter case (Nakamura and Watanabe, 2005; Puelles et al., 2013; Rallu et al., 2002).

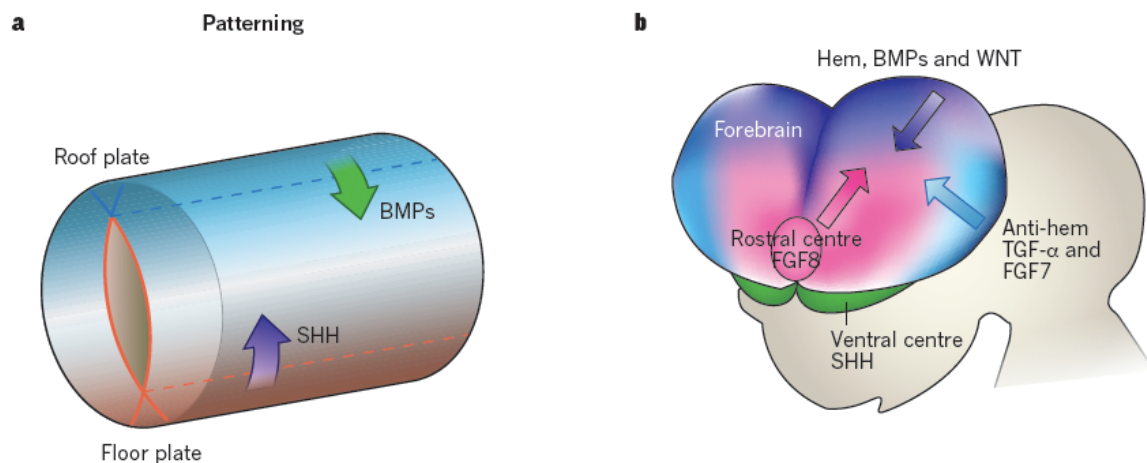


Figure 1. Schematics representing the main signalling pathways involved in central nervous system patterning, as seen in (a) the neural tube and (b) when the main vesicular structures are already specified (*modified from Rowitch and Kriegstein, 2010*).

These five expansions eventually give rise to the structures found in the adult organism (Puelles et al., 2013): the two brain hemispheres (telencephalon), the eyes, thalamus and hypothalamus (diencephalon), the colliculi (mesencephalon), the pons and cerebellum (metencephalon),

various centres regulating involuntary reflexes (myelencephalon).

During these early stages of development the brain is formed thanks to the proliferation of stem cells of the neuroepithelium. These neuroepithelial cells distribute around a central cavity representing the prospective ventricles and constitute a pseudo-stratified layer by performing interkinetic nuclear migration (Kriegstein and Alvarez-Buylla, 2009; Paridaen and Huttner, 2014). The symmetric mode of division ensures a rapid expansion of this cell population by producing other neuroepithelial cells and results in the fast enlargement of the brain primordia within these first developmental phases (Kriegstein and Alvarez-Buylla, 2009; Paridaen and Huttner, 2014; Taverna et al., 2014).

In the following paragraphs the highlight will be on brain development with regards to the mouse, which is the model organism taken into exam during my thesis.

1.2. Neurogenesis in the developing brain

Around embryonic day 9-10 (E9-E10), the neuroepithelium of the neural tube turns into a different population of neural stem cells (NSCs), called radial glia (RG), which expresses genes such as *GFAP*, *GLAST* and *Nestin* (Kriegstein and Alvarez-Buylla, 2009; Paridaen and Huttner, 2014). These cells maintain their soma in proximity to the ventricle in the so-called ventricular zone (VZ), where they constitute a pseudo-stratified layer by proliferating and performing interkinetic nuclear migration to a more limited extent (Götz and Huttner, 2005). Additionally, they extend an apical and a basal process spanning the whole thickness of the developing cortex to maintain contact with both the ventricle and the pial surface, respectively (Kriegstein and Alvarez-Buylla, 2009; Paridaen and Huttner, 2014).

Starting approximately at E9.5, RG cells display asymmetric division mode to maintain their pool while producing a differentiating progeny (Figure 2). In this case, the basal process contacting the pial surface was shown to serve as scaffold for directly generated neurons, guiding their migration to the final destination layer. Additionally, in some brain regions RG cells generate multipolar basal intermediate progenitors (IPs), which locate in the sub-ventricular zone (SVZ) and in turn rapidly amplify the neuronal population by displaying fast rounds of divisions (Figure 2; Kriegstein and Alvarez-Buylla, 2009; Paridaen and Huttner, 2014).

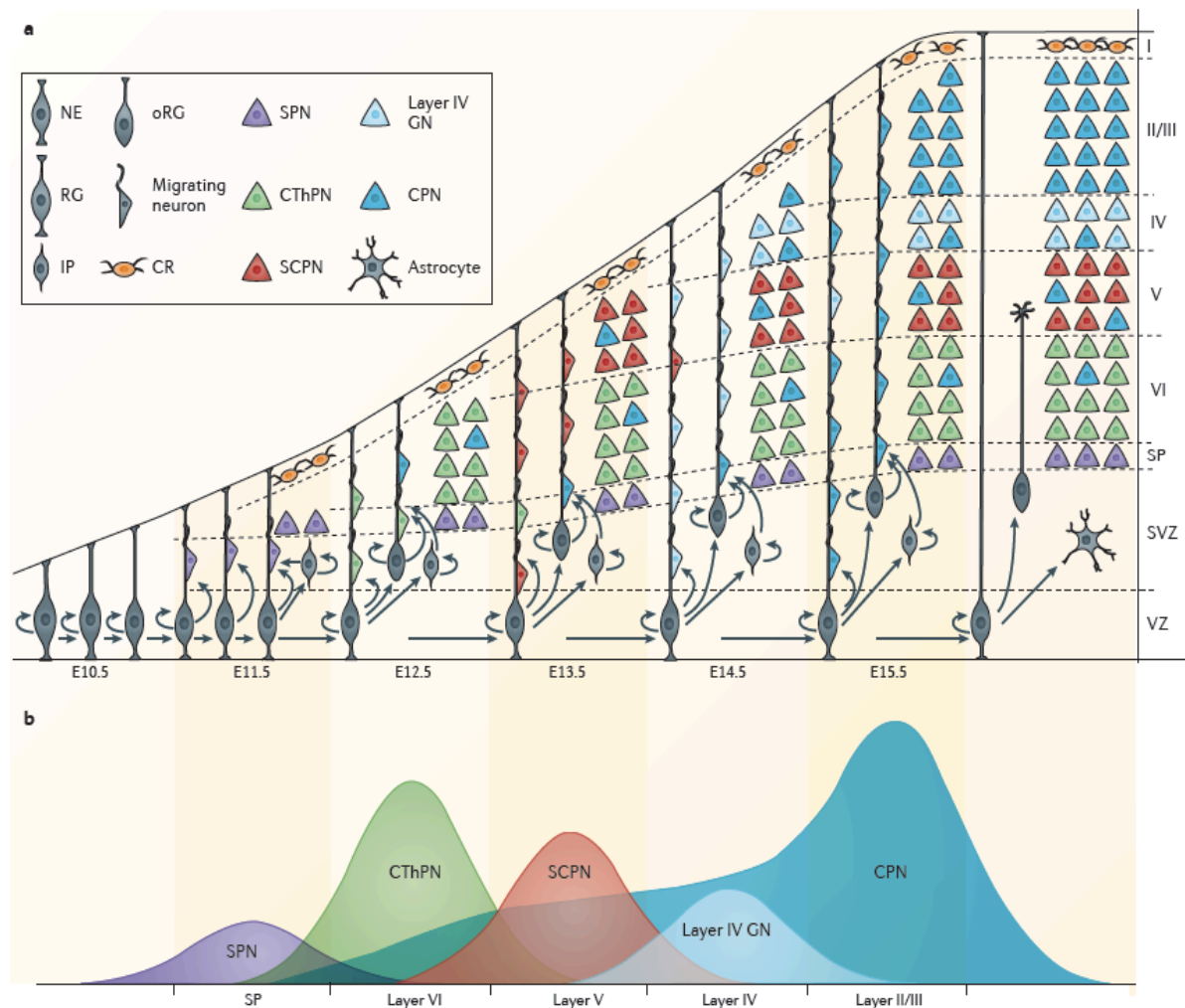


Figure 2. Temporal production of (a) radial glia (RG) cells, intermediate progenitors (IP) and (a,b) layer specific neurons in the dorsal telencephalon (from Greig *et al.*, 2013).

NE=neuroepithelium; oRG=outer radial glia; CR=Cajal-Retzius cell; SPN=sub-plate neuron; CThPN=cortico-thalamic projection neuron; SCPN=sub-cortical projection neuron; GN=granular neuron; CPN=callosal projection neuron

Particularly in Mammals having a high degree of cortical gyrification, but to lesser extent even in mouse, a second population of RG cells can also be observed, namely the outer radial glia (oRG, Figure 2; Borrell and Götz, 2014). Differently from VZ radial glia, these cells do not have the soma in the VZ but rather in the outer sub-ventricular zone (oSVZ), a basal expansion of the SVZ that hosts intermediate progenitors. Additionally, oRG cells can also display a unipolar morphology, by retaining only the basal process towards the pial surface (Borrell and Götz, 2014). These particular populations of stem cells and progenitors have been implicated in the formation of gyri and sulci in gyrencephalic organisms (Borrell and Götz, 2014; Sun and Hevner, 2014).

During late embryogenesis (E18) and until early postnatal stages, RG cells mainly produce (or terminally differentiate into) astrocytes, oligodendrocytes and ependymal cells (Kriegstein and Alvarez-Buylla, 2009; Paridaen and Huttner, 2014; Rowitch and Kriegstein, 2010). Some RG cells instead remain as stem cells in specific areas, where they continue to produce neurons throughout adulthood (see paragraph 1.4).

1.2.1. Shaping the cortex: the dorsal telencephalon

Pax6 expressing RG cells located in the dorsal telencephalon (or pallium) generate neurons directly or produce IPs (characterised by *Tbr2*, *Neurog1* and *Neurog2* expression) that give rise to glutamatergic projection neurons (Figure 2; Arnold et al., 2008; Englund et al., 2005; Imayoshi and Kageyama, 2014). Such neurons populate the cortex by performing an inside-out (apical-basal) radial migration and differentiation following a precise temporal order (Figure 2; Greig et al., 2013; Molyneaux et al., 2007). The first neurons generated (E11.5) are the sub-plate neurons (SPNs), which remain close to the prospective white matter (called intermediate zone during embryogenesis; Greig et al., 2013; Molyneaux et al., 2007). SPNs are then followed by cortico-thalamic projection neurons (E12.5) colonising layer 6 and immunopositive for FoxP2 and *Tbr1* (Ferland et al., 2003; Greig et al., 2013; Molyneaux et al., 2007), layer 5 sub-cortical projection neurons at E13.5 (*Ctip2*-immunopositive; Arlotta et al., 2005; Molyneaux et al., 2007) and layer 4 excitatory spiny neurons at E15.5 (Lodato and Arlotta, 2014; Molyneaux et al., 2007). Finally, callosal projection neurons in layer 2/3 (*Cux1*-immunopositive; Molyneaux et al., 2007; Nieto et al., 2004) are produced starting from E12.5, with a peak of production around E15.5, and finishing at E18.5.

Layer 1 is instead colonised from early stages of development by Cajal-Retzius cells, which have a different origin (Greig et al., 2013).

1.2.2. Shaping the cortex: the contribution of the ganglionic eminence

An area of the developing mouse brain that displays some differences in comparison to the cortex is the ganglionic eminence (GE, or sub-pallium; Figure 3), which is found in the ventral part of the forebrain and can be further distinguished in medial (MGE), lateral (LGE) and caudal (CGE) (Brandão and Romcy-Pereira, 2015; Sultan et al., 2013). While the main characters involved in dorsal telencephalon neurogenesis can still be found, stem cells and progenitors with

a different morphology and localisation are additionally observed in the GE. In particular, compared to the cortex a subset of RG cells and progenitors divides at sub-apical positions and bipolar oRGs cells can be found at higher density (Borrell and Götz, 2014; Pilz et al., 2013). These differences account for the huge amount of GABAergic projection neurons and interneurons produced in this area between E11 and E18 and migrating tangentially to colonise the cortex. The most prominent source of these cells comes from MGE and CGE, together with the pre-optic area (PoA), while the LGE contributes interneurons to the striatum and olfactory bulb (Corbin and Butt, 2011; Sultan et al., 2013).

At the molecular level, several transcription factors and molecular cascades were described for the different GE domains and sub-domains (Figure 3; Corbin and Butt, 2011; Flames et al., 2007). While genes like *Dlx1/2/5/6*, *Gsh2* (also known as *Gsx2*), *Ascl1* and *Olig1/2* are expressed throughout the entire GE, other genes are restricted to more specific areas. In particular, *Er81*, *Sp8*, *Tsh-1* are expressed in the dorsal LGE and *Gsh1* (also known as *Gsx1*), *Nkx6.2*, *Gli1* are in the ventral LGE (Caubit et al., 2005; Corbin and Butt, 2011; Stenman et al., 2003; Waclaw et al., 2006). The MGE can be sub-divided in a dorsal domain expressing the same genes as the ventral LGE plus *Nkx2.1* and *Lhx6*, as well as a ventral domain expressing *Gsh1*, *Lhx6* and *Nkx2.1*. Finally, the CGE expresses the whole cohort of common GE genes as well as *Gsh1* (Corbin and Butt, 2011).

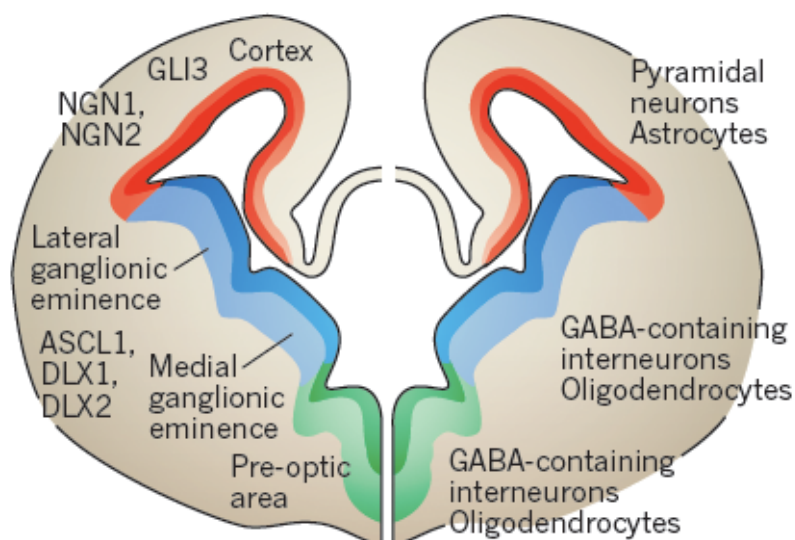


Figure 3. Schematics of the telencephalon as seen during development in coronal section. The different domains and the main expressed genes are indicated on the left side, while the cells produced are indicated on the right (from Rowitch and Kriegstein, 2010).

In regard to extracellular signals, Shh is known to influence the expression of genes in the ventral regions of the developing nervous system, by acting in a gradient that gets lower towards more dorsal regions (see paragraph 1.1; Tole and Hébert, 2013). In the ventral telencephalon, Shh is responsible for the expression of *Nkx2.1* and *Lhx6*, which are critical for the specification of the MGE domain (Brandão and Romcy-Pereira, 2015; Rubenstein and Campbell, 2013). Acting independently of this signalling, also Fibroblast Growth Factor (FGF) pathway plays an important role in specifying the ventral domains, especially through FGF8 (Rubenstein and Campbell, 2013). Instead, less is known about key patterning molecules specific for the LGE, where little Shh signal and, in parallel, little dorsal signals such as Gli3, BMPs and Wnts are expected to be found (Rallu et al., 2002). An exception are Retinoic Acid (RA) and Notch pathways, which are known to be implicated in the specification and survival of progenitors in this area (Rubenstein and Campbell, 2013). The CGE, being the caudal extension of both MGE and LGE, is instead sharing part of the signalling molecules with both these regions (Rubenstein and Campbell, 2013).

The combinatorial expression of all these factors lies at the base of interneuron production in the cortex as well as in striatum, amygdala and olfactory bulbs (OBs).

1.3. Development of the main olfactory bulb

During mouse development, the olfactory bulb is specified from the dorsal telencephalon and is macroscopically observed at E12.5 as small buds in the rostral part of this region, although at the microscopic level several changes take place already before this stage (Treloar et al., 2010). The ventricular cavity can be observed within the presumptive olfactory bulb structure at least until E18, surrounded by neuroepithelium first (Díaz-Guerra et al., 2013) and radial glia cells later, which gradually decrease at postnatal stages (Puche and Shipley, 2001).

Being characterised by both projection neurons and interneurons, the formation of the olfactory bulbs depends on the morphogens and the genes described for dorsal (cortex) and ventral (ganglionic eminences) telencephalic regions, respectively (Díaz-Guerra et al., 2013; Treloar et al., 2010). In particular, excitatory projection neurons (mitral and tufted cells) are generated by olfactory bulb precursors with a pallial origin, whereas inhibitory interneurons arise from the sub-pallium and mainly from the LGE (Blanchart et al., 2006; Puelles et al., 2000). In addition to a different spatial origin, these different cell types display also a different temporal origin:

projection neurons are produced at embryonic stages, as opposed to the mainly postnatal generation of interneurons (Díaz-Guerra et al., 2013), although a small heterogeneous population of interneurons is also produced embryonically by LGE precursors (Tucker et al., 2006) as well as local olfactory bulb progenitors (Vergaño-Vera et al., 2006). Accordingly, the mitral cell layer is the first layer to be distinguished during development, together with the primordia of external plexiform layer and the glomeruli, and followed by the granule cell layer and the internal plexiform layer (Díaz-Guerra et al., 2013; Treloar et al., 2010). At birth, all the layers characteristic of the adult olfactory bulb can already be found (Díaz-Guerra et al., 2013).

1.4. Neurogenic niches in the adult brain

While it is debated whether to some extent neurogenesis in the cortex might still take place in physiological conditions during adulthood (Feliciano and Bordey, 2013), some spatially defined areas are known to maintain active NSCs after the transition from embryonic to postnatal (and then adult) stages. In particular, adult NSCs are found in the sub-granular zone (SGZ) in the dentate gyrus of the hippocampus and in the sub-ependymal zone (SEZ) in the walls of the lateral ventricles (Bond et al., 2015). A third neurogenic niche was more recently described also in the hypothalamic region lining the third ventricle (Rojczyk-Gołębiewska et al., 2014), but it will not be discussed in this work.

1.4.1. The sub-granular zone (SGZ) niche

The dentate gyrus of the adult hippocampus is a V-shaped structure constituted of three main layers, from the most superficial to the deepest: the molecular layer (ML), the granule cells layer (GCL) and the hilus (Figure 4; Toni and Schinder, 2016). The sub-granular zone neurogenic niche is found in the dentate gyrus of the hippocampus, in a thin area between the granule cells layer and the hilus. RG-like NSCs (also called type 1 cells) in this region are found to express *GFAP*, *Prominin*, *Nestin* and *Sox2* as seen for type B cells in the SEZ (paragraph 1.4.2; Beckervordersandforth et al., 2015; Toni and Schinder, 2016). Type 1 cells display a radial morphology with a primary process spanning the entire GCL and branching in the molecular layer or in the superficial portion of the GCL (Figure 4; Gebara et al., 2016) and an end-foot contacting blood vessels (Kempermann et al., 2015). However, through production of intermediate TAPs (type 2 cells) these NSCs produce only granule cells as neuronal progeny,

contrary to the different kind of neurons generated in the different domains of the adult SEZ (Toni and Schinder, 2016). As reviewed in details in Beckervordersandforth et al., 2015, type 2 cells can be further distinguished in type 2a cells expressing *Sox2*, *Tbr2* and *Nestin* and type 2b cells expressing *Tbr2* and (albeit at low levels) *Doublecortin* (*Dcx*). Type 3 cells constitute neuroblasts characterised by *Calretinin* (*CalR*) and *Dcx* gene expression, which give rise to immature neurons extending a short apical process. Finally, mature granule neurons with dendrites spanning the GCL and branching in the molecular layer can be identified based on the expression of *Calbindin* (*CalB*), *Prox1* and *NeuN* (Figure 4).

Both Shh and Wnt signalling pathways play a role also in SGZ neurogenesis, by promoting NSCs maintenance and neuronal differentiation (Beckervordersandforth et al., 2015).

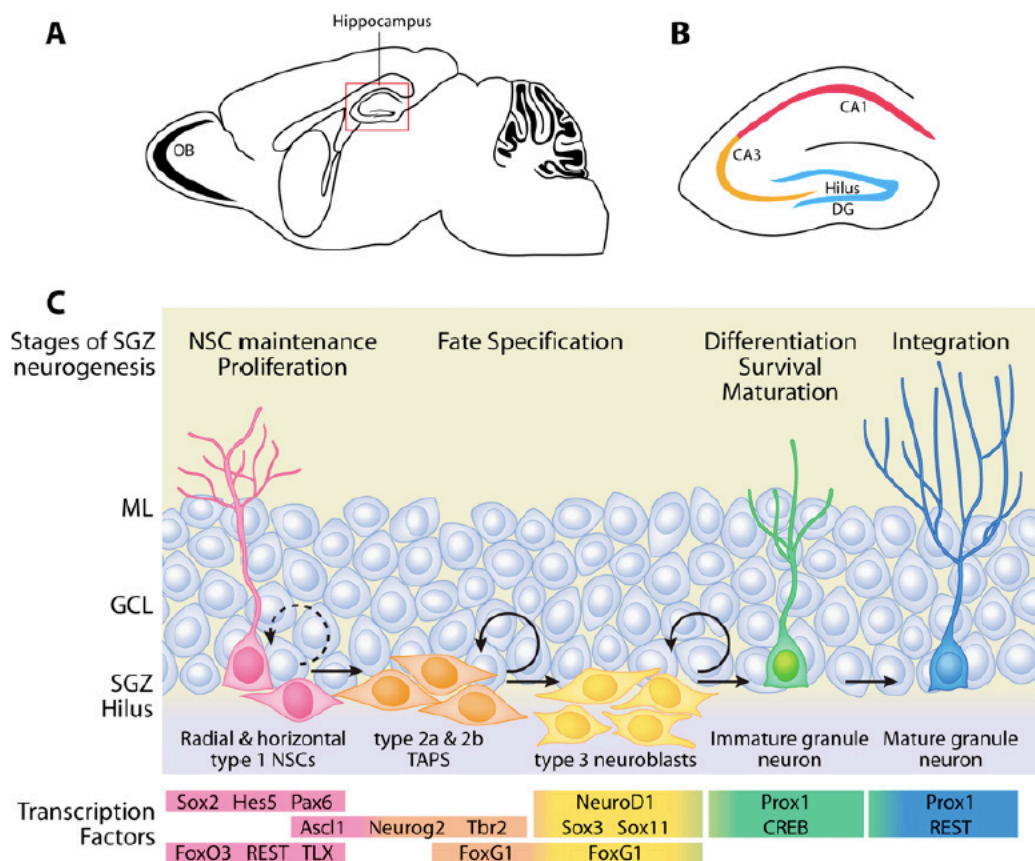


Figure 4. Schematics of the hippocampus (A) and the dentate gyrus (B) location, containing the SGZ neurogenic niche. C) Type 1 cells located in the SGZ produce type 2a and 2b cells, which proliferate to generate type 3 neuroblasts. These cells will then differentiate into granule neurons. The main transcription factors characterising every cell type are indicated (from Hsieh, 2012).

ML=molecular layer; GCL=granule cell layer; DG=dentate gyrus; OB=olfactory bulb

1.4.2. The sub-ependymal zone (SEZ) niche

The sub-ependymal zone neurogenic niche (or ventricular sub-ventricular zone; V-SVZ) lies adjacent to the different walls (dorsal, lateral and medial) of the lateral ventricles, behind an ependymal layer generated during development by the terminal differentiation of some RG cells (see paragraph 1.2; Figure 5). Resident NSCs (B1 cells) have been demonstrated to derive from subsets of embryonic RG (Fuentelba et al., 2015; Merkle et al., 2004). B1 cells share part of their gene expression profile with astrocytes and with RG cells, e.g. *GFAP*, *BLBP*, *Sox2* (Kriegstein and Alvarez-Buylla, 2009) and maintain contact with the cerebro-spinal fluid (CSF) through an apical process that intercalates among ependymal cells forming a sort of pin-wheel structure (Mirzadeh et al., 2008). Moreover, these cells extend a basal process towards nearby blood vessels, thus potentially being exposed to molecules and factors circulating systemically (Figure 5; Shen et al., 2008; Tavazoie et al., 2008).

Morphogens and genes expressed in the embryonic GE as well as in the developing cortex were also described for the adult SEZ, indicating that both regions contribute to the formation of the various SEZ niche domains (Alvarez-Buylla et al., 2013; Young et al., 2007). Among these genes and pathways, the pallial regions contributes to the dorsal SEZ with Wnt signalling and the expression of *Tbr2*, *Pax6* and *Emx1* (Azim et al., 2014a, 2014b, 2015; Fiorelli et al., 2015; Ortega et al., 2013), while the ganglionic eminences constitute the lateral SEZ and express *Gsh1/2*, *Dlx1/2/5/6* (Batista-Brito et al., 2008; Fiorelli et al., 2015; Kohwi et al., 2007; López-Juárez et al., 2013). Consistent with the GE origin, Shh signalling is also active in the lateral SEZ, following a gradient that is higher in the ventral regions (Alvarez-Buylla and Ihrie, 2014; Ihrie et al., 2011). Finally, the medial SEZ derives from the septal area and shares with it the expression of genes such as *Zic1/3* (Inoue et al., 2007; Merkle et al., 2014).

Active NSCs produce fast-proliferating transit amplifying progenitors (TAPs, or C cells) that in turn generate many neuroblasts (A cells; Figure 5), while niche astrocytes produced during development (B2 cells) are believed to separate this neurogenic environment from the nearby striatum (Fiorelli et al., 2015). Such hierarchical system ensures a rapid amplification of the neuronal population in the olfactory bulb, with the highest contribution taking place at the level of TAPs and neuroblasts (Calzolari et al., 2015). Neuroblasts produced in the SEZ gather at the anterior horn of the lateral ventricles to migrate towards the olfactory bulb (see paragraph 1.5), constituting the so-called rostral migratory stream (RMS; Lois et al., 1996; Pencea and Luskin,

2003).

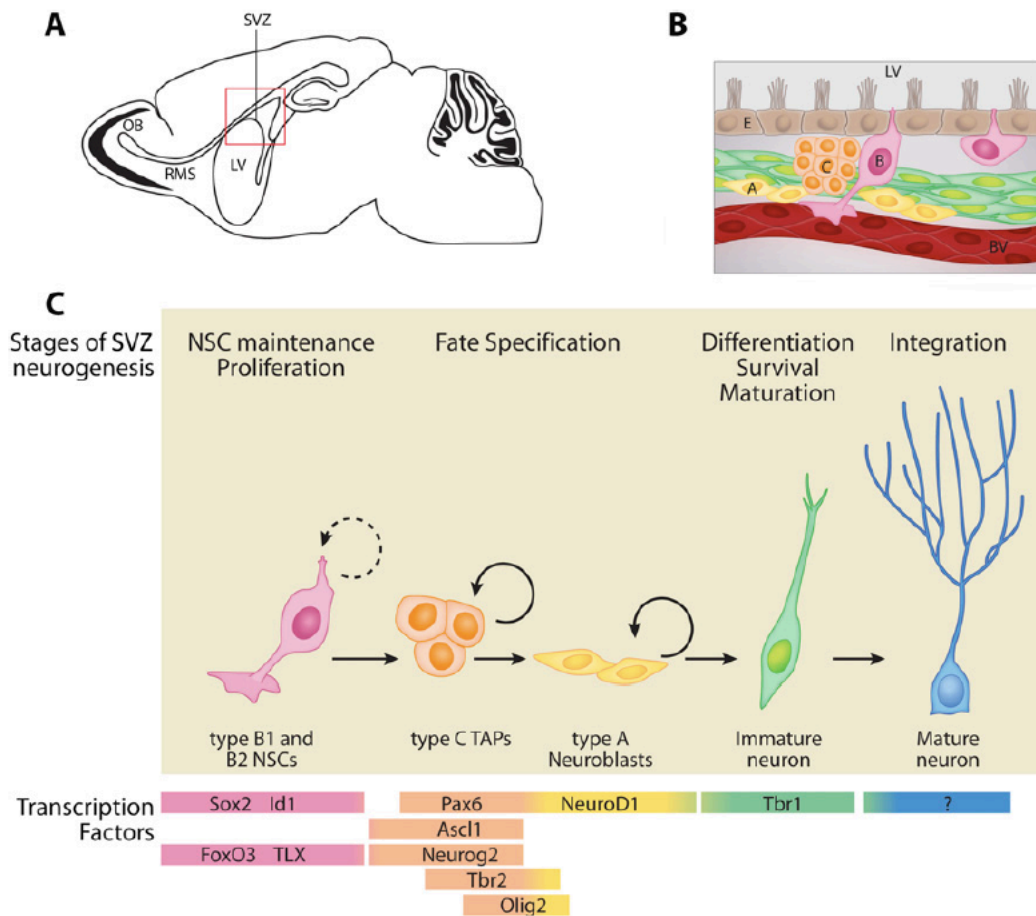


Figure 5. Schematics of the location (A) and the structure (B) of the SEZ (or V-SVZ) niche, with ependymal cells (E), RG cells (B1), TAPs (C) and neuroblasts (A) indicated. Note that B1 cells have an apical process contacting the lateral ventricle (LV) and a basal process contacting a blood vessel (BV). C) B1 cells produce type C TAPs, which in turn generate type A neuroblasts. The latter cells will then differentiate into different type of neurons in the olfactory bulb. Some of the transcription factors characterising every step are indicated, with examples from both dorsal and lateral SEZ domains (from Hsieh, 2012). RMS=rostral migratory stream; OB=olfactory bulb

1.5. The rostral migratory stream (RMS)

Neuroblasts produced by progenitors that are distributed in all SEZ domains (paragraph 1.4.2) eventually gather in the anterior horn of the lateral ventricles to migrate towards the olfactory bulbs, forming the RMS (Lois et al., 1996; Pencea and Luskin, 2003). At least 10000 neuroblasts leave the murine SEZ every day to cover the 5mm-distance separating them from the olfactory bulbs (Whitman and Greer, 2009), with an estimated speed *in vivo* of 40-80 $\mu\text{m}/\text{hour}$ and a motion that results saltatory and occasionally bidirectional (Davenne, 2005; Lledo and Saghatelian, 2005). The overall migration takes up to 7 days (Petreanu and Alvarez-Buylla,

2002; Whitman and Greer, 2009) and can be sub-divided into three steps: initiation, tangential migration and radial migration.

The initiation of migration takes place at the SEZ level and requires neuroblasts to extend a leading process in the direction of the movement (i.e. towards the olfactory bulbs) to start the oriented delamination away from the ventricles. In this regard, the flow of the CSF was found particularly important for the establishment of a SLIT-ROBO gradient, which is implicated in neuroblasts repulsion from the SEZ as well as their correct orientation (Lim and Alvarez-Buylla, 2016; Sawamoto, 2006). Other molecules, such as GSK3 β and PKC ζ , have been associated to the stabilisation of the leading process (Ghashghaei et al., 2007). Interestingly, the olfactory bulb *per se* does not seem to be necessary to trigger the initiation of the migration (Lim and Alvarez-Buylla, 2016).

Neuroblasts successfully leaving the SEZ migrate in organised chains along a vertical descending tract between the striatum and the corpus callosum, before orienting horizontally/rostrally (elbow of the RMS) and finally entering the core of the olfactory bulb constituting a vertical ascending tract (Pencea and Luskin, 2003). This tangential migration does not depend on a glial substrate as seen for embryonic development, but rather relies on cell-cell homophilic interactions of neuroblasts (Lim and Alvarez-Buylla, 2016; Lois et al., 1996) and on the blood vasculature as scaffold (Bovetti et al., 2007; Snapyan et al., 2009; Whitman et al., 2009). Glial cells are also found along the RMS, where they constitute a so-called “glial tube” that does not seem to constitute a physical support for neuroblasts motion. The function of this tube is still partly unclear, but it seems connected to confining/orienting the migration, determining proliferation of a subset of neuroblasts (Ghashghaei et al., 2007) and influencing the speed of the migration through the modulation of GABA signalling (Sun et al., 2010). Neuroblasts express the immature neuron gene *Dcx* and base their migration on different molecular mechanisms including cell-cell and matrix-cell interactions (PSA-NCAM, integrins, tyrosine kinases, matrix metalloproteases), chemoattractive signals including growth factors and neurotrophins (netrin/DCC, Shh, BDNF, VEGF, IGF-1) and chemorepulsive signals (SLIT-ROBO; Ghashghaei et al., 2007; Sun et al., 2010).

In the last step of their journey, neuroblasts enter the olfactory bulb and switch from tangential to radial migration while disengaging from the chains (Ghashghaei et al., 2007). Two main signals promote the detachment of the neuroblasts and the terminal positioning into the appropriate

layers: Reelin, being secreted by mitral cells, and Tenascin R, which is also modulated by olfactory activity (Lim and Alvarez-Buylla, 2016).

While performing this last migration, neuroblasts follow gradual steps of maturation into (mainly) granule neurons by extending dendrites and developing spines (Petreanu and Alvarez-Buylla, 2002; Whitman and Greer, 2009), a process that takes up to 45 days.

1.6. The adult main olfactory bulb

The adult main olfactory bulb is organised in a few layers formed by different neuronal cell types, which interact in a circuitry that has been extensively characterised (Nagayama et al., 2014). The RMS terminates in the core of the OB, where the granule cell layer (GCL) is found. Beyond this layer, several others can be found in the following order: internal plexiform layer (IPL), mitral cell layer (MCL), external plexiform layer (EPL) and glomerular layer (GL; Nagayama et al., 2014). The odour information, arriving from olfactory sensory neurons embedded in the olfactory epithelium, is conveyed by the olfactory nerve to the GL and segregated in the glomeruli according to a defined pattern (Mori et al., 2006a). Here the signal is received by the dendrites of tufted and mitral cells, which represent the only output of the OB towards other brain areas, but not before being properly processed by a cohort of interneurons (Nagayama et al., 2014).

Many different cell types are generated at embryonic stages by precursors residing in different areas along the lateral ventricles or in the OB ventricular zone (Batista-Brito et al., 2008; Díaz-Guerra et al., 2013; De Marchis et al., 2007; Tucker et al., 2006). Mitral cells and tufted cells constitute the output of the olfactory information towards specific cortical areas (Nagayama et al., 2014) and are generated by pallial progenitors at E10-E12 and E13-E16, respectively (Díaz-Guerra et al., 2013; Imamura et al., 2011). Tufted cells are sparsely located at various depth of the EPL, while mitral cells reside in the MCL (Nagayama et al., 2014). Being projection neurons, both cell types are glutamatergic and are generated by *Tbr2*-expressing progenitors located in the OB ventricular zone (Arnold et al., 2008; Imamura and Greer, 2013), similarly with what has been described for the development of the cortex (see paragraph 1.2.1).

Calbindin (CalB) interneurons are instead a subset of periglomerular neurons that is generated predominantly at late embryonic stages (Batista-Brito et al., 2008; Li et al., 2011; De Marchis et al., 2007) by progenitors residing in the LGE (Figure 6; Fiorelli et al., 2015; Merkle et al., 2007). Dopaminergic interneurons expressing tyrosine hydroxylase (TH) are also found in the GL starting from E12.5 (Batista-Brito et al., 2008) and originate from the LGE as well as from progenitors in the OB (Vergaño-Vera et al., 2006). Their production persists until adult stages (see paragraph 1.6.2) from progenitors located in the dorsal SEZ (Batista-Brito et al., 2008; Fiorelli et al., 2015)

Fate-mapping experiments performed by adenoviral targeting of small RG populations at postnatal day 0 (P0; Merkle et al., 2014, 2007, 2004) or by electroporation of distinct ventricular domains (Fernández et al., 2011) allowed elucidating the origin of the various neuronal populations produced at postnatal and adult stages in the olfactory bulb, which are described in the following paragraphs.

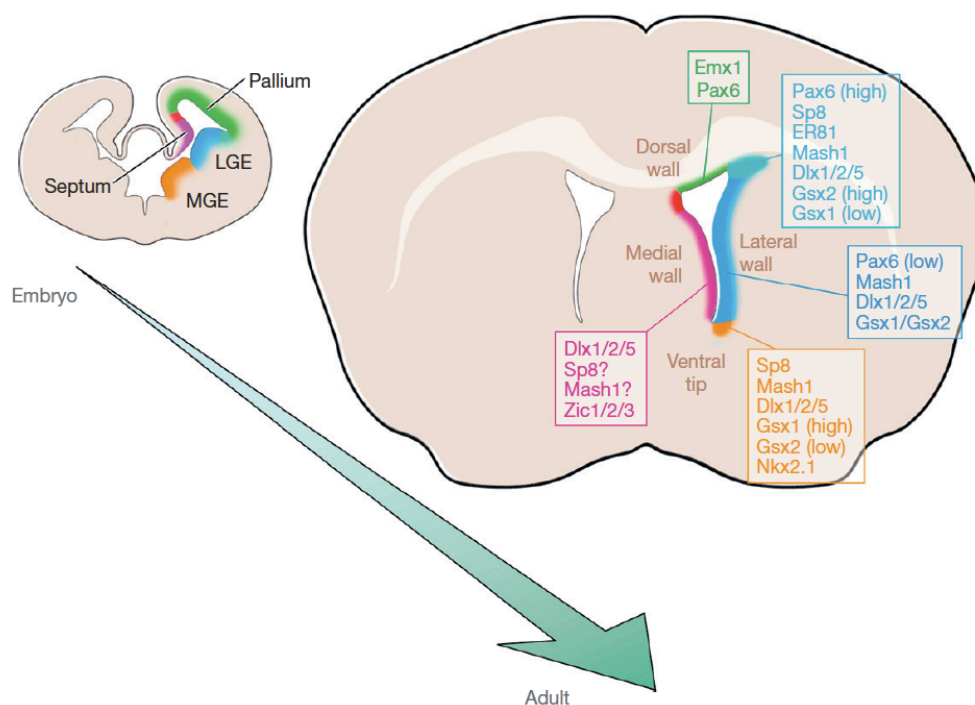


Figure 6. Schematics of the embryonic origin of the SEZ domains in the adult brain, with the main genes that can be found expressed and that specify the neurons generated (from Alvarez-Buylla et al., 2013).

1.6.1. Granule cells

Although being characterised by the absence of an axon and by the expression of GABA, olfactory bulb granule cells are a heterogeneous population both in terms of morphology and in terms of localisation (Lim and Alvarez-Buylla, 2014). These cells are found mainly in the GCL, although a small sub-population expressing the peptide 5T4 is localised in the MCL (Figure 7; Imamura et al., 2006; Merkle et al., 2014; Nagayama et al., 2014). Previous studies described two main granule cell types on the base of the position of the soma, of the complexity of dendritic arbour and on the layer of branching: the deep and the superficial granule cells (Mori et al., 1983; Orona et al., 1983). The former cell type locates in deeper areas of the GCL, bears several basal dendrites and extends a simple branched dendrite in the inner half of the EPL, where it makes dendro-dendritic synapse with mitral cells in the MCL. The latter cell type is instead found in superficial regions of the GCL and has a higher degree of dendrite branching spanning the outer half of the EPL and making contact with the lateral dendrites of tufted cells. Recently, other studies highlighted the presence of other granule cell types, whose function is still not clear (Figure 7; Merkle et al., 2014; Naritsuka et al., 2009).

Granule cell production starts at embryonic stages from LGE progenitors as well as OB local progenitors (Díaz-Guerra et al., 2013; Tucker et al., 2006; Vergaño-Vera et al., 2006), but it further extends into later stages. In particular, superficial granule cells are predominantly produced at early postnatal stages, while deep granule cells production peaks at adult stages (Calzolari et al., 2015; Kelsch et al., 2007; Lemasson et al., 2005; Sakamoto et al., 2014). Moreover, these two granule cell sub-populations have been previously shown to originate from progenitors located in different areas (Figure 7). Deep granule cells are generated in the ventral domain of the lateral SEZ (Fiorelli et al., 2015; Merkle et al., 2007) and are specified by the strong Shh signalling in this area (Figure 6; Alvarez-Buylla and Ihrie, 2014; Ihrie et al., 2011). Superficial granule cells are instead produced in the dorso-lateral SEZ and the signalling pathways in charge of their specification are still not defined (Figure 6; Fiorelli et al., 2015; Merkle et al., 2007).

From the molecular perspective, a sub-population of superficial granule neurons can be distinguished based on the expression of Calretinin (CalR; Alvarez-Buylla et al., 2013). In contrast to the other superficial granule neurons, CalR neurons are generated in the medial SEZ and in the RMS (Kohwi et al., 2007; Merkle et al., 2007). *Sp8* is the gene mainly described for

the specification of these neurons in both GCL and GL (Allen et al., 2007; Chen et al., 2012; Waclaw et al., 2006).

CaMKIV and Er81 were proposed as markers to distinguish deep and superficial granule cells populations, respectively (Saino-Saito et al., 2007). Although Er81 is found in the SEZ as well as in a subset of superficial granule cells and of GL interneurons (Kohwi et al., 2005; Lim and Alvarez-Buylla, 2016; Stenman et al., 2003), CaMKIV expression does not seem to be restricted to the deep GCL (Nagayama et al., 2014). Different metabotropic glutamate receptors (mGluR) would be expressed differentially, with mGluR1 being predominantly in superficial granule cells and mGluR5 being in deep granule cells (Heinbockel et al., 2007; Nagayama et al., 2014).

Particularly interesting is Pax6 protein, whose expression is restricted to the dorso-lateral SEZ by miR-7a opposing gradient (Figure 6; de Chevigny et al., 2012a) and is found in both dopaminergic periglomerular neurons and in a subset of superficial granule cells in the OB (de Chevigny et al., 2012b; Haba et al., 2009; Hack et al., 2005; Kohwi et al., 2005). Interfering with Pax6 function impairs adult neurogenesis and determines the accumulation of deep granule neurons in the OB, with little or no superficial granule neuron generated (Hack et al., 2005; Kohwi et al., 2005).

1.6.2. Periglomerular cells

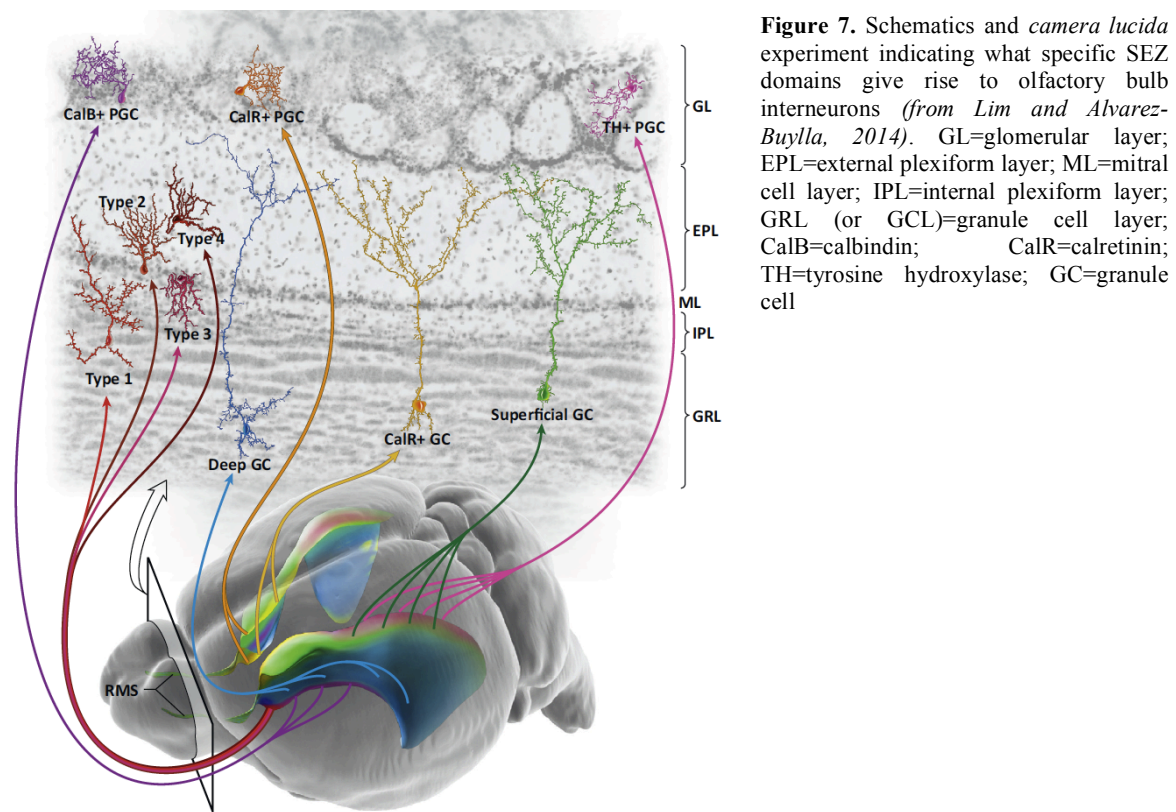
Excluding CalB interneurons, the other two main populations of interneurons in the GL –namely CalR and dopaminergic neurons– are largely (but not exclusively) produced at postnatal and adult stages (Batista-Brito et al., 2008; Díaz-Guerra et al., 2013).

As discussed in the previous paragraph, CalR interneurons are generated in the medial wall of the lateral ventricles as well as in the RMS (Figure 6 and 7; Kohwi et al., 2007; Merkle et al., 2007). The vast majority of these neurons expresses *Sp8*, while nearly half expresses *Er81* (Allen et al., 2007; Waclaw et al., 2006) and a subset expresses *Meis2* (Allen et al., 2007; Lim and Alvarez-Buylla, 2016).

Dopaminergic interneurons, whose production starts at embryonic stages (see paragraph 1.6), are instead mainly generated in the dorsal SEZ (Figure 6) from *Emx1*-, *Dlx1/2/5/6*- and *Pax6/Meis2*-expressing precursors and localise in GL (Agoston et al., 2014; Allen et al., 2007; Batista-Brito et al., 2008; de Chevigny et al., 2012b; Fiorelli et al., 2015; Kohwi et al., 2005, 2007), where

they are typically immunopositive for TH (Figure 7) as well as Er81 (Allen et al., 2007; Cave et al., 2010; Saino-Saito et al., 2007).

Finally, a small population of glutamatergic neurons was reported to be generated in the dorsal SEZ by *Neurog2*- and *Tbr2*-expressing progenitors (Brill et al., 2009; Shaker et al., 2012; Winpenny et al., 2011).



1.7. Neuronal direct reprogramming in vivo: why and how?

Although neurogenesis persists in defined areas of the adult mammalian central nervous system (see paragraph 1.4) and different subtypes of neurons are generated (paragraph 1.4.1 and 1.6), the brain, and particularly the cerebral cortex, has always been poorly amenable for repair strategies following injuries and degenerating pathologies. This difficulty stems from a low capacity of endogenous regeneration, possibly due to a local environment that is not permissive

for the production, maturation and survival of new neurons. Some of these hurdles are encountered also when neural progenitors and/or neurons obtained *in vitro* are transplanted in the cortical parenchyma or when direct reprogramming strategies are applied *in situ* (Akhtar and Breunig, 2015; Yiu and He, 2006).

Reprogramming is the term used to address the forced conversion of a cell type into other cell types. If the latter cells are stem cells with pluripotent characteristics, they are called induced pluripotent stem cells (iPSCs; Singh et al., 2015). The advantage of this method in therapy is the possibility of using easily accessible cell samples from a donor (e.g., skin biopsies) to obtain iPSCs that are eventually differentiated *in vitro* in the cell type needed (Goldman, 2016; Singh et al., 2015). The final cell population can then be used as a model of a particular inheritable pathology or used for transplantation in regenerative medicine approaches (Ichida and Kiskinis, 2015). Therefore, not only reprogramming bypasses the need of human embryos as stem cells source, but it provides also a tool that is genetically compatible with the donor and can be used in the future for personalised medicine.

Direct reprogramming moves even further towards practical applicability of these methods, as it allows forcefully converting a cell type into another cell type without passing through a pluripotent cell state. This approach can be performed *in vitro* and followed by transplantation, but additionally it can be even applied directly *in vivo* where required (Amamoto and Arlotta, 2014; Ichida and Kiskinis, 2015; Tsunemoto et al., 2015). With regards to neuronal conversion *in vitro*, ours and other laboratories described different procedures to obtain specific neuronal subtypes from different cell sources, such as astroglia (Berninger et al., 2007; Blum et al., 2011; Gascón, Murenu et al., 2016; Heinrich et al., 2010; Heins et al., 2002; Masserdotti et al., 2015; Tsunemoto et al., 2015), fibroblasts (Caiazzo et al., 2011; Colasante et al., 2015; Gascón, Murenu et al., 2016; Pang et al., 2011; Pfisterer et al., 2011; Tsunemoto et al., 2015; Vierbuchen et al., 2010) and pericytes (Karow et al., 2012).

Only few attempts to translate these approaches to the adult cortex *in vivo* resulted successful, albeit not always efficient in terms of neuronal numbers and maturation (Smith and Zhang, 2015). The over-expression of *Neurog2* together with the administration of growth factors converts 20% of targeted cells into immature DCX-immunopositive neurons and <1% neurons expressing the mature marker NeuN (Grande et al., 2013). *Sox2* and *Ascl1* over-expression, either singularly or together, bring the percentage of conversion of NG2 glia into DCX-immunopositive neurons to 30% after stab-wound injury, once again with very few NeuN

neurons appearing (Heinrich et al., 2014). A high efficiency of NeuN+ neurons (>90%) is instead achieved when NeuroD1 is delivered in the cortex, although the mode of retroviral injection does not exclude targeting of neural progenitors in the white matter (Guo et al., 2014b). The reduced number of works in *in vivo* neuronal direct reprogramming stresses the importance of developing new strategies and poses the attention on the hurdles that undermine conversion (Vierbuchen and Wernig, 2012). In this thesis I address these questions from an epigenetic and a metabolic perspective, the latter being also described in our recent publication (Gascón, Murenu et al., 2016).

1.8. Epigenetic hurdles in neuronal reprogramming: Polycomb Repressive Complex 1 (PRC1) and Ring1B

The Polycomb Repressive Complex 1 and 2 (PRC1 and PRC2) are two multi-subunit complexes described primarily in *Drosophila* as having a repressing activity on gene expression, particularly of homeotic (Hox) genes during development (Khan et al., 2015). The Mammalian versions of PRCs, though counting on more subunits, still maintain the repressive activity and, in part, the same gene targeting (Figure 8: Laugesen and Helin, 2014). Initially, the mode of action of these complexes was described as tightly hierarchical, with PRC2 starting gene repression by depositing the trimethylation of lysine 27 on histone 3 (H3K27me3) with its catalytic domain Ezh2. Subsequently, PRC1 would specifically recognise this epigenetic mark and bind it, further promoting gene repression by mono-ubiquitylating lysine 119 on histone 2A (H2AK119Ub, Figure 8; Laugesen and Helin, 2014). Although this mechanism is still valid in specific contexts, PRC1 was described as being able to work independently of PRC2 or even to act first to allow PRC2 repressive activity on chromatin (Blackledge et al., 2015, 2014; Leeb and Wutz, 2007; Tavares et al., 2012). Additionally, the ubiquitin-ligase activity was reported to be dispensable in some circumstances (Eskeland et al., 2010; Illingworth et al., 2015; Kondo et al., 2015). The proposed modes of action of PRC1 would strongly depend on its composition, as many other non-canonical variants were more recently described. However, the common link of all variants is the catalytic domain Ring1B or, alternatively, the paralog Ring1A (Laugesen and Helin, 2014).

PRCs are majorly known for their role in maintenance of stem cell characteristics during early

stages of development, by repressing genes associated to lineage choice and differentiation (Boyer et al., 2006; Hirabayashi and Gotoh, 2010b; van der Stoep et al., 2008), and for their involvement in cancer (Laugesen and Helin, 2014; Richly et al., 2011).

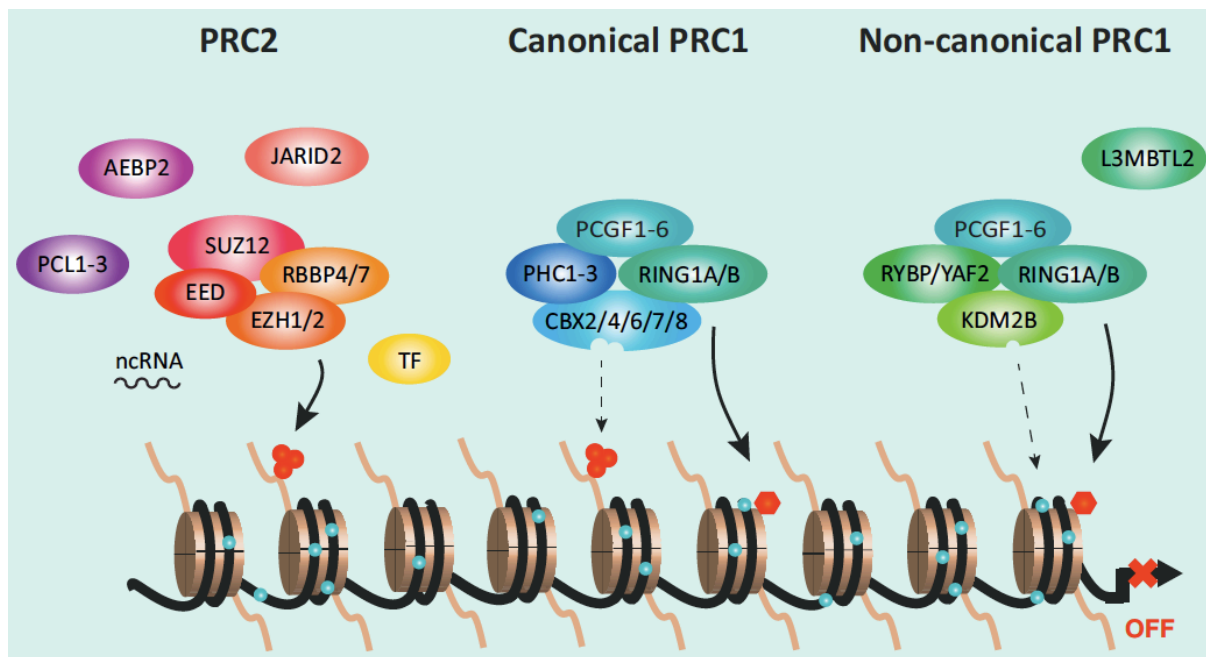


Figure 8. Schematics of PRC2 and PRC1 (canonical/non-canonical) composition, with their mechanism of action. PRC2, once recruited to chromatin by non-coding RNAs (ncRNA) and/or transcription factors (TF), deposits H3K27me3 mark (red circles), which constitutes the docking signal for the canonical PRC1. Non-canonical PRC1 preferentially targets a CpG region (blue circle) and together with the canonical counterpart it promotes the ubiquitylation of H2AK119 (red hexagon). Overall, these mechanisms result in gene repression (from Laugesen and Helin, 2014).

1.8.1. PRC1 and Ring1B in neurogenesis and reprogramming

The E3 ligase Ring1B is important for progression in the embryonic development, as demonstrated by the arrest of gastrulation following its knockout (Morey et al., 2015). *In vitro* experiments on embryonic stem (ES) cells showed that properties like proliferation and self-renewal are lost only when both *Ring1B* and *Ring1A* are deleted (Endoh et al., 2008). Indeed, Ring1A was shown to compensate for Ring1B loss in differentiated cells, taking over its role in mono-ubiquitylating H2A on lysine 119 and repressing PRC1 targets (de Napoles et al., 2004; Endoh et al., 2012; Leeb and Wutz, 2007).

In the developing and postnatal forebrain, the vast majority of PRC1 proteins is expressed, although to different extents and dynamics (Corley and Kroll, 2014; Qi et al., 2013; Vogel et al., 2006). While the inhibition of Polycomb proteins negatively impacts the efficiency of reprogramming into induced pluripotent stem cells (Onder et al., 2012), the canonical PRC1 protein Bmi1 (also known as Pcgf4) was successfully used to reprogram fibroblasts into iPSCs (Moon et al., 2011) and neural progenitors (Tian et al., 2013). Indeed, Bmi1 is important to maintain self-renewal of NSCs both during development and at adult stages (Cao et al., 2012; Corley and Kroll, 2014; Fasano et al., 2007, 2009; Molofsky et al., 2005) and has been associated to protection from oxidative stress in the hippocampus (Cao et al., 2012).

Ring1B loss in olfactory bulb embryonic NSCs also determines a decrease in proliferation and a subsequent increase in neuronal differentiation (Román-Trufero et al., 2009), although in NSCs from the SEZ such alteration in proliferation is not observed (Morimoto-Suzki et al., 2014). In cortical development, Ring1B determines the onset of gliogenesis by repressing Wnt neurogenic targets, such as *Neurogenin1/2* (Hirabayashi et al., 2009) and its deletion prolongs the neurogenic phase while enhancing the production of Ctip2-immunopositive sub-cortical projection neurons (Hirabayashi et al., 2009; Morimoto-Suzki et al., 2014). However, little is currently known about Ring1B and PRC1 role in adult neurogenesis and a possible use in direct conversion into neurons is also unexplored.

1.9. Metabolic hurdles in neuronal reprogramming: oxidative stress

While the role of Ring1B and PRC1 in direct neuronal reprogramming has never been investigated and might therefore represent a candidate approach towards more efficient conversion procedures, oxidative stress has already been described for reprogramming into iPSCs (Hawkins et al., 2016; Kida et al., 2015; Qi et al., 2015) and our recent work shed some light on its role during direct reprogramming of cultured postnatal astrocytes and mouse embryonic fibroblasts (MEFs) into neurons (Figure 9; Gascón, Murenu et al., 2016). In particular, over-expression of *Ascl1* or *Neurog2* starts the conversion process as previously shown (Berninger et al., 2007; Chanda et al., 2014; Heinrich et al., 2010; Liu et al., 2013; Masserdotti et al., 2015; Vierbuchen et al., 2010), but many cells succumb to cell death before managing to acquire a neuronal phenotype. Further analyses showed that oxidative stress is

developed during reprogramming, possibly in the attempt to convert the metabolism of the starting cell population (e.g. anaerobic glycolysis in astrocytes) into the oxidative phosphorylation metabolism that neurons use to satisfy their high energetic demand (Mlody et al., 2016). Indeed, molecules known to alleviate oxidative stress, such as Vitamin D/Calcitriol (Bao et al., 2008) and Vitamin E/ α -Tocopherol/ α -Tocotrienol (Buettner, 1993), drastically improve the final neuronal yield.

Moreover, treating the cultures with compounds known to improve the efficiency of neuronal reprogramming, such as Forskolin (Fk; Liu et al., 2013), also results in a decrease in the levels of oxidative stress (Figure 9), further corroborating the idea that reactive oxygen species (ROS) must be buffered in order to promote a full conversion into neurons. The same result is obtained when the over-expression of either *Ascl1* or *Neurog2* is simultaneous with *Bcl-2* (Figure 9), whose role goes now beyond the mere promotion of cell survival, as we show for the first time by using specific mutants that enhance/impair its anti-apoptotic activity (Gascón, Murenu et al., 2016). The implications of these findings in neuronal reprogramming *in vivo* after cortical grey matter injury are discussed in the Results section.

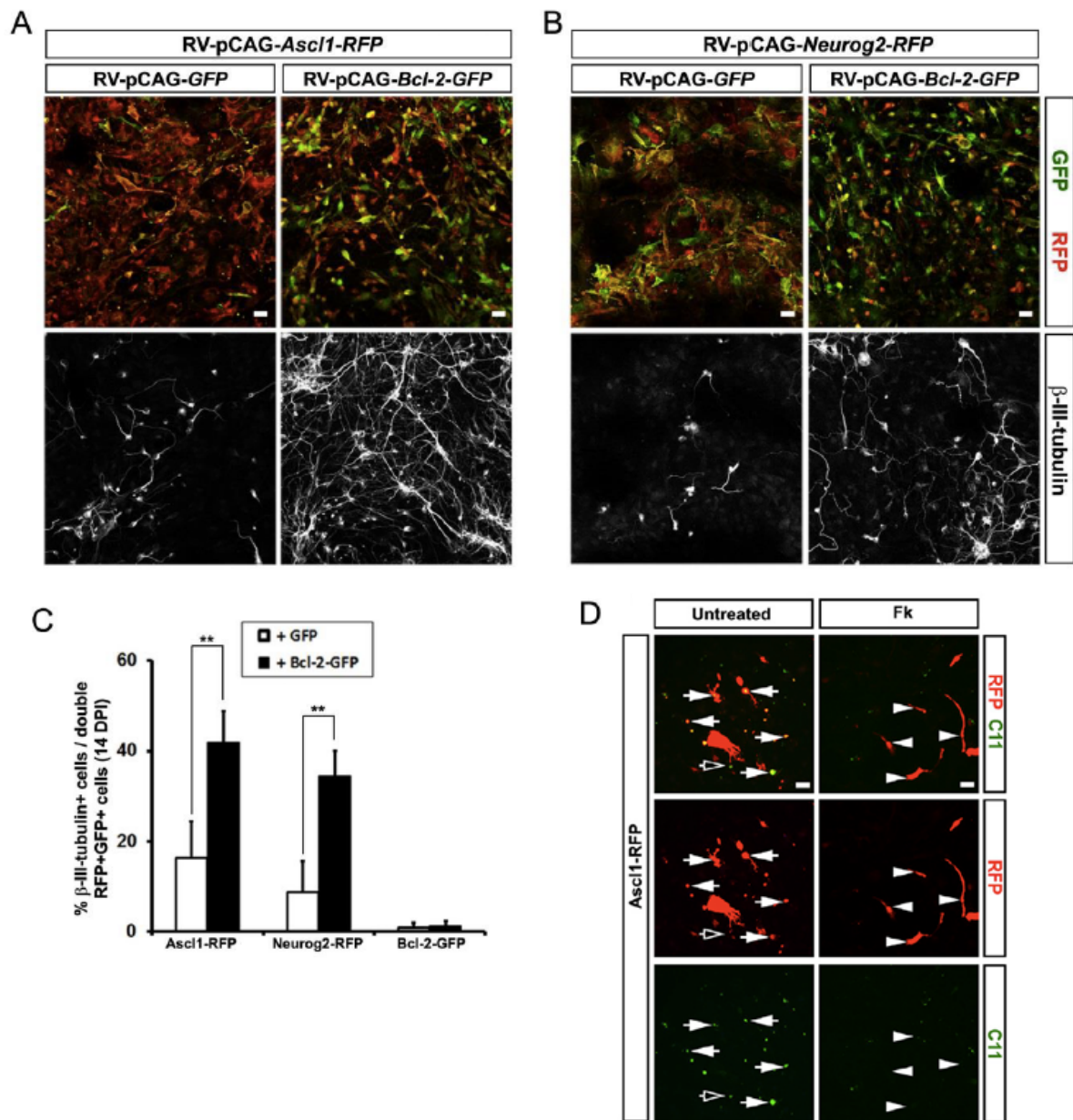


Figure 9. MEFs transduced with retroviruses expressing (A) *Ascl1*-RFP (red) with *GFP* or *Bcl-2*-GFP (green) and (B) *Neurog2*-RFP (Red) with *GFP* or *Bcl-2*-GFP (green). β -III-tubulin shows the immature neurons, whose proportion is quantified in (C). Both the complexity (A, B) and the percentage (C) of immature neurons are drastically improved when *Bcl-2* is over-expressed with either *Ascl1* or *Neurog2*. D) Cultured astrocytes that are pushed towards the neuronal phenotype by over-expression of *Ascl1* (red) are immunopositive for the ROS reporter (C11, green). Treatment with Forskolin, known to enhance reprogramming efficiency, strongly decreases ROS levels (modified from Gascón, Murenu et al., 2016).

2. Results

2.1. Role of metabolism in forced neurogenesis: the starting point

Direct reprogramming of different cell types into mature neurons can be achieved by forcing the over-expression of key transcription factors involved in neurogenesis during development. This approach was described for the first time in our laboratory and it involved the retroviral delivery or plasmid lipofection of *Pax6*, *Neurogenin2* (*Neurog2*), *Ascl1* or *Dlx2* in primary cultures of cortical astrocytes from postnatal mice (Berninger et al., 2007; Blum et al., 2011; Heinrich et al., 2010, 2011; Heins et al., 2002). More specifically, the over-expression of *Neurog2* triggered the generation of glutamatergic neurons in 70% of all transduced cells, while the over-expression of *Ascl1* or *Dlx2* allowed the acquisition of a GABAergic phenotype in 40% of all transduced cells. However, although this approach was successful also in neurospheres obtained from adult mouse cortex upon grey matter injury (Heinrich et al., 2010), the direct conversion of reactive glia cells *in vivo* in a lesion context was rather limited (Buffo et al., 2005; Kronenberg et al., 2010).

In the attempt to investigate the mechanisms underpinning forced conversion into neurons, our laboratory recently showed that oxidative stress is developed during reprogramming of postnatal astrocytes or mouse embryonic fibroblasts (MEFs) with *Neurog2* or *Ascl1*. As a consequence, the acquisition of the neuronal program is impaired by high levels of lipid peroxidation, which ultimately determine cell death (Gascón, Murenu et al., 2016). The simultaneous over-expression of Bcl-2 – a protein mostly known for its anti-apoptotic role – resulted in the achievement of a higher reprogramming rate by potently reducing such oxidative levels, independently of the neurogenic transcription factor and the starting cell population used. Similar results were obtained through administration of molecules like forskolin (Fk), which was already described to improve neuronal conversion (Liu et al., 2013), as well as vitamin D or vitamin E, which are known for their anti-oxidant effect (Bao et al., 2008; Buettner, 1993; Dong et al., 2012).

In this project I investigated the implications of Bcl-2, vitamin D and vitamin E on neuronal reprogramming *in vivo* in combination with *Neurog2* retroviral delivery in the injured cortical grey matter of adult mice.

2.2. Proliferating cells in the lesion site do not include neuronal progenitors

The lesion paradigm used in this study is a unilateral stab-wound injury performed in the cortical grey matter of 8-10 week old mice (Buffo et al., 2005), sparing the deep layers to minimise the risk of involvement of neural progenitors from the underlying white matter. Three days after the

Results

surgery, a micro-injector was used to deliver the retroviral suspension in the lesion. The retroviral approach ensures that only cells in active proliferation express the construct, therefore excluding the expression by endogenous neurons that might be incorrectly considered reprogrammed. Finally, 10 days post-injection (DPI) the animals were perfused and vibrating microtome sections of the brain were analysed by immunohistochemistry.

To exclude the possibility that proliferating neural progenitors migrate to the site of the lesion and alter the results of our analysis, we conducted a preliminary experiment (n=1) by injecting a retrovirus for the green fluorescent protein (GFP) three days after stab-wound injury and analysed it by immunohistochemistry 7 days later. In agreement with a previous work from our lab (Heinrich et al., 2014), mostly NG2-immunopositive oligodendrocyte precursor cells (OPCs; Figure 10A, left panel) and GFAP-immunopositive reactive astrocytes (Figure 10A, right panel) were transduced at this time-point. Moreover, doublecortin (DCX) – a marker of neuroblasts and immature neurons – was found at low levels only in OPCs, as already described in the cortical injury paradigm (Guo et al., 2010).

We therefore confirmed that three days after stab-wound injury no neuronal progenitor can be observed in the site of the lesion and that the retroviral approach ensures targeting only reactive glial cells.

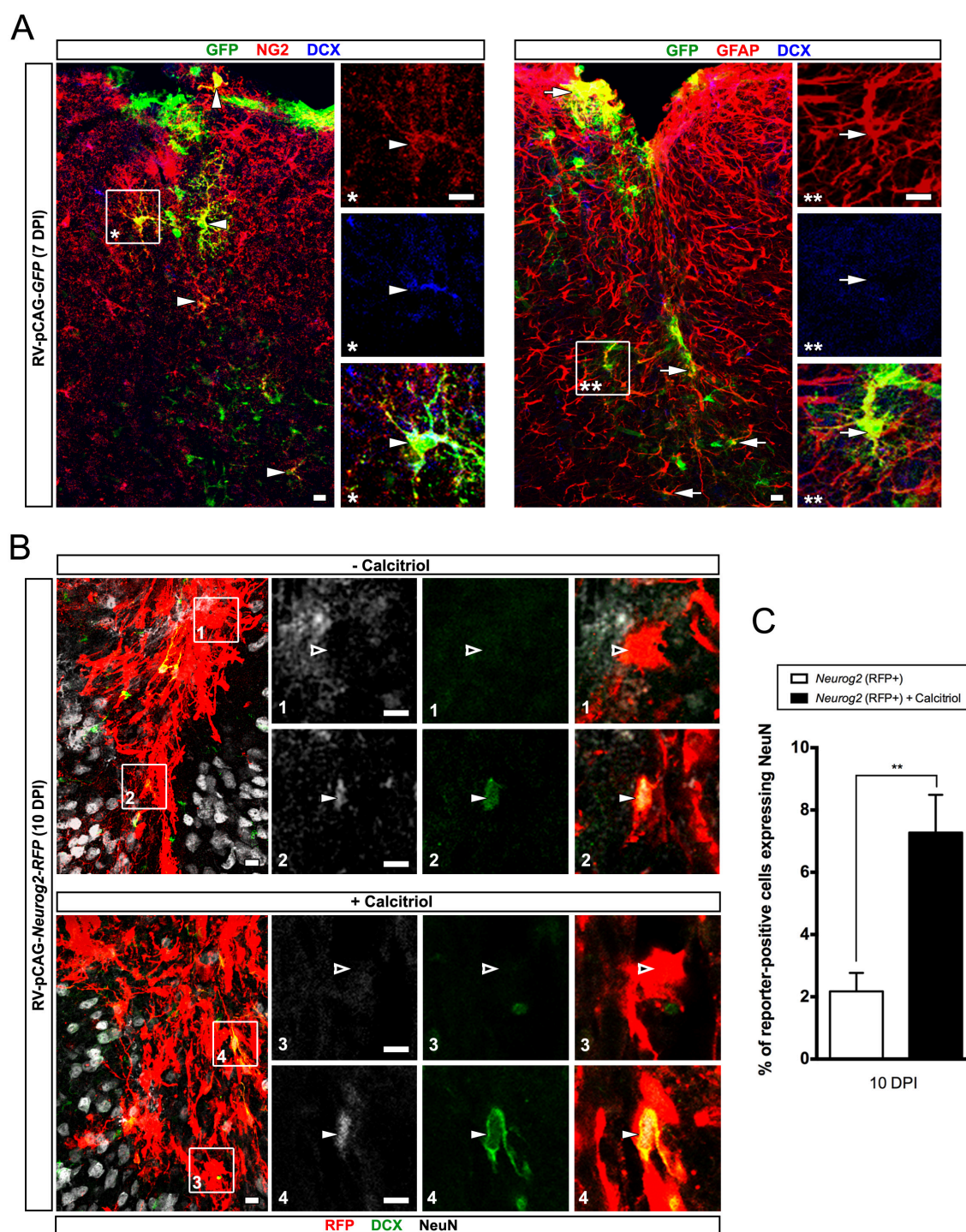


Figure 10. (A-B) Confocal micrographs of mouse sections with cortical grey matter stab-wound injury followed by retroviral injection of different constructs 3 days later and analysed by immunohistochemistry at different time-points. Single optical sections are shown at higher magnification in the insets. (A) Retroviral delivery of a construct encoding for *GFP* analysed at 7 days post-injection (DPI) shows *GFP*-immunopositive cells either positive for *NG2* (arrowheads, left panel) or *GFAP* (arrows, right panel). When detectable, low doublecortin (*DCX*) levels are observed only in *NG2*-immunopositive cells. (B) Retroviral delivery of *Neurog2*-IRES-*RFP* construct followed (lower panels) or not (upper panels) by Calcitriol treatment and analysed at 10 DPI. Transduced cells (*RFP*+) are rarely immunopositive (filled arrowheads) for *DCX* and/or *NeuN* (C) Quantifications of the total *RFP*-immunopositive population show a higher percentage of *RFP*/*NeuN* immunopositive cells when Calcitriol is administered.

Scale bars: 10 μ m. Error bars represent SD. Unpaired t test in C ($n=3$ per condition), ** $p<0.01$

2.3. *Neurog2* over-expression in reactive glia cells does not trigger neuronal conversion

After corroborating the observation that this infection paradigm does not lead to the transduction of neurons and/or neuronal progenitors potentially migrating to the site of injury, I applied the same approach for the injection of neurogenic determinants.

When a retroviral construct encoding for *Neurog2*-IRES-*RFP* was injected in the injured cortex, many cells were found immunopositive for the red fluorescent protein (RFP) at 10 DPI (Figure 10B, top panel). To investigate whether such RFP-positive cells converted into neurons as a consequence of *Neurog2* over-expression, we performed immunostainings for DCX. In agreement with previous experiments from our laboratory, few cells resulted immunopositive for DCX, with the intensity of the signal considerably weaker than in immature neurons of the hippocampal sub-granular zone. To further analyse the nature of the transduced cells we performed an immunostaining for NeuN (also known as Fox-3), which is normally found in almost all mature neurons in the brain. Among all RFP-positive cells, only 2% of them (Figure 10C) expressed detectable levels of NeuN while failing to adopt a neuronal-like morphology (i.e., small round soma, long thin processes).

Therefore, we confirmed that *Neurog2* over-expression alone is not sufficient to efficiently reprogram reactive glia cells *in vivo* and that additional measures must be adopted to ameliorate the final acquisition of a neuronal phenotype.

2.4. Calcitriol improves neuronal reprogramming initiated by *Neurog2*

Microarray analysis of MEFs transduced with *Ascl1* showed that vitamin D receptor (*Vdr*) is the most up-regulated transcription factor when also Fk is administered to the culture (Gascón, Murenu et al., 2016). Furthermore, the cross-analysis of the genes up-regulated by *Ascl1* after treatment with Fk or co-expression of A(70)-*Bcl-2* – a mutant form of Bcl-2 that displayed the best effects in terms of reprogramming – further indicated that cells undergoing successful reprogramming activate a strong response against oxidative stress (Gascón, Murenu et al., 2016). For this reason, 2 days after the injection of *Neurog2*-IRES-*RFP* we set out to administer the *Vdr* agonist Calcitriol and analyse the effects at 10 DPI (Figure 10B). Interestingly, although only a small proportion (7%, Figure 10C) of RFP-immunopositive cells displayed a detectable NeuN signal, Calcitriol administration resulted in a 3.5-fold significant increase in the percentage of NeuN-positive transduced cells compared to the condition without Calcitriol administration.

However, the morphology of such cells was again lacking clear neuronal-like features.

All in all, these data suggest that *Vdr* downstream targets may partially facilitate *Neurog2* reprogramming capacity, albeit still insufficient to allow for a high conversion rate.

2.5. The simultaneous over-expression of *Neurog2* and *Bcl-2* results in large numbers of reprogrammed neurons

Continuous time-lapse imaging experiments in postnatal astrocytes showed that *Bcl-2* over-expression together with *Ascl1* boosts the acquisition of the neuronal phenotype and dramatically increases the final neuronal yield. Surprisingly, such potent effect is not determined by *Bcl-2* re-known anti-apoptotic activity, but rather by a less known role in antagonizing oxidative stress (Gascón et al., 2016) that is effective also when other cell types (i.e. MEFs) or neurogenic transcription factors (i.e. *Neurog2*) were used.

To test whether *Bcl-2* role *in vitro* could be exerted also *in vivo*, we co-infected the cortex of adult mice with *Neurog2*-IRES-*RFP* and *Bcl-2*-IRES-*GFP* upon grey matter stab-wound injury and then analysed the brains at 10 DPI (Figure 11A). Following immunostaining, we observed that 50-60% of all transduced cells expressed both retroviral constructs and displayed neuronal-like features, while the single-transduced cells (either GFP- or RFP-positive) maintained a glial morphology (Figure 11B). Despite being weakly immunopositive for DCX, a striking percentage of co-transduced cells expressed distinct levels of NeuN (75%, Figure 11C, D). Interestingly, the soma size of converted cells was notably smaller than the soma size of neighbouring neurons, suggesting that more time might be required for these cells to develop a proper neuronal morphology (see NeuN immunostaining in Figure 11C).

The analysis of *Neurog2* single-transduced cells in this paradigm showed a percentage of NeuN-immunopositive cells 4-fold higher than in *Neurog2*-IRES-*RFP* single-infected mice (8%, Figure 11D and 10C). This discrepancy could be caused by a low expression of *GFP* reporter in some co-transduced cells, thus incorrectly leading to consider such cells as single-transduced.

Taken together, these data show that the forced expression of *Bcl-2* considerably improves *Neurog2*-mediated conversion into neurons, both in terms of final yield and in the acquisition of neuronal-like features.

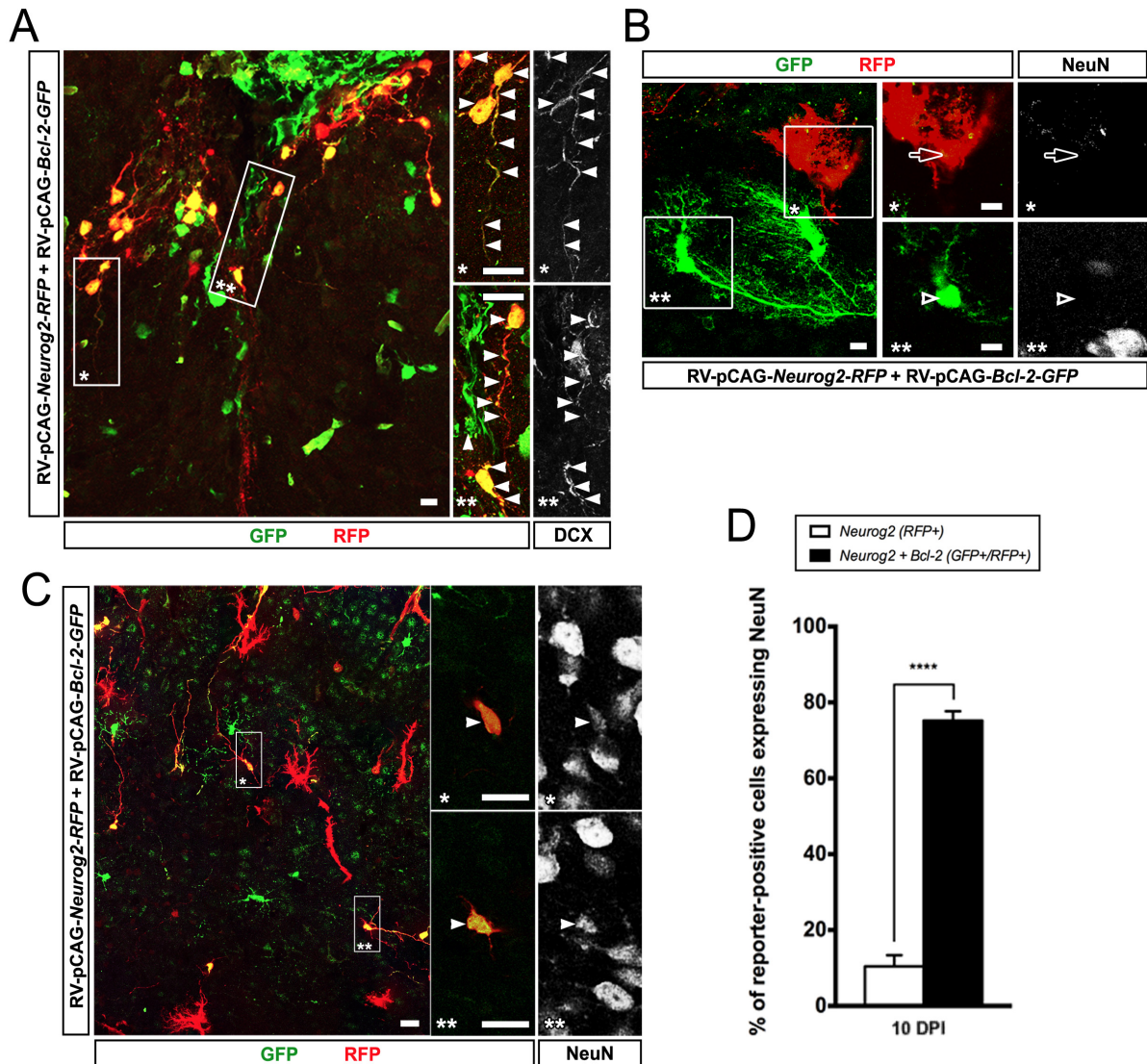


Figure 11. (A-C) Confocal micrographs of mouse sections with cortical grey matter stab-wound injury followed by retroviral injection of *Neurog2*-IRES-RFP and *Bcl-2*-IRES-GFP 3 days later and analysed by immunohistochemistry at 10 DPI. Single optical sections are shown at higher magnification in the insets. (A) Co-transduced cells adopt an elongated morphology and are weakly DCX-immunopositive (arrowheads). (B) Single-transduced cells (RFP+, empty arrows; GFP+, empty arrowheads) do not express detectable NeuN levels, contrary to many of the co-transduced cells (C, arrowheads). (D) Quantifications of RFP- or RFP/GFP-immunopositive cells expressing NeuN show a striking increase in percentage when Bcl-2 (GFP+) is co-administered.

Scale bars: 10 μ m. Error bars represent SD. Unpaired t test in D (n=3 per condition), ****p<0.0001

2.6. *Bcl-2* and Calcitriol bring neuronal reprogramming in vivo to unprecedented levels

Following the results obtained with the simultaneous over-expression of *Neurog2* and *Bcl-2*, we next asked whether in this paradigm Calcitriol could have additional beneficial effects.

For this reason, after performing a cortical grey matter stab-wound injury and subsequent

Neurog2/Bcl-2 co-infection, we administered Calcitriol to the mice (2 DPI) and then analysed the brain sections at 10 DPI (Figure 12A). Strikingly, the percentage of co-transduced cells immunopositive for NeuN rose to 87%, significantly higher than in co-infected animals not treated with Calcitriol (Figure 12B). While some single *Neurog2*-transduced (RFP+) cells were found immunopositive for NeuN (Figure 12A, C), single *Bcl-2*-transduced (GFP+) cells never showed a detectable NeuN signal (Figure 12C). Interestingly, reprogrammed neurons appeared far more complex upon Calcitriol treatment, with long and ramified processes often spanning the entire thickness of the sections and occasionally reaching either the pial surface or the white matter (Figure 12D).

Besides performing the immunostaining for NeuN we checked also if Myt1L, a gene that was previously used for direct conversion into neurons (Pang et al., 2011; Vierbuchen et al., 2010), labelled all neuronal populations in the brain as reported (unpublished, courtesy of Marius Wernig).

Indeed, Myt1L-immunopositive cells in the cortex co-labelled with NeuN, whereas in other brain regions (i.e. the olfactory bulb) Myt1L signal was detected in neuronal populations known to be immunonegative for NeuN (Bagley et al., 2007; Mullen et al., 1992; Winpenny et al., 2011; Figure 12E). Importantly, the expression of Myt1L in OPCs was detected neither in the intact cortex nor in the injured cortex (when instead they result weakly immunopositive for DCX; Figure 12F), allowing us to reliably use this marker to further prove the neuronal nature of our co-transduced cells. As expected, the vast majority of *Neurog2/Bcl-2* co-transduced cells resulted immunopositive for Myt1L (Figure 12G), but did not show any detectable signal for MAP2 –a known marker for neuronal dendrites (Figure 12H).

Similarly to what we observed in the mice infected with *Neurog2* alone, Calcitriol significantly increased the rate of conversion of RFP+ single-transduced cells also in this paradigm, resulting in 22% of RFP-immunopositive cells expressing detectable levels of NeuN (Figure 12B). Even in this case such percentage is considerably higher than the percentage obtained from *Neurog2* single-infected mice treated with Calcitriol, possibly due once again to the difficult detection of GFP-protein levels in some co-transduced cells.

All in all, Calcitriol ameliorates the rate of conversion elicited by *Neurog2* alone or in combination with *Bcl-2* and enhances the development of complex processes at 10 DPI.

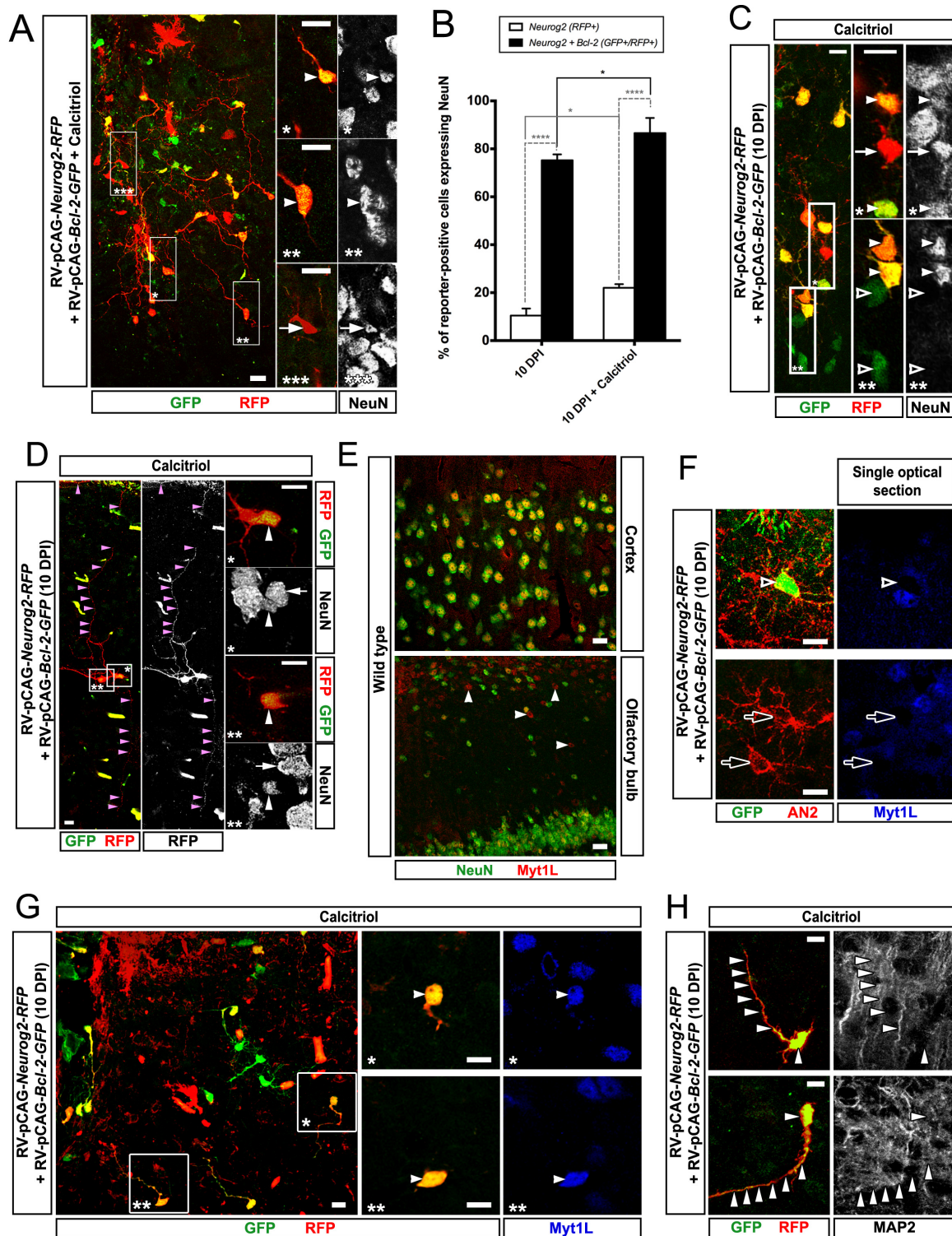


Figure 12. (A, C-E, G, H) Confocal micrographs of mouse sections with retroviral injection of *Neurog2/Bcl-2* and Calcitriol treatment, analysed by immunohistochemistry at 10 DPI. Single optical sections are shown at higher magnification in the insets. (A) Co-transduced cells (RFP+/GFP+, arrowheads) often show detectable levels of NeuN; occasionally, also RFP+ single-transduced cells are immunopositive for NeuN (arrow). (B) Percentage of RFP+ and RFP+/GFP+ transduced cells immunopositive for NeuN, with or without treatment with Calcitriol. Note that in presence of Calcitriol all values result increased. (C) Example of co-transduced (arrowhead) and RFP+ single-transduced (arrow) cells immunopositive for NeuN after Calcitriol treatment. Note that GFP+ single-transduced cells (empty arrowhead) are immunonegative for NeuN. (D) Calcitriol administration determines the extension of long processes (purple arrowheads) in *Neurog2/Bcl-2* co-transduced cells. Note that the soma of such cells (white arrowheads) is considerably smaller than the soma of neighbouring neurons (arrows), as indicated by NeuN staining.

Figure 12 (continues from previous page). (E) Immunostaining for Myt1L perfectly matches NeuN signal in the cortex, but recognises also NeuN-immunonegative neurons (arrowheads) in the olfactory bulbs of wild type animals. (F) AN2-immunopositive oligodendrocyte precursors, either GFP+ single-transduced (empty arrowhead) or non-transduced (empty arrows), are never immunopositive for Myt1L, contrary to what observed for DCX. (G) Co-transduced cells are often immunopositive for Myt1L, but not for the dendritic marker MAP2 (H).

Scale bars: 10 μ m, except 20 μ m in E. Error bars represent SD. Two-way ANOVA with Tukey's post-hoc test in B (n=3 per condition), *p<0.05, ****p<0.0001

2.7. Reprogrammed neurons dramatically decrease in number over time

After assessing and describing the *in vivo* conversion potential of *Neurog2* and *Bcl-2*, we set out to determine the survival rate of reprogrammed cells at later time-points.

At 20 DPI, cells co-transduced with *Neurog2* and *Bcl-2* retroviral constructs were still immunopositive for NeuN (Figure 13A) and bore a neuronal-like morphology, comparably to what observed at 10 DPI at the same conditions. However, the total number of reprogrammed neurons was dramatically decreased compared to the earlier time-point (5 neurons/section at 20 DPI, n=1; 12 neurons/section at 10 DPI, n=3; 3-6 sections/mouse analysed), suggesting that over time a massive number of converted cells do not manage to survive. The single administration of Calcitriol at 2 DPI slightly improved the survival rate of co-transduced neuronal cells (8 neurons/section, n=1; 3-6 sections/mouse analysed), which still showed distinct NeuN (Figure 13A) and Myt1L (Figure 13B) signal. Both in Calcitriol treated and untreated conditions single-transduced cells were still observed at 20 DPI.

Despite the lower absolute number of reprogrammed cells, the surviving ones occasionally displayed mature neuronal features, e.g. thicker processes reminiscent of dendrites and long thin processes (possibly axonal) with boutons-like enlargements (Figure 13C).

As a consequence of what we observed at 20 DPI, 2 months after the retroviral injection (60 DPI) the reprogrammed neurons found in the injured cortex were even fewer (1 neuron/section, n=1; 3 sections analysed), although the administration of Calcitriol partially improved their number (3 neurons/section, n=2; 3-4 sections/mouse analysed; Figure 13D). However, even at such a late time-point single-transduced cells maintaining their glial origin could be observed, strongly suggesting that mostly reprogrammed neurons undergo cell death despite the over-expression of *Bcl-2*.

Therefore, we concluded that cells undergoing conversion still die at later time-points and that *Bcl-2* over-expression is not sufficient to prevent it. In this paradigm, the single Calcitriol administration at 2 DPI brings little improvement, suggesting that for long-term survival additional or alternative approaches might be required.

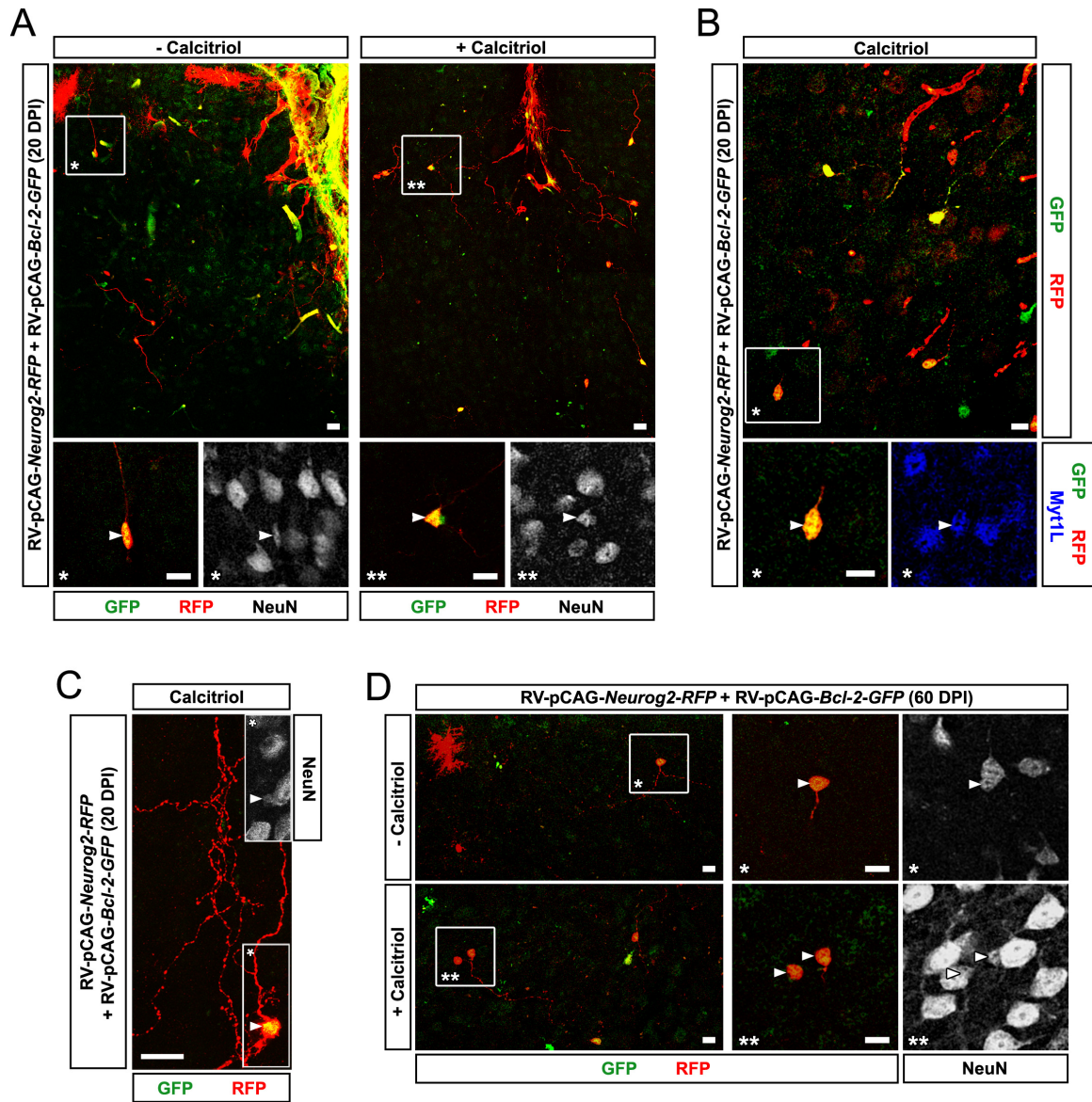


Figure 13. (A-D) Confocal micrographs of mouse sections with retroviral injection of *Neurog2/Bcl-2* with/without Calcitriol treatment, analysed by immunohistochemistry at 20 and 60 DPI. Single optical sections are shown at higher magnification in the insets. (A, B) Few co-transduced cells can be observed at 20 DPI, regardless of Calcitriol treatment. Note that such cells often express NeuN (A, arrowheads) and Myt1L (B, arrowheads). (C) Example of co-transduced cell at 20 DPI and after Calcitriol treatment showing NeuN signal (arrowhead) and high level of morphological complexity. (D) Fewer co-transduced cells (all immunopositive for NeuN, arrowheads) can be observed at 60 DPI, with little improvement after a single Calcitriol treatment.

Scale bars: 10 µm.

2.8. Several administrations of Calcitriol are required to promote long-term survival and further maturation of reprogrammed neurons

The single administration of Calcitriol at 2 DPI had beneficial effects on both the percentage and the maturation of reprogrammed neurons assessed at 10 DPI. In particular, the higher neuronal yield could be a result of an increased number of co-transduced cells pushed into conversion and/or a higher number of neurons surviving the conversion process. In the latter case, while Calcitriol effects are evident at short time-points (10 DPI) the same would not necessarily take place at longer time-points, i.e. during further maturation and integration of reprogrammed cells, ultimately determining the massive decrease in numbers described at 60 DPI.

For this reason, I administered Calcitriol at 2 DPI and once per week after 10 DPI, for a total of 3 times. Following this approach, at 30 DPI the number of reprogrammed cells was considerably higher than previously observed (8 neurons/section, n=1; 4 sections analysed; Figure 14A). Moreover, these co-transduced cells were immunopositive for NeuN, developed long processes and had a soma size almost comparable to the soma of endogenous neurons (NeuN immunostaining in Figure 14A). Therefore, we concluded that multiple administrations of Calcitriol improve survival and maturation of reprogrammed neurons.

Following these preliminary results, we used the same protocol to analyse the mice at 60 DPI (Figure 14B). Intriguingly, not only the number of recombined cells was notably higher than previously described for this time-point (7 neurons/section, n=1; 3 sections analysed), but also the cell complexity was enhanced. As a matter of fact, many co-transduced cells showed an increased soma size (Figure 14B, NeuN immunostaining) and long processes spanning the whole cortical thickness (Figure 14C), bearing spine-like structures or real spines (Figure 14D). The diverse degree of development of reprogrammed cells could indicate a different speed in maturation or could reflect intrinsic differences that ultimately affect the way co-transduced cells respond to the simultaneous over-expression of *Neurog2* and *Bcl-2*, as well as the stimulation of Vdr downstream pathways.

Taken together, these data indicate that reprogrammed neurons are able to survive up to 2 months and develop complex structures (i.e. spines, bigger soma), provided that Calcitriol is administered for longer periods.

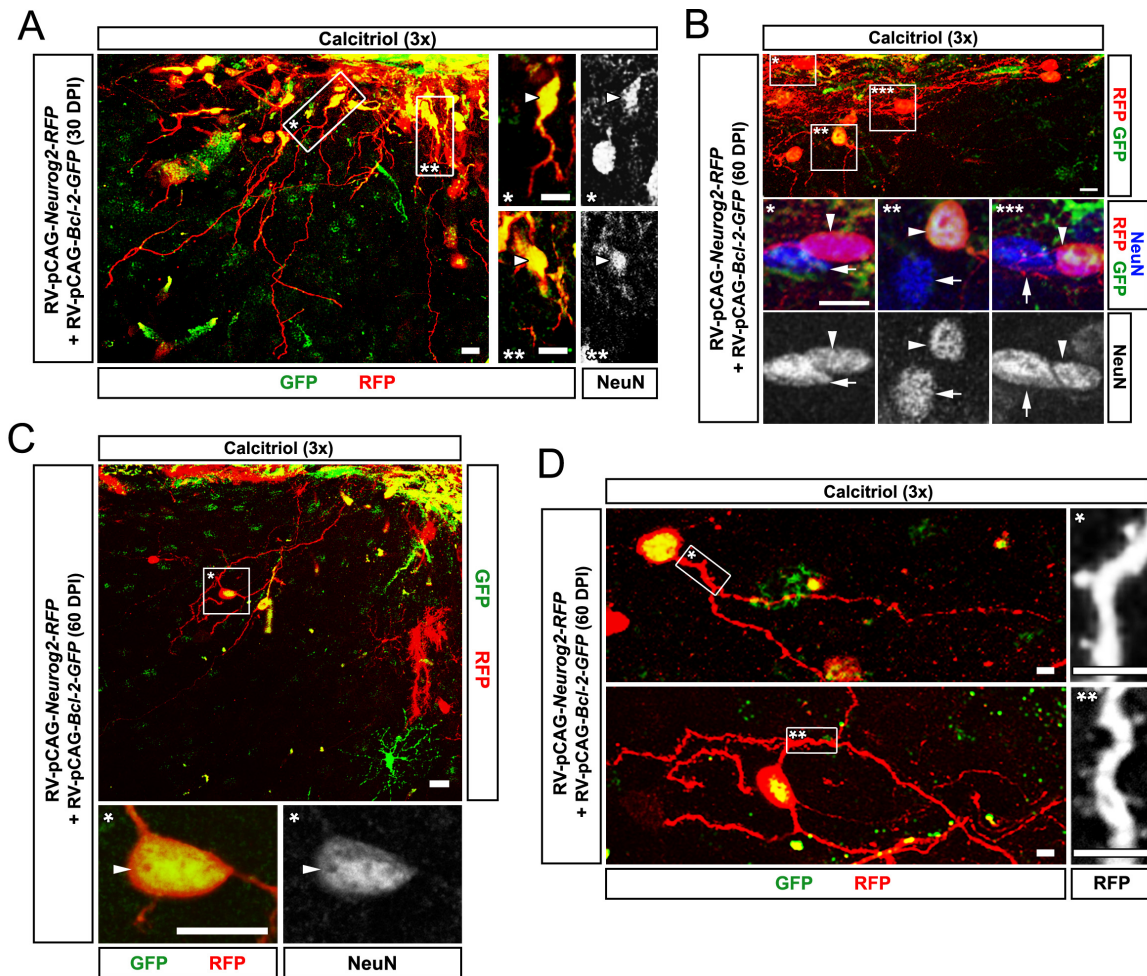


Figure 14. Confocal micrographs of mouse sections with retroviral injection of *Neurog2/Bcl-2* after multiple Calcitriol treatments, analysed by immunohistochemistry at 30 and 60 DPI. Single optical sections are shown at higher magnification in the insets. (A) Several administrations of Calcitriol improve the total number of co-transduced cells at 30 DPI. Most of these cells are immunopositive for NeuN (arrowheads). (B) More co-transduced cells can be observed at 60 DPI after multiple administration of Calcitriol. Not only these cells are immunopositive for NeuN (arrowheads), but their soma size is almost comparable to the soma size of neighbouring neurons (arrows). (C, D) Example of neurons immunopositive for NeuN (C, arrowhead) with big soma size, found after co-infection with *Neurog2/Bcl-2* and multiple treatment with Calcitriol. Some of these neurons display also long branches and different degree of spine development (D; lower panel shows the same neuron as in C).

Scale bars: 10 µm, except 5 µm in D.

2.9. α -Tocotrienol potently enhances neuronal maturation

As the *in vitro* experiments suggested, the oxidative stress resulting from the onset of conversion is responsible for the impairment of the reprogramming process and for the consequent cell death following lipid peroxidation. Bcl-2, Vdr and Calcitriol all act as potent anti-oxidants, thus allowing for a faster and more efficient conversion into neurons. However, these molecules are

likely to activate a diverse range of cellular pathways, possibly also collateral to the mere anti-oxidant response. Therefore, to further prove that oxidative stress and lipid peroxidation are the key events undermining reprogramming efficiency, α -Tocopherol or α -Tocotrienol (two different forms of Vitamin E) were added to the cultures after *Ascl1* over-expression, as molecules that do not rely on the activation of cellular signalling in order to antagonize oxidative stress. In agreement with our hypothesis, reprogramming efficiency considerably improved after treatment with these molecules, while drastically reducing lipid peroxidation (Gascón, Murenu et al., 2016).

To check the extent to which α -Tocotrienol exerts the same effects in our *in vivo* reprogramming paradigm, we administered this compound 2 days after the injection of *Neurog2/Bcl-2*, similarly to what described for Calcitriol. At 10 DPI a high percentage of co-transduced cells (88%) was immunopositive for NeuN (Figure 15A, B), with a significant increase compared to the same condition without any Vitamin administration (Figure 15B) and similarly to what observed after Calcitriol treatment. However, differently from any tested condition at 10 DPI, the vast majority of reprogrammed cells displayed complex process ramifications and a thick apical neurite that occasionally bore spine-like structures (Figure 15C). Moreover, the morphology acquired by these reprogrammed neurons was considerably enhanced, with the soma volume being significantly bigger than the soma volume of cells reprogrammed in the absence of any Vitamin (Figure 15D). Interestingly, Calcitriol treatment failed to improve the soma volume of reprogrammed neurons to the extent of α -Tocotrienol (Figure 15D), corroborating the observation that the direct reduction of oxidative stress promoted by α -Tocotrienol boosts the maturation of reprogrammed neurons.

Single *Neurog2*-transduced (RFP-immunopositive) cells also responded to α -Tocotrienol administration generating NeuN-immunopositive neurons in 20% of the cases, with a significant 3-fold increase compared to the single-transduced cells without any subsequent Vitamin treatment (Figure 15B). However, pilot long-term experiments showed that the single administration of α -Tocotrienol is not sufficient to guarantee survival of reprogrammed neurons until 60 DPI, as it was the case for Calcitriol single administration (not shown).

Therefore, we concluded that α -Tocotrienol has similar effects as Calcitriol on the final neuronal yield at 10 DPI, but additionally it also improves the maturation of the reprogrammed neurons to unprecedented levels for this early time-point. Several administrations of α -Tocotrienol might be necessary to promote survival and consolidation of reprogrammed neurons at longer time-points.

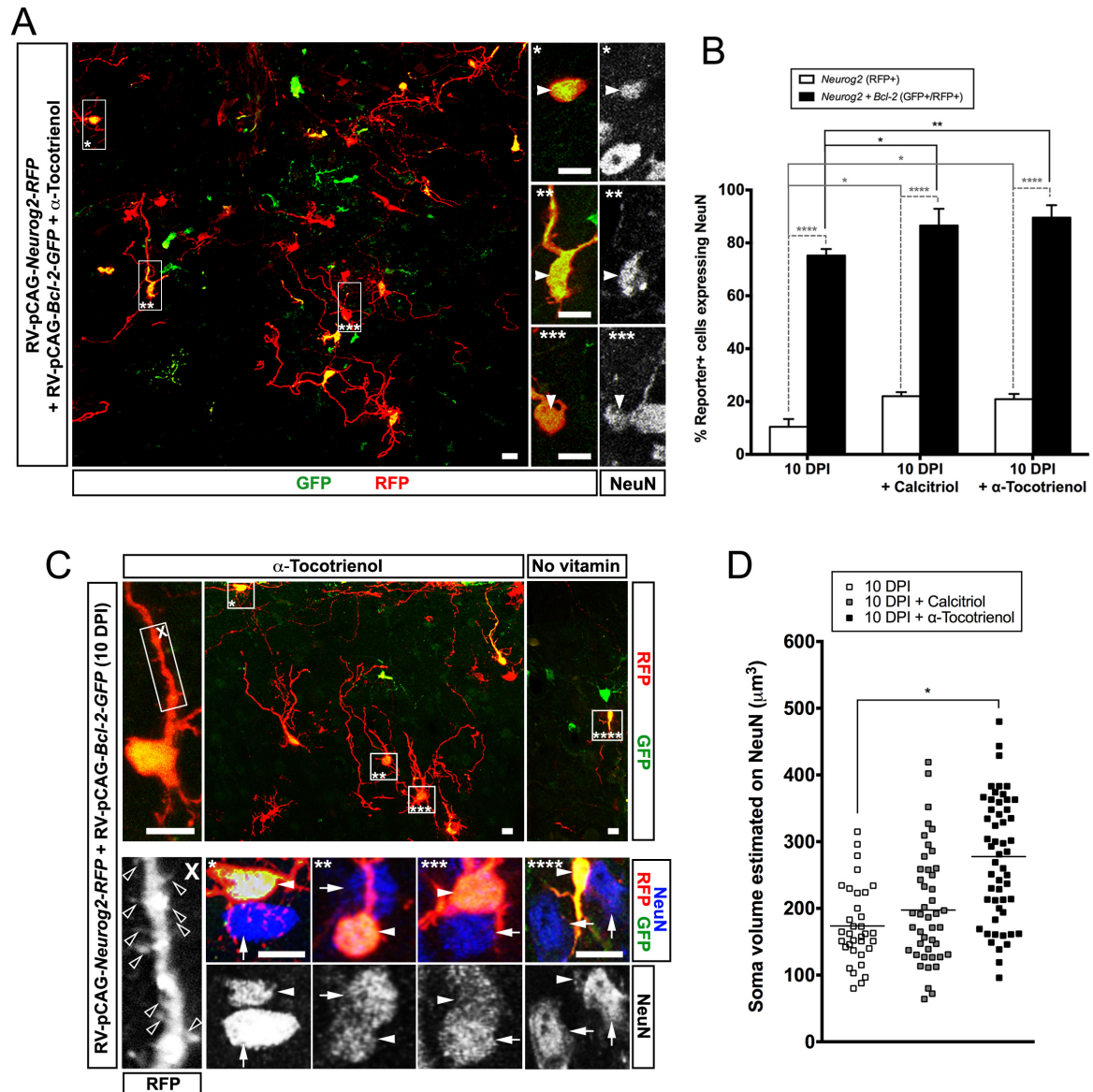


Figure 15. (A, C) Confocal micrographs of mouse sections with retroviral injection of *Neurog2/Bcl-2* after α -Tocotrienol treatment (see Material and Methods), analysed by immunohistochemistry at 10 DPI. Single optical sections are shown at higher magnification in the insets. (A) Most co-transduced cells are immunopositive for NeuN (arrowheads) at 10 DPI after α -Tocotrienol treatment. (B) Quantification of single- (RFP+) and co-transduced cells (RFP+/GFP+) immunopositive for NeuN at 10 DPI, with Calcitriol, α -Tocotrienol or no treatment. Note that Calcitriol and α -Tocotrienol have similar effect on the percentage of reprogrammed neurons, both single- and co-transduced. (C) As a result of α -Tocotrienol treatment, co-transduced cells (arrowheads) have spine-like structures already at 10 DPI (left panel, empty arrowheads) and a soma size more comparable to the soma size of neighbouring neurons (arrows). Reprogrammed neurons obtained without any vitamin treatment are considerably smaller than neighbouring neurons and are shown as comparison (right panel). (D) Quantification of the soma volume of co-transduced cells in all conditions described at 10 DPI, based on NeuN immunohistochemistry. Note that only α -Tocotrienol significantly increases the soma size of reprogrammed neurons.

Scale bars: 10 μ m. Error bars represent SD. Two-way ANOVA with Tukey's post-hoc test in B (n=3 per condition, except n=4 for α -Tocotrienol condition); One-way ANOVA with Tukey's post-hoc test in D (n=3 per condition, except n=4 for α -Tocotrienol condition), *p<0.05, **p<0.01, ***p<0.0001

2.10. Reprogrammed neurons express deep layer markers

The administration of α -Tocotrienol after co-infection with *Neurog2/Bcl-2* resulted in the best efficiency of conversion and neuronal maturation already at 10 DPI. For this reason, we used such paradigm to further investigate the identity of reprogrammed neurons, mainly focusing in the expression of layer-specific markers.

In particular, immunostainings for Ctip2, which labels layer 5 subcortical neurons (Arlotta et al., 2005; Molyneaux et al., 2007), resulted in 80% of all co-transduced cells being immunopositive regardless of their layer of localisation (Figure 16A, E). Most of the remainder neurons (20%) were immunopositive for the layer 6 marker FoxP2 (Figure 16B, E; Ferland et al., 2003; Molyneaux et al., 2007), although the intensity of the signal was considerably lower than in endogenous neurons. Accordingly, no reprogrammed neuron was found immunopositive for upper layer markers, such as Cux1 (Figure 16C, E; Molyneaux et al., 2007; Nieto et al., 2004) or Satb2 (Figure 16C, E; Britanova et al., 2008).

Finally, I immunostained for the neurotransmitter GABA (Figure 16D) and found that no reprogrammed cell expressed detectable levels of this protein, while some transduced non-converted astroglia were weakly immunopositive, as expected from the role of astrocytes in GABA production (Robel and Sontheimer, 2015).

All in all, we concluded that neurons obtained after reprogramming with *Neurog2/Bcl-2* and administration of α -Tocotrienol at 10 DPI have a deep layer identity, further specifying their phenotype as excitatory pyramidal neurons.

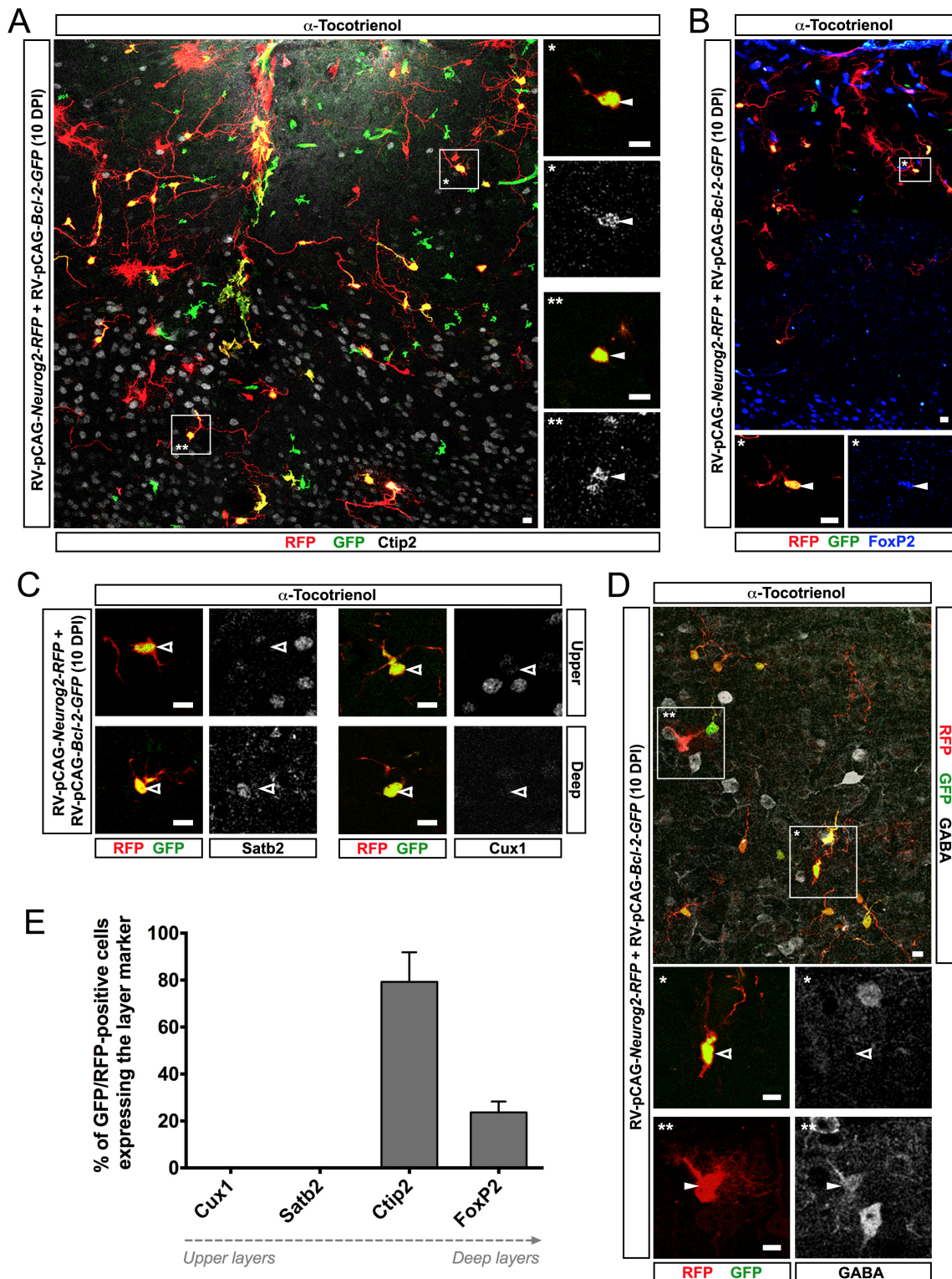


Figure 16. (A-D) Confocal micrographs of mouse sections with retroviral injection of *Neurog2/Bcl-2* after α -Tocotrienol treatment, analysed by immunohistochemistry at 10 DPI. When present, insets show single optical sections at high magnification. (A, B) Most co-transduced cells are Ctip2-immunopositive (A, arrowheads) regardless of the layer they are located into, while only occasionally they are immunopositive for FoxP2 (B, arrowheads). (C) Regardless of the upper (first panel row) or deep (second panel row) layer location, co-transduced cells were never found immunopositive for Satb2 or Cux1 (empty arrowheads). (D) Reprogrammed co-transduced cells are immunonegative for GABA (empty arrowhead), while RFP+ single-transduced cells with astroglial morphology are weakly immunopositive (arrowhead). (E) Quantifications of co-transduced cells immunopositive for the markers in A, B and C show that reprogrammed neurons have a deep layer identity.

Scale bars: 10 μ m. Error bars represent SD. In E, n=2 for Cux1 and Satb2; n=3 for Ctip2 and FoxP2.

2.11. α -Tocotrienol and Calcitriol co-administration might further improve efficiency of conversion and neuronal maturation after *Neurog2* over-expression

Calcitriol and α -Tocotrienol showed similar but at the same time different effects in the conversion of reactive glia cells into neurons. The extent to which the overall neuronal yield was improved was highly comparable between the two approaches, with regards to both *Neurog2* single-transduced cells and *Neurog2/Bcl-2* co-transduced cells. However, while Calcitriol seemed to mostly enhance the efficiency of conversion, α -Tocotrienol potentially accelerated the acquisition of mature neuronal features, such as a bigger soma size, thick basal processes and spine-like structures.

As these observations seem to highlight partially different mechanisms of action, we next asked whether the simultaneous administration of Calcitriol and α -Tocotrienol at 2 DPI could exert a synergistic effect both in final neuronal yield and in maturation of cells co-transduced with *Neurog2-IRES-RFP* and *Bcl-2-IRES-GFP*. Preliminary results at 10 DPI indicate a high rate of NeuN-immunopositive neurons among the co-transduced population (Figure 17A), as predicted after the experiments with Calcitriol or α -Tocotrienol administration at the same time-point. Furthermore, the neurites of such converted cells showed a high complexity of branchings, development of spine-like structures (Figure 17B) and a soma size bigger than observed in *Neurog2/Bcl-2* co-infection experiments in the absence of any vitamin. However, the extent to which both conversion rate and acquisition of these mature neuronal features took place still remains to be quantitatively evaluated.

All in all, these preliminary data suggest that the combination of both vitamins does not seem to interfere with the proportion of cells undergoing efficient neuronal reprogramming after *Neurog2/Bcl-2* over-expression, as well as the achievement of a mature neuronal morphology. Future experiments might aim at elucidating the effects of Calcitriol and α -Tocotrienol co-administration on mice infected by *Neurog2*-expressing retrovirus, to test whether this simultaneous treatment can partially mimic the role of Bcl-2.

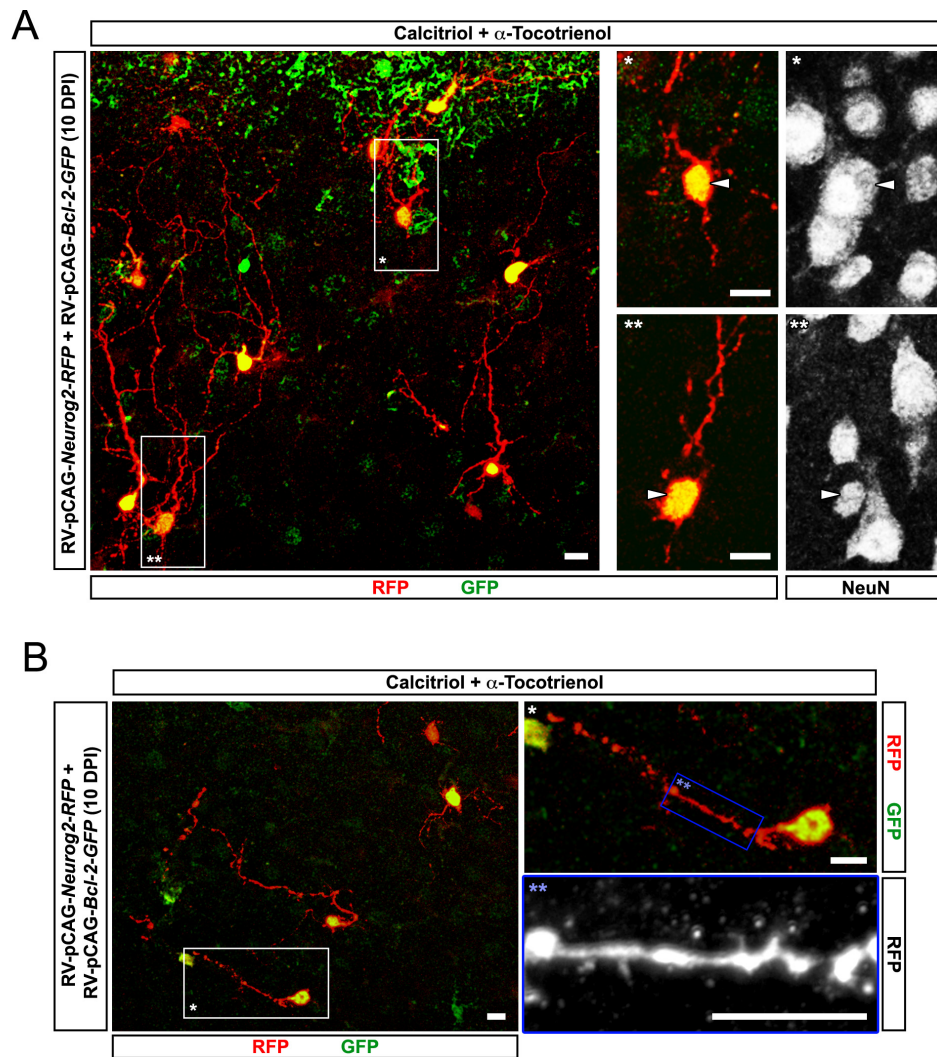


Figure 17. Confocal micrographs of mouse sections with retroviral injection of *Neurog2/Bcl-2* after α -Tocotrienol and Calcitriol co-treatment, analysed by immunohistochemistry at 10 DPI. Single optical sections are shown at higher magnification in the insets. Co-transduced cells are often NeuN-immunopositive (A, arrowheads) and occasionally display mature features, e.g. spine-like structures (B).

Scale bars: 10 μ m.

2.12. Role of epigenetics in forced and endogenous neurogenesis: the starting point

Polycomb Repressive Complexes (PRCs) have been widely implicated in maintenance of stemness as well as in differentiation into diverse lineages (Di Croce and Helin, 2013), by inhibiting gene expression through specific histone modifications. In particular, PRC1 determines the mono-ubiquitination of Lysine 119 residue on histone 2A (H2AK119Ub) through its catalytic domain Ring1B/Rnf2. Although PRC1 comes in many different compositions, Ring1B protein was always found in all variants described so far (reviewed in Gil and O’Loghlen, 2014).

With regards to the nervous system, Ring1B was shown to determine the onset of the astrogenic phase during mouse corticogenesis by repressing key proneural genes like *Neurogenin1* (*Neurog1*; Hirabayashi et al., 2009). Accordingly, *Ring1B* knockout prolonged the length of the neurogenic phase and resulted in higher numbers of glutamatergic neurons being generated in the embryonic cortex. However, little is known about the role of Ring1B in adult neurogenesis as well as in the generation of GABAergic neurons.

As this gene was described to act as a block in embryonic neuronal corticogenesis, we speculated that a similar mechanism of repression could take place also in differentiation towards GABAergic neurons *in vitro* as well as *in vivo*. Therefore, aiming at the use of Ring1B in direct neuronal reprogramming, in this project we investigated the impact of its knockdown in *in vitro* paradigms of forced neuronal differentiation and further move to *in vivo* genetic deletion approaches to tackle its role in adult neurogenesis.

2.13. Ring1B knockdown in neural stem cells impairs forced neuronal differentiation triggered by *Dlx2*

In order to study the role of Ring1B in loss-of-function experiments, miRNAs against its sequence were previously designed and tested by Dr. Sergio Gascón. HEK293 cells were co-transfected with a construct encoding for Ring1B together with one encoding for scramble miRNA or Ring1B miRNA and a total of 3 different Ring1B miRNAs were tested. The subsequent Western Blot analysis confirmed a reduction in Ring1B protein levels when either one of Ring1B miRNA constructs was provided. After cloning the 3 miRNA sequences in chain, a culture of postnatal day 5 (P5) astrocytes was transfected with this construct and the effects on

Results

Ring1B expression were further confirmed by immunohistochemistry. Therefore, we concluded that miRNA-mediated silencing is effectively leading to a sensitive reduction in Ring1B protein levels, as estimated by Western Blot and immunohistochemistry.

Next, to address the role of Ring1B in forced neuronal differentiation *in vitro* we used E14 mouse primary NSCs, which we expanded in culture in a medium containing epidermal growth factor (EGF) and fibroblast growth factor 2 (FGF-2) for a maximum of 13 passages (P13; Figure 18A). In these conditions, upon withdrawal of the growth factors NSCs preferentially differentiate into glia. Therefore, we decided to force the differentiation into neurons by transfecting the cells with a construct expressing a neurogenic determinant together with the red fluorescent protein (*RFP*).

Being a key gene for the generation of GABAergic neurons in embryonic and adult neurogenesis (Brill et al., 2008; Petryniak et al., 2007) and a moderately efficient determinant in direct neuronal reprogramming of postnatal astrocytes (Heinrich et al., 2010), I chose *Dlx2* for our paradigm (*Dlx2*-IRES-*RFP*) and I co-transfected it with a construct expressing either scrambled miRNA or a combination of 3 different Ring1B miRNA. Contrary to our hypothesis, immunostaining for β -III-tubulin at 6 days post-transfection (DPT) revealed a reduction in the percentage of RFP-immunopositive neurons by $\frac{1}{3}$ when Ring1B was knocked down (Figure 18B, C).

To test whether this effect is general for neural stem cells or rather restricted to embryo-derived ones, we performed a pilot experiment co-transfecting *Dlx2* with scrambled miRNA or miRNA against Ring1B in primary cultures of adult neural stem cells obtained from the sub-ependymal zone (SEZ; Figure 18D). Also in this case, the final percentage of transfected cells that turned into β -III-tubulin-immunopositive neurons was lower when Ring1B was knocked down, in agreement with the observation in NSCs (Figure 18E).

Therefore, we concluded that Ring1B does not inhibit neurogenesis of GABAergic neurons, contrary to what described at embryonic stages for glutamatergic neurons.

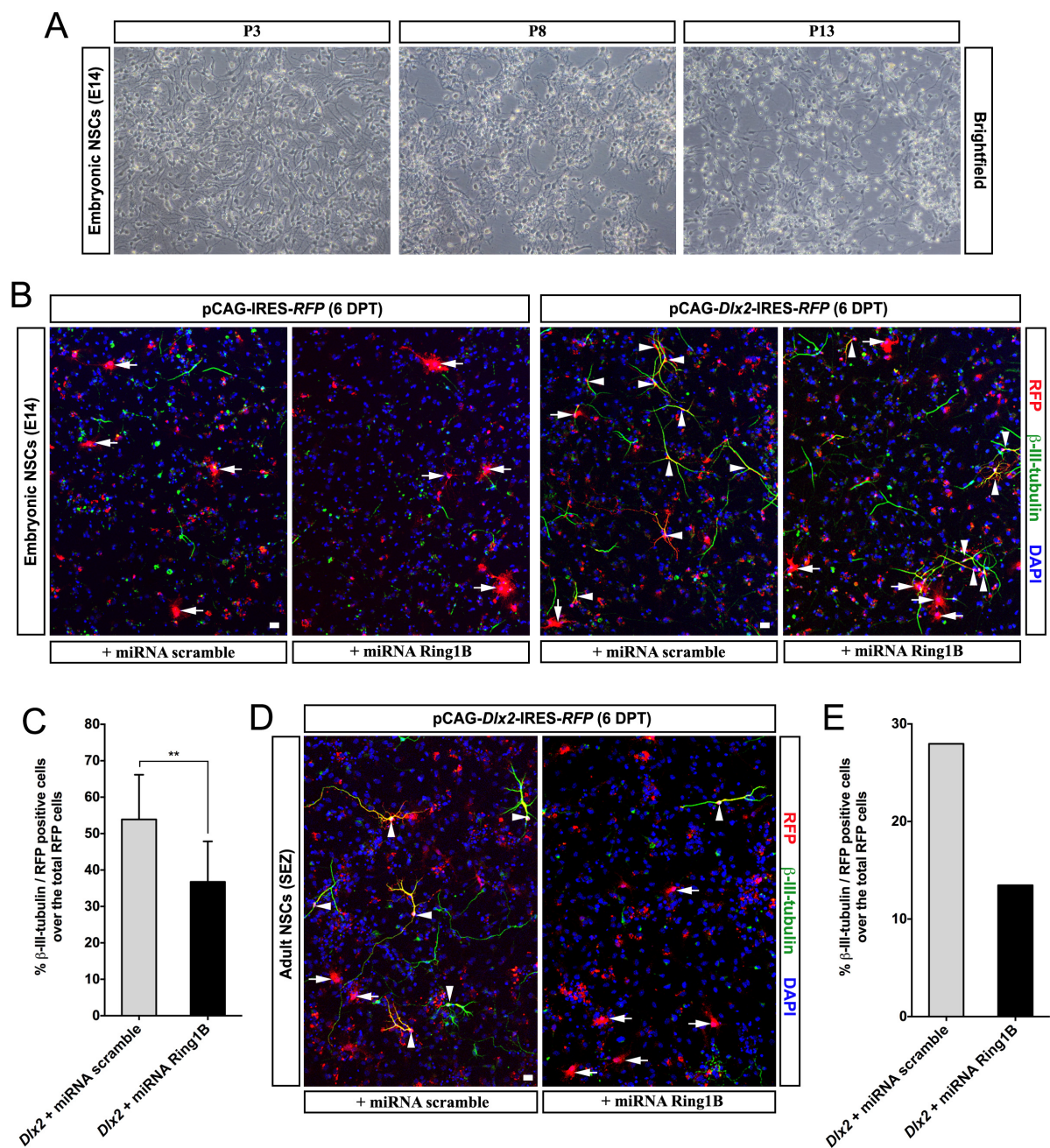


Figure 18. (A) Brightfield pictures of E14 NSCs primary cultures at different passages (P), maintained in Expansion Medium (see Material and Methods). (B) E14 NSCs transfected with a plasmid encoding for miRNA scramble or miRNA Ring1B (left panel) at 6 DPT do not differentiate into β-III-tubulin-immunopositive neurons when RFP is co-transfected (arrows). Transfection of a plasmid encoding for *Dlx2*-IRES-RFP (right panels) results in higher-rate neuronal differentiation (arrowheads) at 6 DPT, but to a lesser extent when miRNA Ring1B is co-transfected. (C) Quantifications of NSCs at different passages (6 DPT) transfected with *Dlx2* (RFP+) together with miRNA scramble or miRNA Ring1B indicate a lower percentage of β-III-tubulin-immunopositive neurons when Ring1B is knocked down. Results from cultures at different passages were compared between each other and then pooled together for this analysis. (D) Adult NSCs from the subependymal zone (SEZ) transfected with *Dlx2* (RFP+) and miRNA scramble differentiate into β-III-tubulin-immunopositive neurons (arrowheads) to a larger extent than cells co-transfected with miRNA Ring1B, which turn mostly glial (arrows). (E) Quantifications of the experiment in D, showing that Ring1B knockdown in adult NSCs results in a lower proportion of RFP+/β-III-tubulin+ neurons at 6 DPT.

Scale bars: 20 μm. Error bars represent SD. Ratio-paired t test in C (n=4 per condition); n=1 per condition in E.

2.14. Ring1B protein is expressed in a generalised manner in the adult brain

As the experiments in embryonic and adult neural stem cells *in vitro* suggested that Ring1B rather favours the generation of neurons, we focused on how adult neurogenesis is influenced by this gene. In fact, the two main neurogenic niches in the adult mammalian brain, namely the SEZ of the lateral wall of the lateral ventricle and sub-granular zone (SGZ) of the hippocampus, produce mostly GABAergic granule neurons.

To check the expression pattern of the protein in the adult brain, we immunostained wild type sections for Ring1B, as well as for general glial and neuronal markers (Figure 19A). A first look at the overall brain showed that the vast majority of DAPI+ nuclei co-localised with Ring1B signal. Indeed, among the cells immunopositive for this protein we found GFAP+ astroglial cells, NG2+ oligodendrocyte precursor cells (OPCs), Doublecortin+ (DCX) neuroblasts and NeuN+ neurons, while Iba1+ microglial cells seem to express lower levels. Thus, this analysis indicates that a broad range of different cell types expresses Ring1B protein in the mouse brain at adult stages.

2.15. Ring1B protein is not detected 7 days after inducing the knockout of the gene

Next, we asked what effects the deletion of *Ring1B* gene exerted on adult neural stem cells, focusing on the SEZ - rostral migratory stream (RMS) - olfactory bulb (OB) system. To address this point, we generated an inducible line crossing Ring1B-floxed mice (Ring1B^{F/F}, courtesy of Miguel Vidal; Calés et al., 2008) with Glast^{CreERT2}/CAG-GFP mice (Mori et al., 2006b; Nakamura et al., 2006). The administration of Tamoxifen in the resulting mouse line (Ring1B^{F/F}/Glast^{CreERT2}/CAG-GFP) determines the excision of Ring1B gene and GFP activation specifically in adult neural stem cells and astrocytes (Ring1B^{Δ/Δ}/Glast^{CreERT2}/GFP). Likewise, as control we used Ring1B^{+/+}/Glast^{CreERT2}/GFP mice, which we induced as described for *Ring1B* knockout mice.

To determine the dynamics of Ring1B protein turnover, we analysed the SEZ of mice sacrificed at 4, 5 and 7 days post-induction (DPI; Figure 19B). Immunostainings for GFP and Ring1B revealed that at 4 DPI nearly half of the recombined cells in the SEZ already lost Ring1B signal (46%, Figure 19C) and the proportion dropped to 21% at 5 DPI. Accordingly, at 7 DPI no GFP+ cell in the SEZ had a detectable Ring1B signal. Therefore, we concluded that the turnover of this protein takes nearly one week after inducing the gene deletion.

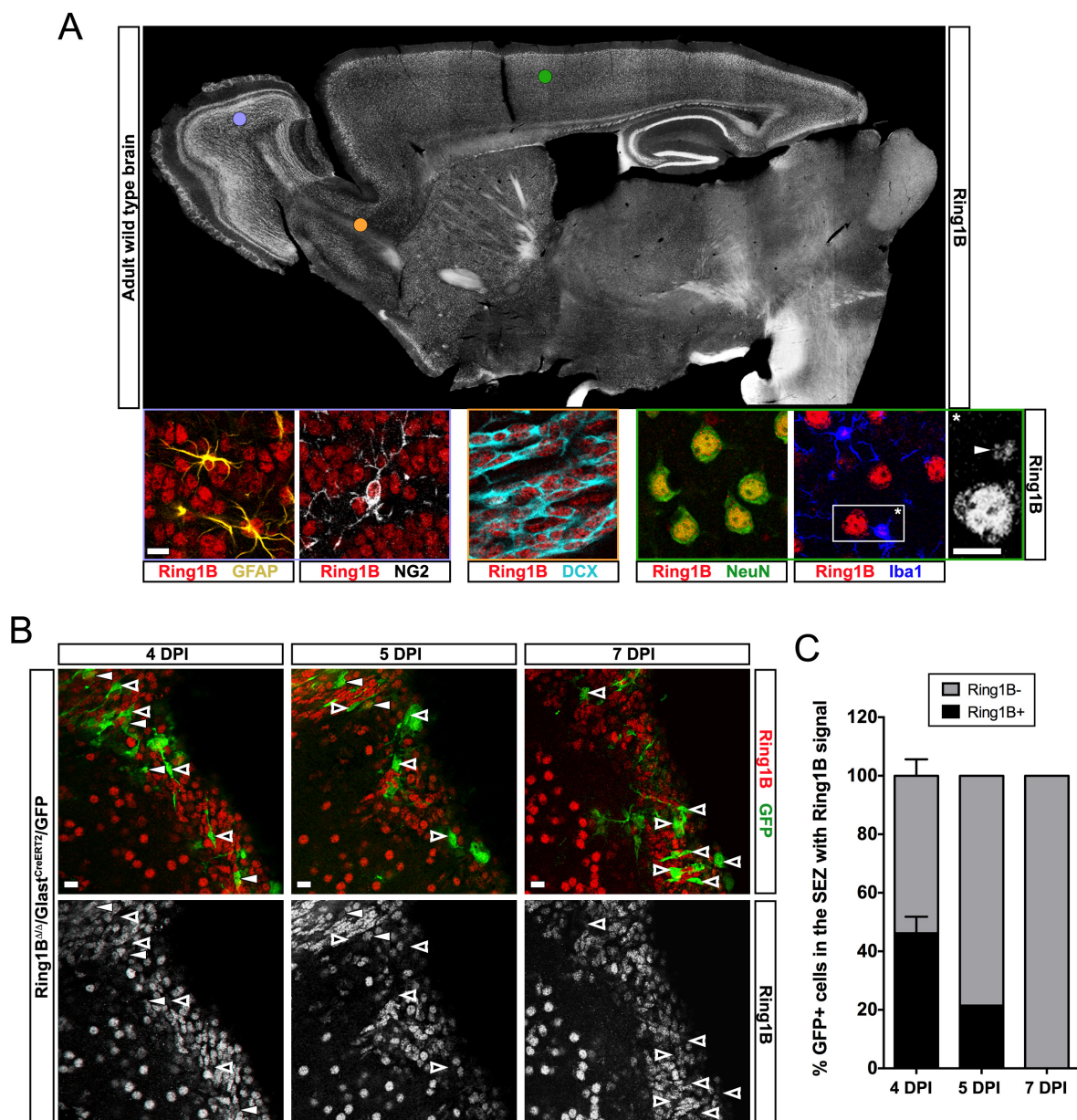


Figure 19. (A, B) Micrographs of mouse brain sagittal sections analysed by immunohistochemistry. Coloured dots show position of insets with high magnification in single optical sections of the area in the boxes. (A) Epifluorescent micrograph with overview of a wild type brain immunostained for Ring1B showing that astroglial cells (GFAP), oligodendrocyte precursors (NG2), neuroblasts (DCX) and neurons (NeuN) express high levels of Ring1B, while microglia (Iba1) seems to express at lower levels. The confocal micrographs of the different cell types is taken from different regions of the mouse brains, i.e. the olfactory bulb (violet boxes), the rostral migratory stream (RMS, orange box) and the cortex (green boxes). (B) Confocal micrographs with immunostainings for Ring1B and GFP in the SEZ of Ring1B^{Δ/Δ} mice at 4, 5 and 7 days post Tamoxifen induction (DPI; see Material and Methods). Note that over time the proportion of Ring1B-/GFP+ cells (empty arrowheads) increases at the expense of Ring1B+/GFP+ cells (arrowheads), as depicted in the histogram in C.

Scale bars: 10 μ m. Error bars represent SD. In C, n=3 for 4 and 7 DPI, n=2 for 5 DPI.

2.16. *Ring1B* knockout does not affect cell identity or proliferation in the SEZ and the RMS

Ring1B excision and *GFP* expression in NSCs is inherited to their progeny, namely the TAPs and the neuroblasts. As neuroblasts need 5-7 days to cover the 5mm-long distance from the SEZ to the core of the olfactory bulb and an additional month to mature into granule neurons (Whitman and Greer, 2009), we decided to analyse the effects of *Ring1B* knockout at 45 DPI.

A first inspection of the sections did not uncover any striking phenotype in the SEZ *Ring1B*-deficient mice, with many *GFP*⁺ neuroblasts leaving this area in the direction of the OB and forming a well-defined RMS. As Polycomb complexes have been also implicated in maintenance of stemness and proliferation, we started our in-depth investigation by immunostaining for Ki67, which labels all cell cycle stages except G₀ (Figure 11A). Compared to *Ring1B*^{+/+} mice, *Ring1B*^{Δ/Δ} mice did not show any significant difference in the proportion of *GFP*⁺/Ki67⁺ cells, neither in the SEZ nor in the elbow of the RMS (30-35% in both areas, Figure 11B).

Therefore, these data suggest that adult neural stem cells and migrating neuroblasts do not exhibit any major defect after *Ring1B* knockout, neither in the SEZ nor in the elbow of the RMS.

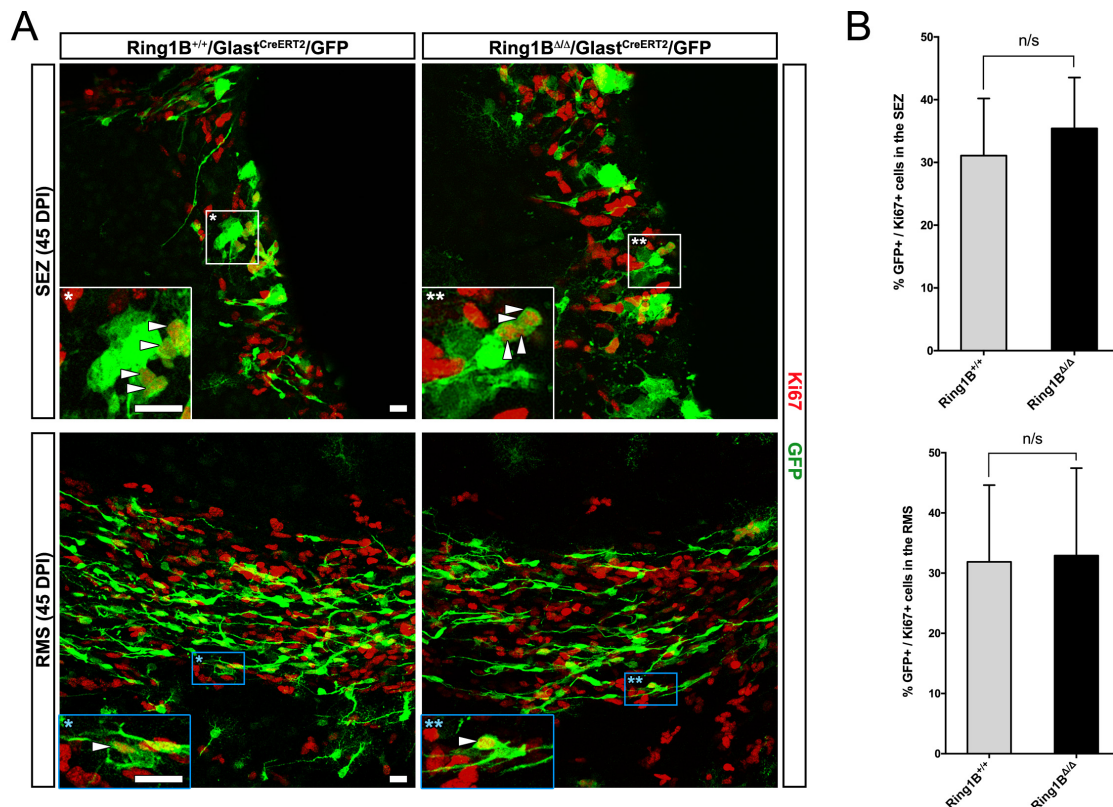


Figure 20 (previous page). (A) Confocal micrographs of mouse brain sagittal sections (Ring1B $\Delta\Delta$ and Ring1B $^{+/+}$) showing the SEZ and the RMS after immunohistochemistry for GFP and Ki67 at 45 DPI. Insets show high magnification of the area in the boxes (white for the SEZ, blue for the RMS), with arrowheads indicating GFP+/Ki67+ immunopositive cells. (B) Quantifications of the proportion of GFP+/Ki67+ cells in the SEZ (upper histogram) and in the RMS (lower histogram) indicate no difference in proliferation between Ring1B $\Delta\Delta$ and Ring1B $^{+/+}$ mice.

Scale bars: 10 μ m. Error bars represent SD. Unpaired t test in B (n=3 for Ring1B $^{+/+}$, n=4 for Ring1B $\Delta\Delta$), n/s not significant.

2.17. *Ring1B* knockout leads to an increase in the proportion of superficial granule cells

Next we focused on the olfactory bulbs, which represent the final stage of migration and differentiation of the neuroblasts leaving the SEZ. Interestingly, already at first glance Ring1B-deficient GFP+ cells with a neuronal morphology were rarely observed in the deep granule cell layer (GCL) of the OB (Figure 21A), although it was reported that the main cell type generated during adult neurogenesis is the deep granule neuron (Sakamoto et al., 2014). Indeed, sagittal and coronal sections showed that the strong reduction of neural GFP+ cells in the deep GCL was not regionally restricted but rather took place in all areas of the OB. To better evaluate the extent of this phenotype, I quantified the percentage of GFP+ cells (morphologically distinguished in neuronal or astroglial; Figure 21B) that were found in the deep and in the superficial part of the GCL in both Ring1B $^{+/+}$ and Ring1B $\Delta\Delta$ mice. The two areas of the GCL were defined by arbitrarily dividing the region comprised between the superficial edge of the GCL and the RMS into two equal bins. While in my Ring1B $^{+/+}$ mice neural GFP+ cells distributed equally between the defined deep and superficial GCL bins, Ring1B $\Delta\Delta$ mice had a significantly higher number distributed in the superficial GCL bin (Figure 21C). Such difference was not observed in the astroglial GFP+ population, which in both conditions resulted similarly distributed within the two GCL areas.

Interestingly, although the relative density of all GFP+ cells differed between the superficial and deep GCL of both mouse lines, the total density of GFP+ cells in the whole GCL did not significantly vary (Figure 21C). To exclude the possibility of a bias introduced by a different recombination rate of the mice used for the evaluation, I quantified the density of GFP+ astroglial cells in the cerebral cortex, which are not affected by *Ring1B* deletion (Figure 21D). As expected, we found no significant difference between Ring1B $^{+/+}$ and Ring1B $\Delta\Delta$ mice, indicating a comparable recombination rate in the mice analysed.

Therefore, these data suggest that the reduced number of recombined cells in the deep GCL of Ring1B $\Delta\Delta$ mice might be the result of a re-specification of deep granule neurons into superficial granule neurons or a re-localisation of the formers into the superficial GCL, rather than selective cell death of recombined deep granule neurons.

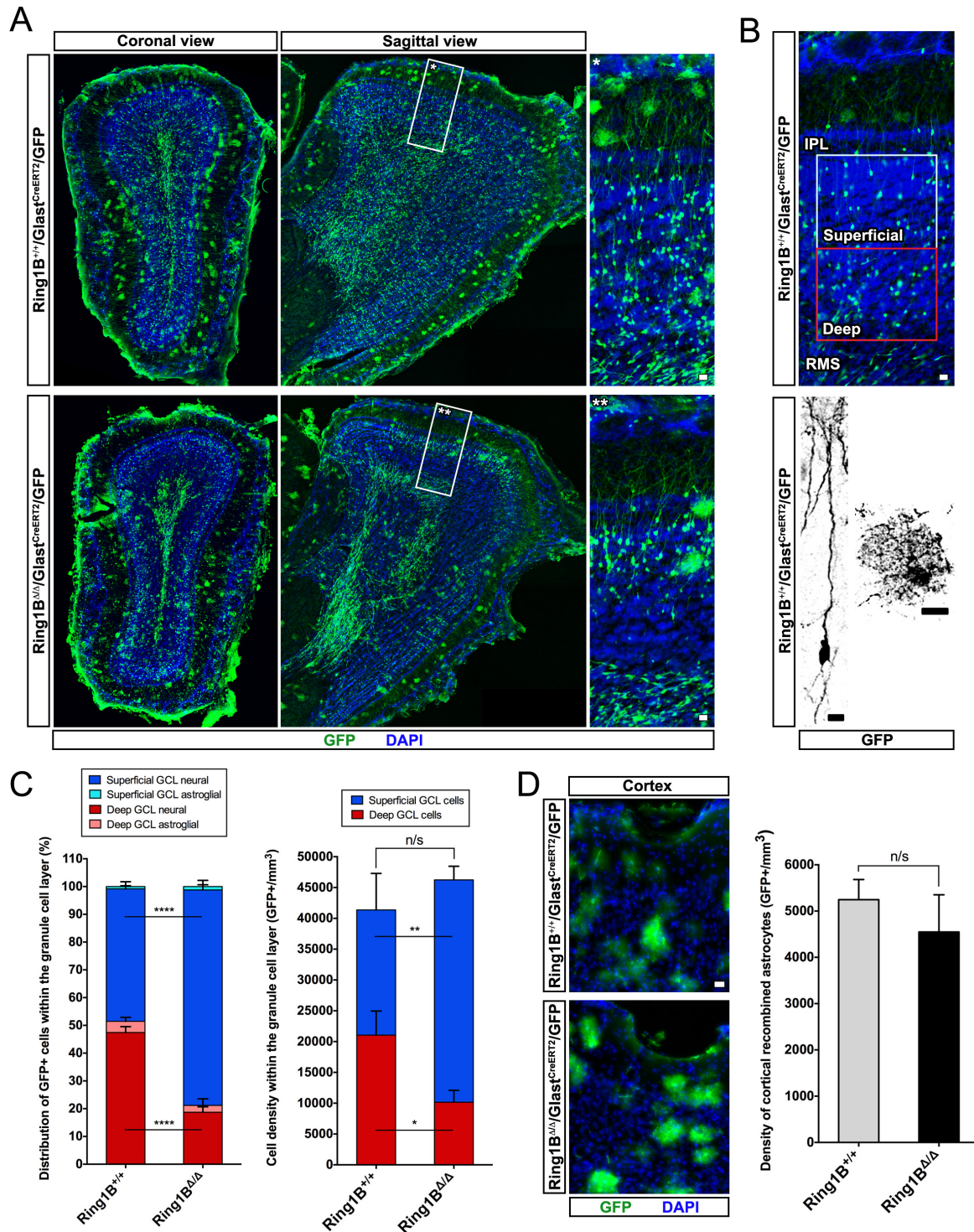


Figure 21. (A) Confocal micrographs of mouse coronal and sagittal sections (Ring1B^{+/+} and Ring1B^{Δ/Δ}) displaying the olfactory bulbs after immunostaining with GFP, with insets showing higher magnification of the areas in the boxes. (B) Confocal micrograph of a Ring1B^{+/+} olfactory bulb with the areas used for the quantifications in C (upper panel). Two equal bins (blue and red boxes) of known size are defined to cover the granule cell layer (GCL) between the RMS and the inner plexiform layer (IPL). GFP-immunopositive cells are classified as neuronal (lower panel, left cell) or astroglial (lower panel, right cell) according to their morphology. (C) Quantification of GFP-immunopositive cells in the GCL of Ring1B^{+/+} and Ring1B^{Δ/Δ}, as indicated in B. Both the percentage (left histogram) and the density (right histogram) of GFP+ cells in the superficial GCL are significantly increased in Ring1B^{Δ/Δ} mice. (D) Epifluorescent micrographs of the cortex of Ring1B^{+/+} and Ring1B^{Δ/Δ} mice, with quantification of the density of GFP-immunopositive astroglial cells. Note that the density of these cells in the cortex does not significantly change and is used to indicate a similar recombination rate between the two mouse lines.

Scale bars: 10 μ m. Error bars represent SD. Two-way ANOVA with Bonferroni post-hoc test in C (n=3 per condition). Unpaired t test in D (n=3 per condition), n/s not significant.

2.18. *Ring1B*-deficient superficial granule neurons do not change OB subtype identity

In the superficial granule cell layer two main neuronal populations can be found, which are distinguished based on the expression of the protein Calretinin (CalR; Lim and Alvarez-Buylla, 2014). Such populations have also a different spatial origin, as CalR⁺ granule neurons are preferentially generated by NSCs located in the SEZ of the medial wall, while CalR⁻ superficial granule neurons originate from NSCs in the SEZ of the dorso-lateral wall (Obernier et al., 2014). To check whether the increased proportion of GFP⁺ neurons in the superficial GCL is caused by the specific enrichment in CalR⁺ population, we performed immunohistochemical analysis of this protein in sections from Ring1B^{+/+} and Ring1B^{Δ/Δ} mouse lines at 45 DPI (Figure 22A). The quantification of GFP⁺/CalR⁺ cells in the GCL showed no difference between the two conditions (7% in Ring1B^{+/+}, 8% in Ring1B^{Δ/Δ}; Figure 22B), suggesting that the higher number of recombined neurons in the superficial GCL is not caused by a selective enrichment of the CalR⁺ population in this region.

Next, we asked whether the additional GFP⁺ neurons in the superficial GCL expressed markers usually found in other OB layers. For this reason, we immunostained the sections for Calbindin (CalB; periglomerular cells), Tyrosine Hydroxylase (TH; dopaminergic periglomerular cells) and Parvalbumin (neurons in the external plexiform layer) and checked in the GCL for any abnormal expression of these markers in recombined cells (Batista-Brito et al., 2008). Similarly to Ring1B^{+/+} mice, virtually no GFP⁺ cell in the superficial GCL of Ring1B^{Δ/Δ} was found immunopositive for any of these markers (Figure 22C, D).

Thus, we concluded that Ring1B-deficient neurons in the superficial GCL do not belong to the CalR population and do not express markers of neurons usually found in other layers within the olfactory bulbs.

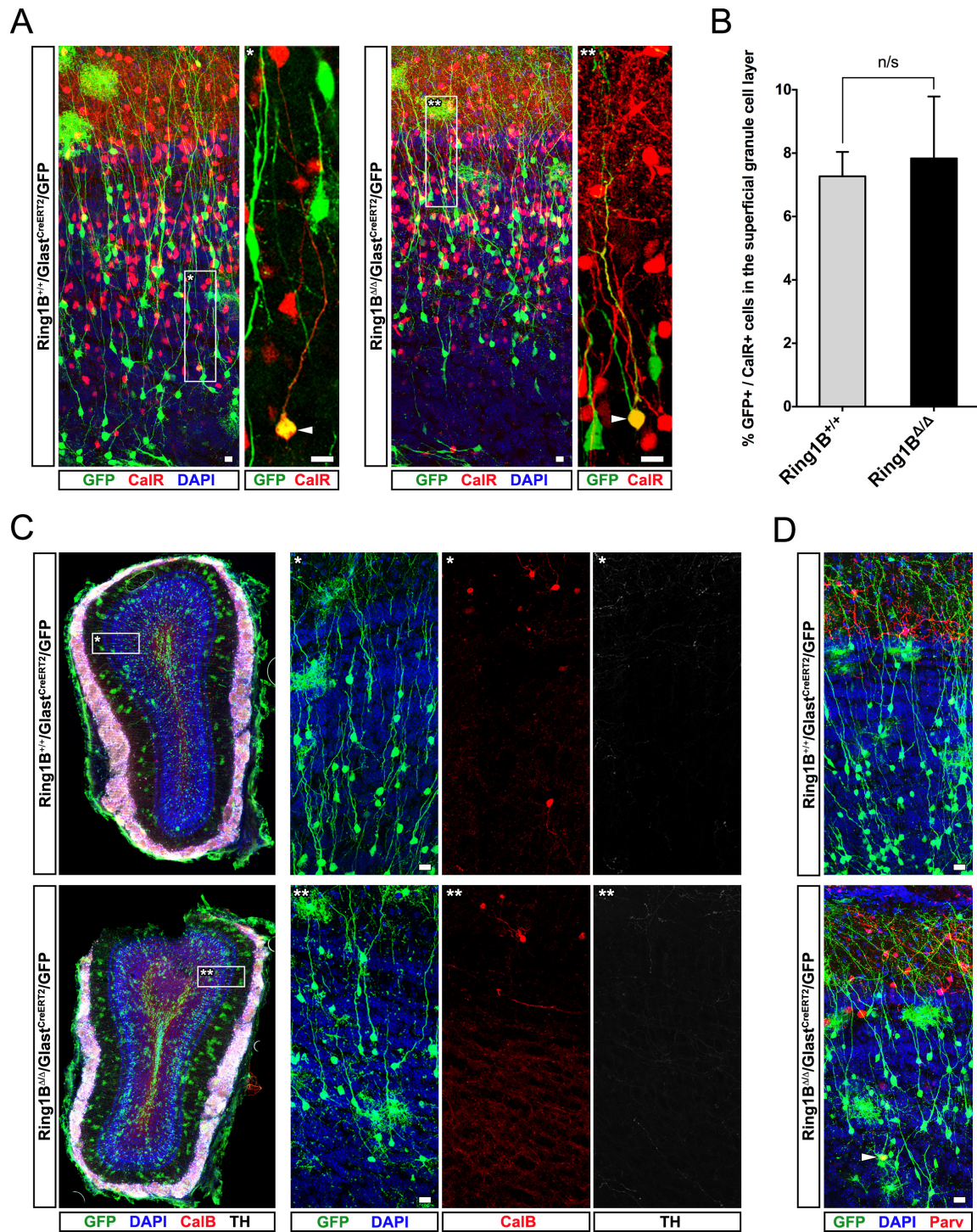


Figure 22. (A) Confocal micrographs of olfactory bulb sagittal sections (Ring1B^{+/+} and Ring1B^{Δ/Δ}) at 45 DPI after immunostaining with GFP and Calretinin (CalR), with insets showing higher magnification of the areas in the boxes. Note that in both conditions only a few GFP-immunopositive cells are also CalR-immunopositive (arrowheads). (B) Quantifications of the experiment in A. The percentage of GFP+/CalR+ cells in the GCL does not significantly vary between Ring1B^{+/+} and Ring1B^{Δ/Δ} mice. (C) Confocal micrographs of olfactory bulbs coronal sections (Ring1B^{+/+} and Ring1B^{Δ/Δ}) at 45 DPI after immunostaining with GFP and Calbindin (CalB) and tyrosine hydroxylase (TH), with insets showing higher magnification of the areas in the boxes. Note that no ectopic GFP+/CalB+ or GFP+/TH+ cell can be observed in the GCL of both mouse lines. (D) Confocal micrographs of olfactory bulbs sagittal sections (Ring1B^{+/+} and Ring1B^{Δ/Δ}) at 45 DPI after immunostaining with GFP and Parvalbumin (Parv). Only in sporadic cases GFP+/Parv+ (arrowhead) can be observed in the GCL of Ring1B^{+/+} and Ring1B^{Δ/Δ} mice.

Scale bars: 10 μ m. Error bars represent SD. Unpaired t test in B (n=3 for Ring1B^{+/+}, n=4 for Ring1B^{Δ/Δ}), n/s not significant.

2.19. Initial phenotype characterisation in the olfactory bulbs

As previously mentioned, the density of recombined neurons in the GCL of Ring1B^{Δ/Δ} mice was comparable to the density of neurons in the GCL of Ring1B^{+/+} mice (Figure 21C). The CalR-immunonegative neurons normally found in this area are so far poorly characterised molecularly and very heterogeneous in morphology (Merkle et al., 2014; Naritsuka et al., 2009). Indeed, the main differences concerning such cells are the micro-domains they originate from, the final position within the GCL and the overall morphology (Lim and Alvarez-Buylla, 2014).

To elucidate which neuronal subpopulations are mainly responsible for the specific enrichment in the superficial GCL of Ring1B^{Δ/Δ} mice, the cytoplasmic fluorescence of a reporter protein can be used for a semi-automatic dendrite tracing analysis. As the density of recombined cells within the superficial GCL does not allow a precise tracing due to the vast overlapping of the processes, 10 days after inducing the recombination (10 DPI) I injected a retrovirus encoding for RFP in the elbow of the RMS (Figure 23A). Immunohistochemistry performed 21 days after the injection (31 DPI) showed only few cells immunopositive for both GFP and RFP (Figure 23B), whose morphology could be efficiently traced using the sole RFP signal (Figure 23C).

Therefore, this approach allows tracing the dendritic arborisation of neurons and obtaining information like length and branching points. Additionally, the data collected can also be used to perform a 3D reconstruction and a Sholl analysis of the overall arborisation (Figure 23C, D), thus helping to determine the identity of the recombined neurons within the GCL.

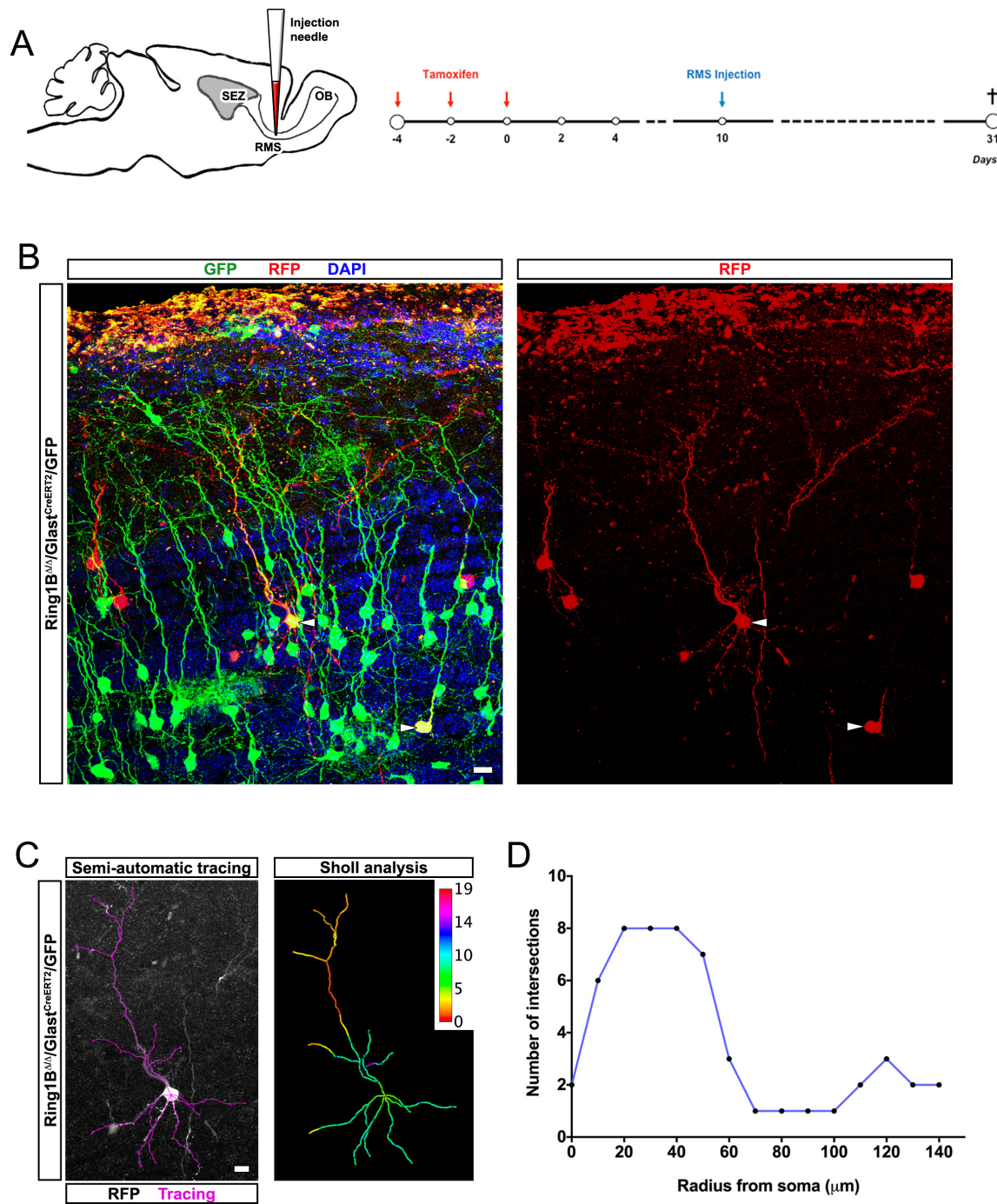


Figure 23. (A) Schematic of mouse sagittal brain (left) and timeline of the experiment. The site of the retroviral injection of the vector encoding for RFP is depicted. Note that the injection is performed 10 days after inducing recombination, to allow for Ring1B protein loss in GFP-immunopositive cells. (B) Confocal micrograph of olfactory bulb sagittal sections (Ring1B^{Δ/Δ}) at 31 DPI, showing two GFP/RFP-immunopositive cells (arrowheads). (C) Semi-automatic tracing of one of the two GFP/RFP-immunopositive cells indicated in B, with related colour-coded Sholl analysis indicating the number of intersections along the traced processes. (D) Histogram based on the Sholl analysis in C, representing the number of intersections as a function of the distance from the cell soma.

Scale bars: 10 μm.

2.20. *Ring1B* loss results in accumulation of neuroblasts in the core of the OB

Both sagittal and coronal views of the olfactory bulbs revealed a second difference in *Ring1B*^{Δ/Δ} mice, specifically in the RMS within the core. Indeed, the density of recombined cells in this area was significantly higher in mice lacking *Ring1B* (Figure 24A, B), despite the comparable recombination rate between mouse lines (Figure 21D) and the equal proliferation rate (Figure 20B) assessed in the elbow of the RMS.

As the olfactory bulbs constitute the final target of neuroblasts migration and determine the start of their terminal differentiation, we asked whether *Ring1B* loss could lead to a premature onset of the differentiation program. However, immunostainings for the neuronal marker NeuN excluded this possibility, as recombined cells in the OB core of both mouse lines were rarely found immunopositive (Figure 24A). Similarly, we next investigated the expression of glial markers in the same region. While few recombined cells in clusters were expressing the oligodendroglial marker NG2 in both *Ring1B*^{+/+} and *Ring1B*^{Δ/Δ} mice (Figure 24C), a higher percentage of cells immunopositive for the astroglial marker GFAP was observed, albeit comparable in the two genotypes (Figure 24C, D). As expected, the vast majority of recombined cells expressed DCX, well in agreement with the neuroblast nature of such cells (Figure 24C, D). To further corroborate this observation, we used non-induced *Ring1B*^{+/+} and *Ring1B*^{F/F} mice and triggered recombination by injecting a retrovirus encoding for CreGFP fusion protein in the SEZ (Figure 25A, B). Contrary to Tamoxifen induction, this approach ensured targeting the neuronal lineage and sparing the resident astrocytes, which could potentially influence the phenotype in the OB core. In line with the immunohistochemistry for glial markers, 28 days after retroviral delivery *Ring1B*^{Δ/Δ} neuroblasts in the olfactory bulbs were never found immunopositive for GFAP (Figure 25C), while *Ring1B*^{Δ/Δ} neurons tended to localise in the superficial GCL as previously observed (Figure 25B).

Therefore, we concluded that neuroblasts accumulate in the OB core of *Ring1B*^{Δ/Δ} mice possibly due to a migration defect, as they do not prematurely differentiate into neurons nor differentiate towards the glial lineage.

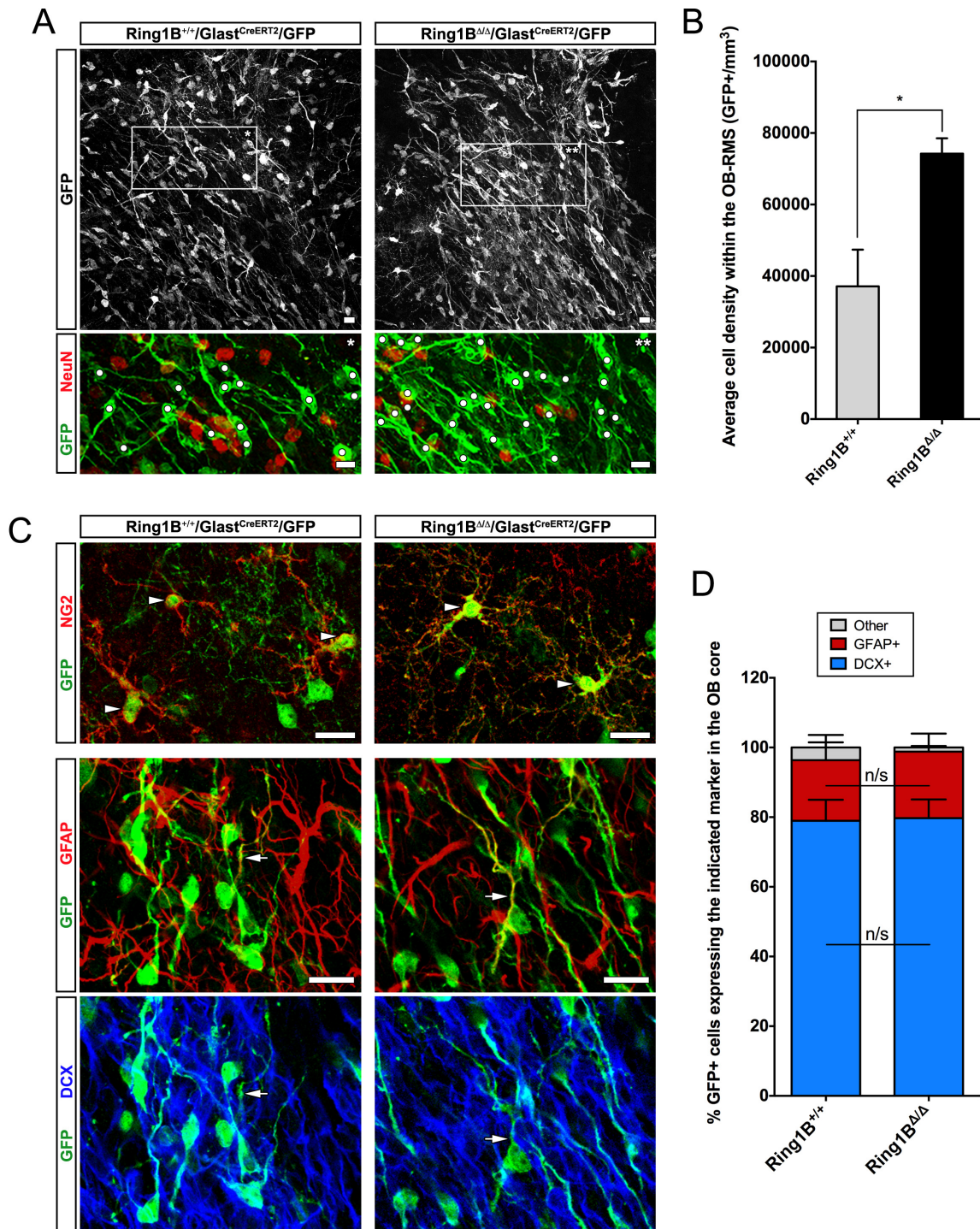


Figure 24. (A, C) Confocal micrographs of the core of the olfactory bulbs in sagittal sections at 45 DPI after immunostaining for GFP, NeuN, NG2, GFAP, NG2 or DCX, with insets showing higher magnification of the areas in the boxes. (A) GFP-immunopositive cells in the core of the olfactory bulbs do not co-express NeuN, but their density (B) is significantly higher in Ring1B^{ΔΔ} mice. White dots in A label each neuroblast. (C) Occasionally, small clusters of NG2/GFP-immunopositive cells (arrowheads, upper panel) can be observed in both conditions, although to a much lesser extent than GFAP/GFP-immunopositive cells (arrows, lower panel), which are accordingly immunonegative for DCX. (D) Quantifications of GFP+ cells immunopositive for GFAP or DCX. Note that there is no difference in the proportion of these populations between Ring1B^{+/+} and Ring1B^{ΔΔ} mice.

Scale bars: 10 μ m. Error bars represent SD. Unpaired t test in B (n=3 per condition), two-way ANOVA with Bonferroni post-hoc test in D (n=3 per condition), n/s not significant, *p<0.05

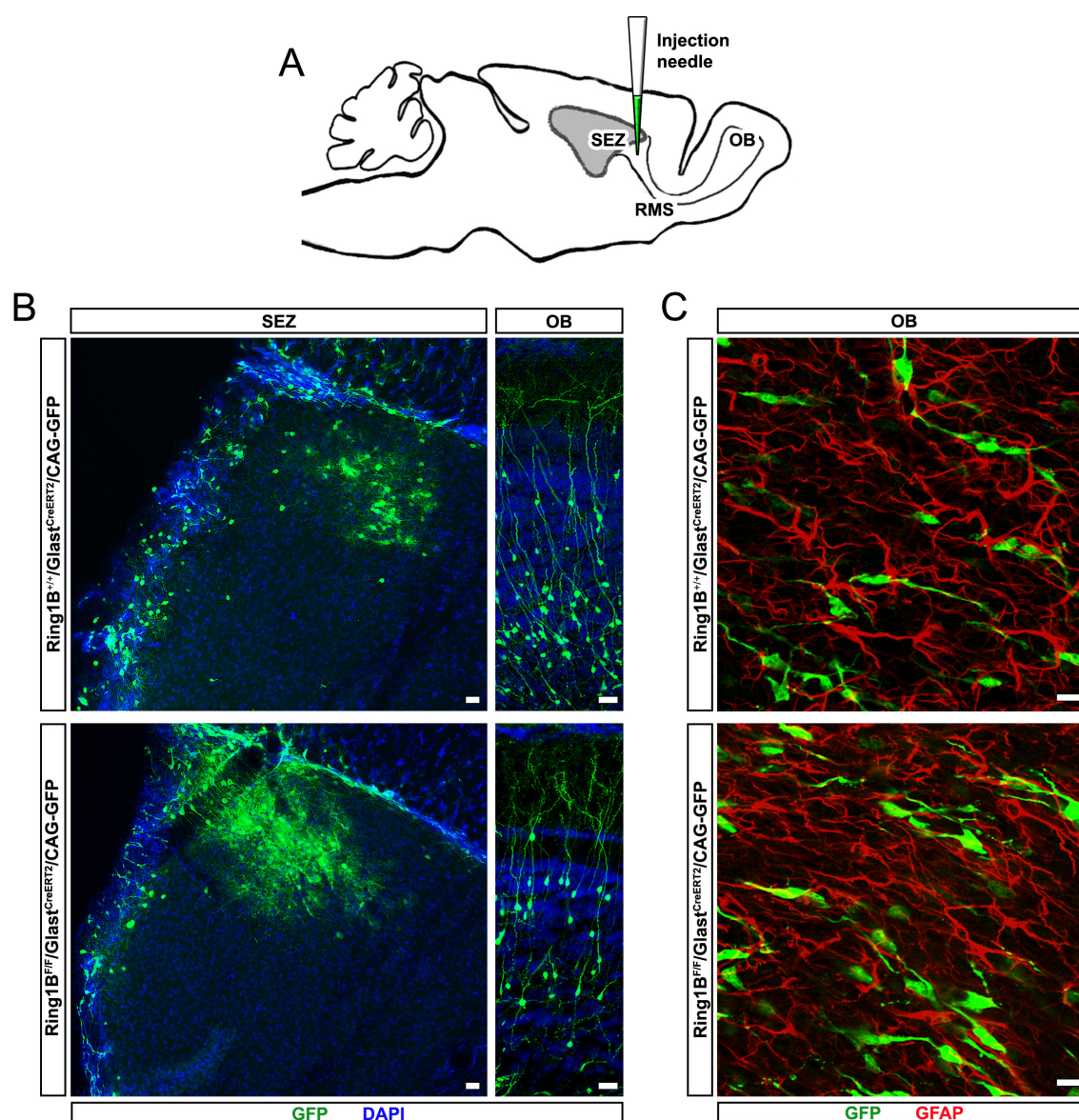


Figure 25. (A) Schematic of mouse sagittal brain, with ventricle in grey. The site of the retroviral injection of the vector encoding for CreGFP fusion protein is depicted. For this experiment, mice are not induced with Tamoxifen. (B) Epifluorescent micrograph of the SEZ (left panel) and confocal micrograph of the OB (right panel) 28 days after retroviral injection. Note that in Ring1B^{F/F} mice many GFP-immunopositive cells preferentially locate in the superficial half of the GCL. (C) Confocal micrograph of the core of the olfactory bulbs showing that GFP-immunopositive cells do not express GFAP.

Scale bars: 10 μ m.

2.21. Wild type neuroblasts can differentiate in the deep granule cell layer of *Ring1B* knockout mice

The results of the selective retroviral induction in the SEZ excluded the potential trans-differentiation of neuroblasts into GFAP-immunopositive astroglia within the OB core, but did not elucidate if the whole GCL environment in *Ring1B*^{Δ/Δ} mice is permissive for radial migration and differentiation.

To assess whether the deep GCL environment is not altered by *Ring1B* deletion, I induced *Ring1B*^{+/+} and *Ring1B*^{F/F} mice and after 10 days I injected a retrovirus encoding for RFP in the elbow of the RMS, as described earlier (Figure 23A). Following 21 days from the injection, RFP-immunopositive neurons in *Ring1B*^{Δ/Δ} mice were found also in the deep GCL, while GFP-immunopositive neurons were mostly found in the superficial GCL (Figure 26A). This result suggested not only that the deep GCL of *Ring1B*^{Δ/Δ} mice allows for radial migration of the neuroblasts, but also that it is permissive for neuronal differentiation of wild type neuroblasts. Immunostainings for Reelin in the mitral cell layer – one of the main molecules responsible for neuroblasts detachment and radial migration (Hack et al., 2002) – further hinted that the correct environmental cues are present in the OB of *Ring1B*-deficient mice (Figure 26B).

Interestingly, GFP/RFP immunopositive neurons in *Ring1B*^{+/+} mice were found at every level of the GCL, while in *Ring1B*^{Δ/Δ} mice they were localised only in the superficial GCL (Figure 26A), therefore implying that already at 10 DPI *Ring1B*-deficient neuroblasts in the RMS are prompted to localise in this specific area.

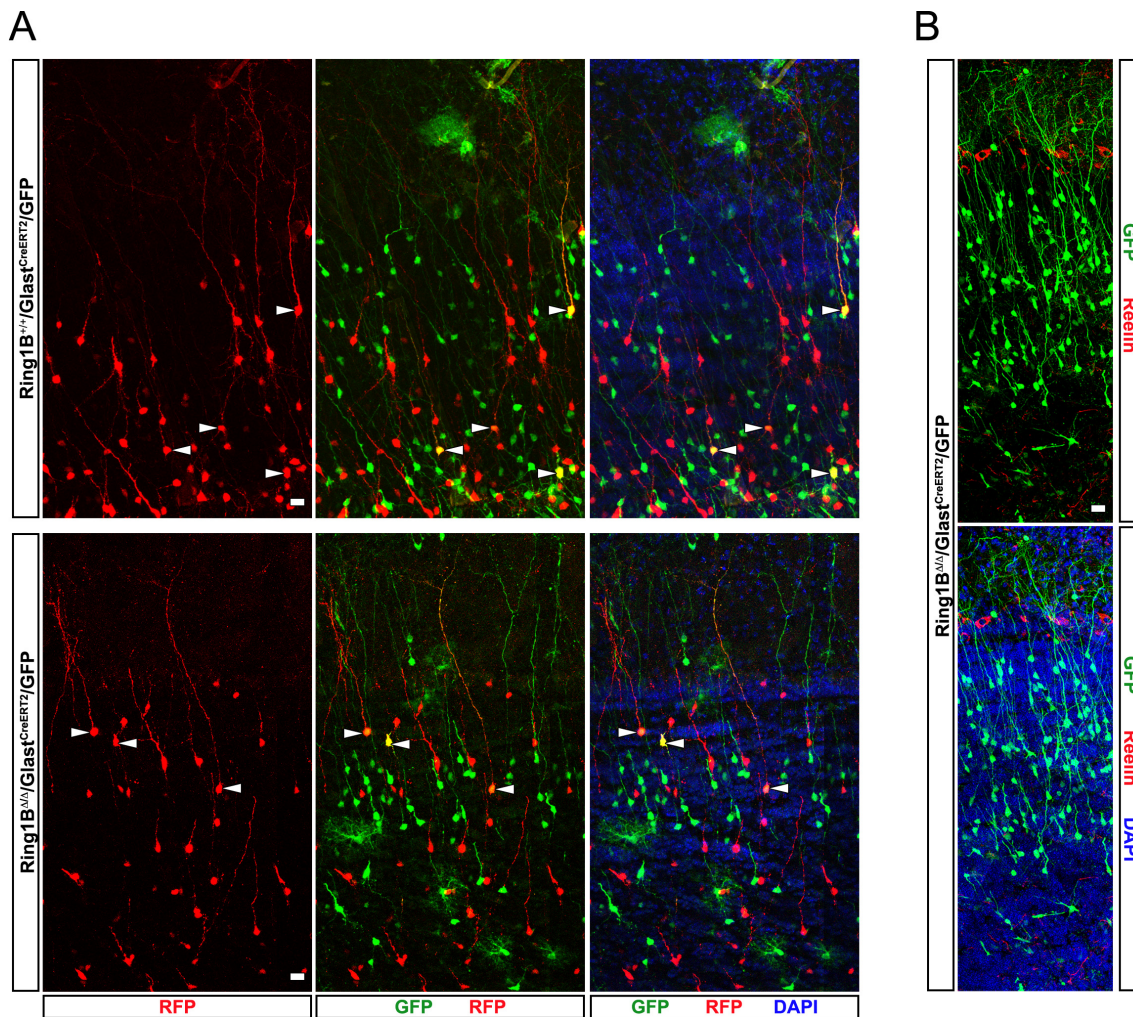


Figure 26. (A) Confocal micrograph of olfactory bulbs sagittal sections at 31 DPI (21 days after injection) showing that in Ring1B^{+/+} mice GFP/RFP-immunopositive cells (arrowheads, upper panel) locate sparsely within the GCL, while in Ring1B^{Δ/Δ} mice (arrowheads, lower panel) such cells are found only in the superficial GCL. Note that RFP-only labelled cells with a neuronal morphology are also found in the deep GCL of Ring1B^{Δ/Δ} mice. (B) Confocal micrographs olfactory bulbs sagittal sections of Ring1B^{Δ/Δ} mice immunostained for GFP and Reelin at 45 DPI. Note that Reelin strong signal can be observed in the mitral cell layer, as described in the main text.

Scale bars: 10 μ m.

2.22. Initial phenotype characterisation in the dentate gyrus of the hippocampus

An initial analysis of the phenotype of Ring1B^{Δ/Δ} mice was also performed where the second main neurogenic niche – the sub-granular zone, or SGZ – can be found, namely in the dentate gyrus of the hippocampus. In this region 20% of Ring1B-deficient granule cells (GFP-immunopositive) was abnormally located in the hilus, compared to only 2% in Ring1B^{+/+} mice (Figure 27A, B). Moreover, semi-automatic tracing of DCX-immunonegative granule neurons revealed a higher length of the dendritic tree in Ring1B^{Δ/Δ} mice as well as a higher number of

Results

branches (tracing and quantifications performed by Dr. David Petrik; Figure 27C, D).

Therefore, our preliminary data from the dentate gyrus of Ring1B^{Δ/Δ} mice suggest a phenotype also in this region and prompts further investigation to unravel similarities and differences with the data collected in the olfactory bulbs.

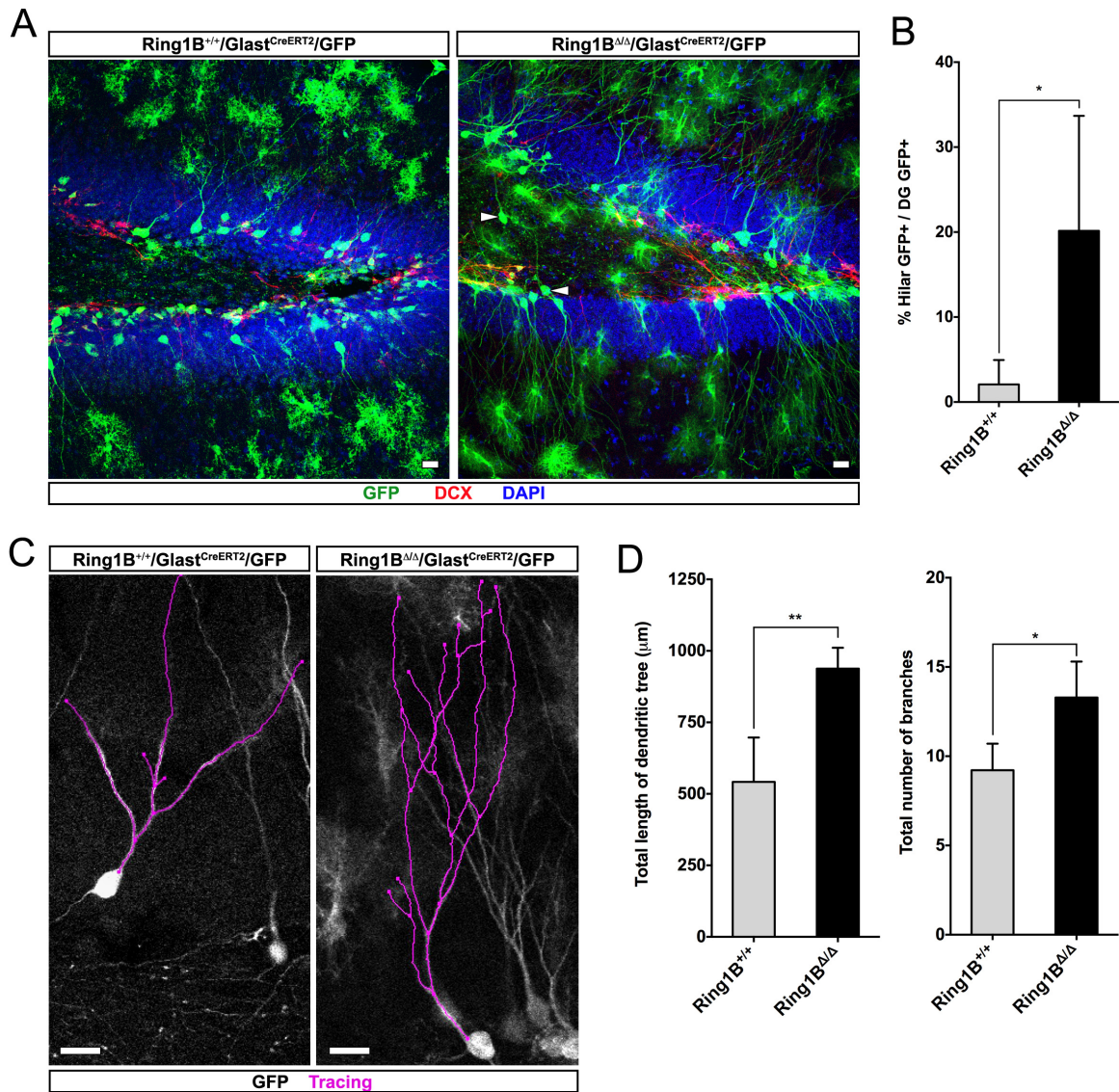


Figure 27. (A) Confocal micrograph of hippocampi sagittal sections (Ring1B^{+/+} and Ring1B^{Δ/Δ}) at 45 DPI after immunostaining with GFP and DCX. GFP-immunopositive cells incorrectly located in the hilus (arrowheads) are more frequently observed in Ring1B^{Δ/Δ} mice. (B) Quantifications of GFP-immunopositive cells within the hilus over the total GFP-immunopositive population in the sub-granular zone (SGZ) show a higher proportion of these cells in Ring1B^{Δ/Δ} mice. Only DCX-immunonegative cells with neuronal morphology are taken into consideration. (C) Semi-automatic tracing of GFP-immunopositive cells in the dentate gyrus of the hippocampus showing a higher degree of complexity of granule cells in Ring1B^{Δ/Δ} mice. (D) Quantifications based on the semi-automatic tracing in C indicating that granule cells in Ring1B^{Δ/Δ} mice have longer processes and a higher number of branches.

Scale bars: 10 μm. Error bars represent SD. Unpaired t test in B (n=5 per condition), D (n=5 for Ring1B^{+/+} mice and n=3 for Ring1B^{Δ/Δ} mice in the dendritic length analysis; n=5 per condition in the branches analysis), *p<0.05, **p<0.01

3. Discussion

The mechanisms underlying direct reprogramming into neurons, and particularly the major roadblocks of the conversion procedure, are still largely unknown. In the projects presented in this thesis I tackled this scientific question from two diverse perspectives. On the one side, after identifying oxidative stress as barrier in direct neuronal reprogramming *in vitro* (Gascón, Murenu et al., 2016), I extended the concept *in vivo* and brought the efficiency of conversion to unprecedented levels by over-expressing *Bcl-2* and administering Calcitriol or α -Tocotrienol. On the other side, I used a candidate approach by exploring the role of Ring1B – Polycomb Repressive Complex 1 catalytic protein – in *in vitro* forced differentiation into neurons mediated by *Dlx2*, further moving *in vivo* to address an unexpected new role in adult neurogenesis.

3.1. *Bcl-2* shows a new role beyond the known anti-apoptotic effect

Our data show that *Bcl-2* over-expression allows for *Neurog2*-mediated neuronal conversion of reactive glia *in vivo* in a model of cortical grey matter injury. Although it is still not known which effects are specifically obtained in this context, *Bcl-2* is predominantly known to act as an anti-apoptotic molecule in the cytoplasm by binding (and inhibiting) the activity of pro-apoptotic proteins like Bax and Bak (Czabotar et al., 2014). *Bcl-2* also modulates calcium-dependent mechanisms by acting on inositol 1,4,5-trisphosphate receptors (InsP₃Rs) on the endoplasmic reticulum, in turn regulating Ca²⁺ levels in the cellular milieu (Chen et al., 2004). Nonetheless, already described in the past are *Bcl-2* effects on oxidative stress and particularly on the levels of the anti-oxidant molecule glutathione (GSH), which binds to *Bcl-2* BH3 domain and is ultimately shuttled to the mitochondria (Zimmermann et al., 2007) or sequestered in the nucleus (Voehringer et al., 1998). In this scenario, the results that we obtained with *Bcl-2* over-expression in neuronal reprogramming *in vivo* are well-explained by the finding that oxidative stress is developed during forced conversion of non-neural cells into neurons (Gascón, Murenu et al., 2016). Indeed, we cannot exclude that *Bcl-2* might play merely an anti-apoptotic role also in our *in vivo* paradigm, by rescuing cells entering the reprogramming process from a premature cell death. However, the absolute number of reprogrammed neurons is dramatically decreasing over time, suggesting that *Bcl-2* over-expression is not sufficient to prevent death of these cells in the long run. Equally important, *Bcl-2* co-transduction allows for a faster reprogramming triggered by *Neurog2*, compared to what described for this neurogenic determinant in previous works (Grande et al., 2013) and in agreement with our *in vitro* experiments (Gascón, Murenu et al., 2016).

Interestingly, while Bcl-2 was never described in direct reprogramming into neurons, a member of its protein family – namely Bcl-x_L – was recently utilised in the generation of medium spiny neurons (Victor et al., 2014). Though the involvement of Bcl-x_L in this work seems purely linked to cell survival, different effects were previously described for Bcl-2 compared to this molecule. In particular, while the anti-apoptotic role is similar for both factors, Bcl-2 – but not Bcl-x_L – is able to promote axonal regeneration following optic nerve crush (Jiao et al., 2005) by regulating the intracellular Ca²⁺ influx at the endoplasmic reticulum. Additionally, Bcl-2 expression has its peak in the developing nervous system and decreases at adult stages, but it is retained in the peripheral nervous system and in the immature neurons generated during adult neurogenesis in the hippocampus (Akhtar et al., 2004; Ceizar et al., 2016; Sasaki et al., 2006). Instead, Bcl-x_L is not only expressed during nervous system development but also in mature neurons from the adult brain (Akhtar et al., 2004; Chang et al., 2007; Nakamura et al., 2016).

All these observations corroborate the idea of partially different functions of Bcl-2 compared to Bcl-x_L and suggest additional roles of Bcl-2 beyond the mere apoptosis antagonism, with the cellular localisation of this factor that can somehow be linked specifically to such roles.

3.2. Oxidative stress and metabolism influence reprogramming

In our work we bring up for the first time oxidative stress as a major roadblock in direct reprogramming into neurons, independently of the cell types and the neurogenic determinants used for the conversion (Gascón, Murenu et al., 2016). While the involvement of oxidative stress in direct reprogramming into neurons was not addressed until now, it was previously described that a sharp and transient oxidative burst takes place when performing reprogramming into induced pluripotent stem cells (iPSCs; Kida et al., 2015; Qi et al., 2015). However, iPSCs are cells characterised by a fast proliferation, whereas in our protocol of direct reprogramming proliferation does not seem to play a relevant role, as assessed *in vitro*. The sources of the high production of reactive oxygen species (ROS) in our conversion paradigm might rather reside in the different nature of the starting and final cell types. Indeed, astroglial cells have a glycolytic metabolism, while neurons strongly rely on oxidative phosphorylation to cope with their high energetic demand (Bélanger et al., 2011). For this reason, we rather favour the hypothesis of oxidative stress as a result of a sharp conversion from one cell type (glial) to another (neuronal), not paralleled by an equally fast change in metabolism.

Bcl-2 over-expression and vitamin E treatment proved to be efficient in alleviating oxidative

stress and potentiating reprogramming into neurons *in vitro*. While the levels of oxidative stress in our reprogramming paradigm *in vivo* remain to be assessed, it is legitimate to assume that similar mechanisms take place also in this context. In fact, we showed that the same treatments used *in vitro* exerted unprecedented results *in vivo* and particularly the renowned anti-oxidant vitamin E retained the best effects in terms of conversion efficiency and final maturation of our reprogrammed cells, strongly suggesting that oxidative stress and lipid peroxidation play an important role also in direct reprogramming into neurons *in vivo*. We speculate that other vitamins could have a beneficial effect in this context, as demonstrated by the use of vitamin C in iPSCs reprogramming (Chen et al., 2013; Esteban et al., 2010) and more recently in the generation of neurons with a defined medium (He et al., 2015).

Although our results *in vitro* indicated a cell intrinsic mechanism for vitamin D and E, we cannot exclude an additional role on inflammation and scar formation in our paradigm of cerebral cortex grey matter injury, due to the systemic administration of these vitamins *in vivo*. Indeed, vitamin D can prevent and/or counteract fibrosis in liver as well as in pancreas (Ding et al., 2013; Sherman et al., 2014), suggesting a beneficial effect of its pathway on the regulation of inflammation and immune response. Therefore, the high efficiency of reprogramming that we observed could be the result of the reduction of oxidative stress levels as well as a reduction of the tissue reaction following the lesion.

3.3. Reprogrammed neurons *in vivo* adopt a deep layer identity

We showed that in our paradigm of neuronal conversion in the cortical grey matter after stab-wound injury the vast majority of the reprogrammed cells with a neuronal morphology (80%) expresses Ctip2, indicative of a deep layer identity (Arlotta et al., 2005; Molyneaux et al., 2007). Neurog2 was already described to be important in the specification of neurons in the dorsal telencephalon as well as in the specification of the laminar identity of a subset of deep layer cortical neurons during mouse development (Fode et al., 2000; Schuurmans et al., 2004). Interestingly, Neurog2 also plays a role in development of upper layer pyramidal neurons by specifying axonal projection towards the callosum (Hand and Polleux, 2011), suggesting that this neurogenic determinant has different roles in different populations of neurons. While no direct correlation between Neurog2 and Ctip2 was previously observed (Masserdotti et al., 2015), Neurog2 seems to have a role in Fezf2 regulation (François Guillemot, oral communication). Fezf2 is responsible for the differentiation and proper axon targeting of layer 5 subcortical

projection neurons (Arlotta et al., 2005; Chen et al., 2005b; Lodato et al., 2014; Molyneaux et al., 2005) and was shown to act upstream of Ctip2 (Chen et al., 2005a). Therefore, the deep layer identity of our reprogrammed neurons could be explained by a cascade of event initiated by *Neurog2* over-expression and leading to Ctip2 up-regulation mediated by Fezf2. Moreover, the correct conversion towards deep layer pyramidal neurons is also confirmed by the absence of Satb2 signal. Satb2 and Ctip2 expression is known to be mutually exclusive, with Satb2 directly repressing Ctip2 and being negatively regulated by Fezf2 (Alcamo et al., 2008; Chen et al., 2008; Srinivasan et al., 2012).

All in all, we showed that *Neurog2* and *Bcl-2* over-expression is sufficient to promote the conversion of reactive glia into neurons and that the further treatment with vitamin D or vitamin E exerts the best results in terms of conversion efficiency and final neuronal maturation. Bcl-2 and vitamin D/vitamin E treatment would mainly act by antagonising oxidative stress, which is produced during direct neuronal reprogramming and ultimately represents a major roadblock for the conversion procedure (Gascón, Murenu et al., 2016).

Besides metabolism, the chromatin and epigenetic state of the starting cell population are known to play a role in this paradigm. Indeed, in direct neuronal reprogramming of MEFs with Ascl1, Brn2 and Myt1L (Vierbuchen et al., 2010), Ascl1 is able to bind also compacted chromatin and to precede Brn2 and Myt1L binding (Wapinski et al., 2013), a feature that was described for pioneering transcription factors (Vierbuchen and Wernig, 2012; Zaret and Carroll, 2011). Moreover, epigenetics has also proven to be an important aspect in reprogramming into iPSCs, as specific factors (DOT1L, YY1, SUV31H1) decrease the conversion efficiency while others (e.g. the main subunits of Polycomb Repressive Complex 1 and 2) are rather required.

3.4. Ring1B is necessary for neuronal differentiation into the GABAergic lineage

After alleviating a major roadblock in direct reprogramming *in vivo*, we further moved to tackling the same question from an epigenetic perspective, by addressing the role of the renowned Polycomb Repressive Complex 1 (PRC1) in forced neuronal differentiation. Particularly, we focused in loss-of-function experiments by impairing the expression of Ring1B, the main catalytic protein of this complex. This approach ensured affecting not only the canonical PRC1 but also all PRC1 variants described so far (Kondo et al., 2015), although it is not clear to which extent Ring1A – the alternative catalytic protein for this complex – can compensate for Ring1B loss in this paradigm, as previously described for embryonic stem cells

and embryonic fibroblasts (Leeb and Wutz, 2007; de Napoles et al., 2004).

In cultures from E14 embryonic NSCs and adult NSCs from the SEZ we found the forced differentiation into neurons mediated by *Dlx2* to be less efficient when *Ring1B* was knocked down. *Ring1B* was shown to antagonize the production of glutamatergic neurons *in vivo* by regulating the expression of Wnt downstream targets (such as *Neurogenin1*), thus determining the end of the neurogenic phase and the onset of the gliogenic phase during corticogenesis (Hirabayashi et al., 2009). Furthermore, *Ring1B* regulates the expression of *Fzf2* to correctly specify subcortical projection neurons in the developing cortex (Morimoto-Suzki et al., 2014). Our observation unexpectedly showed a role of *Ring1B* in regulating the differentiation of adult generated GABAergic neurons, suggesting a tightly regulated target specificity of PRC1 depending on the developmental stage (embryonic versus adult) and the lineage choice (glutamatergic versus GABAergic). Indeed, we showed that adult *Ring1B*^{Δ/Δ}/*Glast*^{CreERT2}/GFP mice do not have alterations in the overall density of recombined cells within the olfactory bulb granule cell layer. Moreover, such cells do not undergo a change towards a non-neuronal phenotype (i.e. astroglial or oligodendroglial), indicating that *Ring1B* deletion at adult stages in the SEZ-RMS-OB system does not lead to fate switch as seen during development.

3.5. *Ring1B* regulates specific neurogenic determinants

Our data indicate that *Ring1B* deletion does not affect cell proliferation of recombined cells in the SEZ as well as during migration in the RMS and overall it does not lead to major alterations in these areas. These results are in agreement with a recent work indicating that *Ring1B* loss *in vivo* does not determine increased proliferation or premature cell cycle exit of neural precursor cells (NPCs) located in the embryonic ventricular zone (Morimoto-Suzki et al., 2014). Moreover, this work elucidates a role of *Ring1B* in NPCs rather than in post-mitotic neurons. In this regard, although the phenotypes we described take place in the olfactory bulb, the effects on gene regulation could start already in stem cells and progenitors at the level of the SEZ and eventually manifest only during differentiation. As previously shown, the different granule cell populations in the olfactory bulbs arise in a precise temporal order from neural stem cells that have a specific spatial distribution along the telencephalic ventricles (Fiorelli et al., 2015; Lim and Alvarez-Buylla, 2014). Particularly, superficial granule cells are generated mainly at early postnatal stages in the dorso-lateral domain of the SEZ, while deep granule cells arise from the ventral domain predominantly during adulthood (Calzolari et al., 2015; Fiorelli et al., 2015; Kelsch et

al., 2007; Lemasson et al., 2005; Merkle et al., 2007; Sakamoto et al., 2014). While it is known that sonic hedgehog (Shh) signalling is the major determinant in the ventral SEZ (Alvarez-Buylla and Ihrie, 2014; Ihrie et al., 2011), little is known about the signalling(s) characterising the dorso-lateral niche. Wnt pathway is playing an important role in the dorsal SEZ, where it is involved in the generation of cortical glutamatergic neurons during development and in the production of oligodendrocyte precursors at adult stages (Azim et al., 2015, 2014a, 2014b; Fiorelli et al., 2015; Ortega et al., 2013, as well as dopaminergic and glutamatergic periglomerular neurons in the olfactory bulb (Fiorelli et al., 2015). However, it still remains to be elucidated to which extent Wnt signalling is involved also in the generation of superficial granule neurons in the olfactory bulb and whether other pathways concur to specify this particular cell fate.

3.6. Migration or subtype specification?

Our data have shown that the deep granule cell population is virtually not specified after *Ring1B* deletion, while the superficial granule cell population increases significantly in density. One hypothesis to explain this phenotype could be that *Ring1B* deletion leads to the sudden accessibility and active transcription of genes connected to the superficial granule cell lineage in the neural precursors arising from the ventral SEZ. This event would re-specify the deep granule cell population to a superficial granule cell fate, while not necessarily affecting the overall granule cell density in the olfactory bulb (Figure 28). Though previous attempts to distinguish the different subpopulations of GCL neurons have led to the description of some markers expressed in the superficial GCL as well as in the mitral cell layer and in periglomerular neurons, e.g. Calretinin, Er81, Sp8, 5HT3aR, 5T4 (Allen et al., 2007; Batista-Brito et al., 2008; Chen et al., 2012; Imamura et al., 2006; Kohwi et al., 2005; Kosaka and Kosaka, 2012; Waclaw et al., 2006), the transcriptional code underlying the specification of deep and superficial granule neurons is still largely unknown. However, since some of the mentioned genes are largely expressed within the dopaminergic periglomerular cell lineage (Agoston et al., 2014; Cave et al., 2010), it is legitimate to speculate that superficial granule cells partially share their molecular signature with this population, whose progenitors in the SEZ are located in a nearby area (see previous paragraph). One example is the tyrosine hydroxylase (*TH*) gene, whose protein expression is rather restricted to the glomerular layer, while the transcript is found also in the mitral and superficial granule cell layer (Kohwi et al., 2005).

A second hypothesis to explain the increased density of neurons in the superficial GCL of Ring1B^{Δ/Δ}/Glast^{CreERT2}/GFP would not involve a selective re-specification of deep granule neurons into superficial granule neurons, but rather the incorrect localisation of deep granule neurons in the superficial GCL (Figure 28). This scenario would not only suggest a migration defect of those differentiating neuroblasts that are generated in the ventral SEZ, which might however maintain their final identity as deep granule neurons in the new area of destination, but it would also explain the increased neuroblasts density in the core of the OB as the result of an impaired radial migration. Indeed, previous studies in *C. elegans* showed that the deletion of Ring1B most similar gene (*SPAT-3A*) leads to impaired migration of HSN neurons (Karakuzu et al., 2009), as well as to an incorrect axonal outgrowth. Moreover, Ring1B and Ring1A depletion in human pancreatic cancer cells was shown to affect migration during epithelial-mesenchymal transition (Chen et al., 2014) by regulating the expression of key adhesion molecules such as E-cadherin.

Therefore, Ring1B might be involved in the regulation of the switch from tangential to radial neuroblasts migration, as well as to their final localisation in certain olfactory bulb areas and the terminal differentiation into subtype-specific neurons. Transcriptome analysis of SEZ and OB-core samples dissected at the earliest time-point when Ring1B immunohistochemistry signal is not detected after recombination (i.e., 7 days later) might help elucidating the first events that take place after *Ring1B* induced deletion.

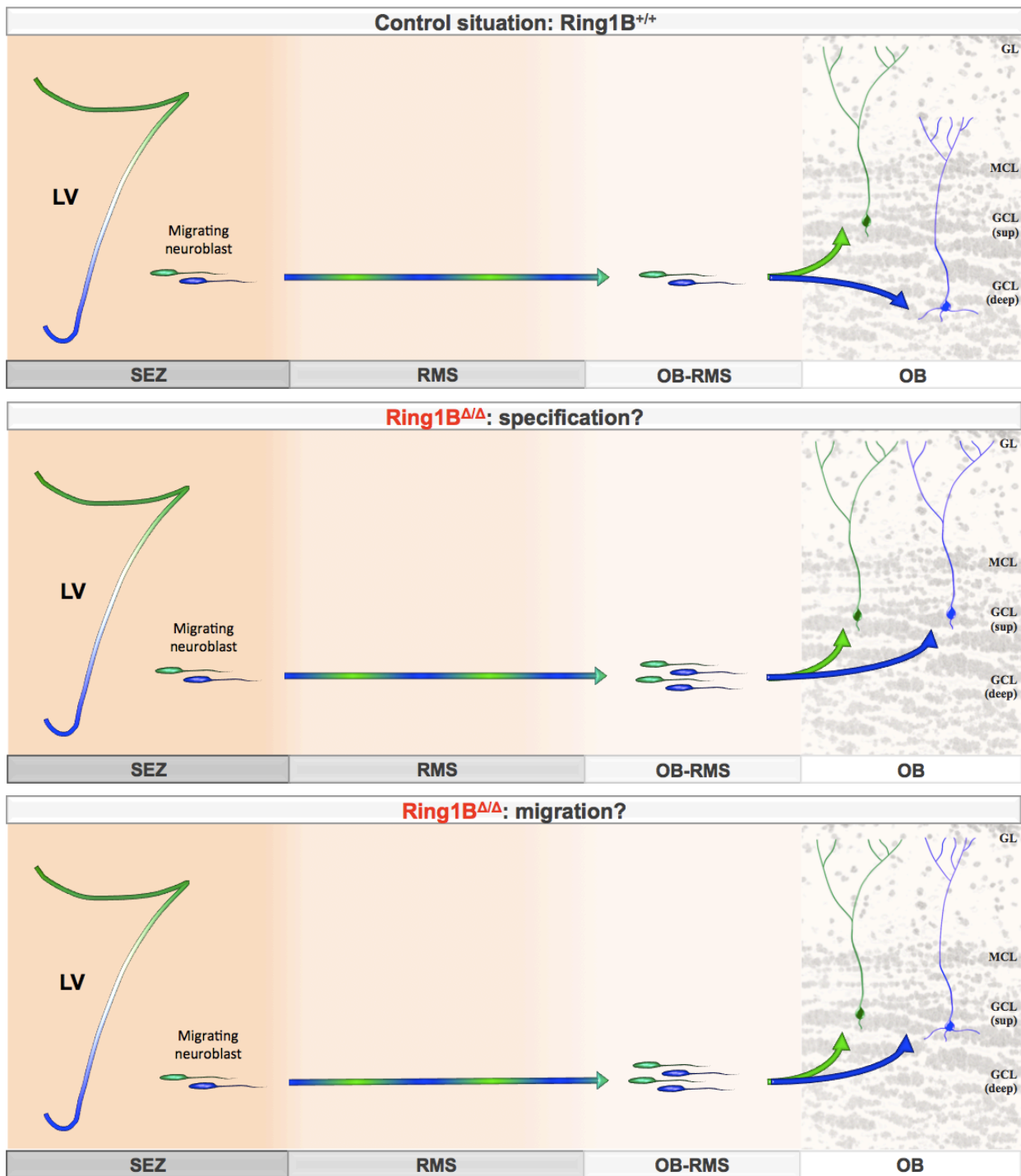


Figure 28. Schematics of the hypotheses behind the phenotypes observed in *Ring1B*^{Δ/Δ} mice. In control animals (upper panel), neuroblasts generated in the dorsal (green) and ventral (blue) SEZ walls migrate to the olfactory bulbs through the RMS. Once inside the OB core (OB-RMS), the neuroblasts derived from the dorsal SEZ progenitors (green) become superficial granule cells, while the ones derived from the ventral SEZ progenitors (blue) become deep granule neurons. In *Ring1B*^{Δ/Δ} mice (middle and lower panels), neuroblasts accumulate in the OB-RMS. Moreover, while dorsal SEZ-derived neuroblasts would still make superficial granule cells, ventral SEZ-derived neuroblasts would either re-specify into superficial granule cell (specification hypothesis, middle panel) or maintain a deep granule cell identity but locate in the superficial GCL (migration hypothesis, lower panel).

LV=lateral ventricle, SEZ=sub-ependymal zone, RMS=rostral migratory stream, OB=olfactory bulb, GCL=granule cell layer, MCL=mitral cell layer, GL=glomerular layer

4. Materials and Methods

4.1. Experimental animals

The described experiments were mainly conducted on young adult mice (8-11 weeks old), both females and males. Mice at embryonic day 14 (E14) were used for cultures of cerebral cortex in adherent conditions.

For *in vitro* experiments and *in vivo* reprogramming, C57BL/6J wild type mice were used.

For adult neurogenesis experiments *in vivo*, Ring1B^{F/F} transgenic mice (courtesy of Miguel Vidal; Calés et al., 2008) were previously crossed with Glast^{CreERT2}/CAG-GFP transgenic mice (Mori et al., 2006b; Nakamura et al., 2006). The resulting mouse line (Ring1B^{F/F}/Glast^{CreERT2}/CAG-GFP) expresses the Tamoxifen-inducible recombinase Cre (CreERT2) in the GLAST locus - specifically in neural stem cells and astrocytes. In the reporter line generated by Nakamura et al., 2006 the GFP gene is preceded by a floxed STOP codon and its expression is consequentially turned on upon Cre activation. Therefore, administration of Tamoxifen determines the excision of Ring1B gene (and GFP activation) specifically in adult neural stem cells and astrocytes (Ring1B^{Δ/Δ}/Glast^{CreERT2}/CAG-GFP, referred to as Ring1B^{Δ/Δ} in the main text). Ring1B^{+/+}/Glast^{CreERT2}/CAG-GFP mice were used as experimental controls in this paradigm and referred to as Ring1B^{+/+}.

All mice were chow-fed and kept with abundance of water in a 12-hour light/dark cycle.

4.2. Genotyping

Mouse tails were collected and used for DNA extraction with technical support of Detlef Franzen. The following primers, PCR cycles and solutions were used to characterise the genotype of all transgenic mice used in this study.

<u>Glast^{CreERT2}</u>	Primer F8	5'-GAGGCACTTGGCTAGGCTCTGAGGA-3'
	Primer R3	5'-GAGGAGATCCTGACCGATCAGTTGG-3'
	Primer CER1	5'-GGTGTACGGTCAGTAAATTGGACAT-3'
	94°C	Pause
	94°C	5 min
	35 cycles	94°C 30sec
		56°C 40sec
		72°C 40sec
	72°C	5min
	4°C	

Materials and Methods

Glast^{CreERT2}	Volume (μl)
H₂O	10
25 mM MgCl	2.5
Buffer (10x)	2.5
Primer F8	1
Primer R3	0.5
Primer CER1	0.5
Q-Solution/Betaine	5.0
dNTPs	0.5
Taq	0.5
DNA	2
Final volume	25

GFP reporter II Primer AG2 5'-CTGCTAACCATGTTCATGCC-3'
 Primer CAT2 5'-GGTACATTGAGCAACTGACTG-3'
 95°C 5min
 30 cycles 95°C 30sec
 55°C 30sec
 72°C 1min
 72°C 10min
 4°C

GFP reporter II	Volume (μl)
H₂O	12
25 mM MgCl	1.5
Buffer (10x)	2.5
Primer 1 (AG2)	1
Primer 2 (CAT2)	1
Q-Solution/Betaine	5.0
dNTPs	0.5
Taq	0.5
DNA	1
Final volume	25

<u>Ring1B^{F/F}</u>	Primer Forward	5'-GGAAATGCAATGGTATCAATGTATATG-3'
	Primer Reverse	5'-GCTAGCGATGTGGCTATG-3'
	94°C	Pause
	94°C	1min
	30 cycles	94°C 20sec
		60°C 20sec
		72°C 1min
	72°C	30sec
	4°C	

Ring1B^{F/F}	Volume (µl)
H₂O	15.5
25 mM MgCl	1.5
Buffer 10x	2.5
Primer Forward	0.5
Primer Reverse	0.5
DMSO	1.0
dNTPs	0.5
Taq	1.5
DNA	1.5
Final volume	25

4.3. Dissection of the embryonic cerebral cortex and primary culture in adherent conditions

Isolation and culture of cortical neural stem cells (NSCs) from mice at embryonic day 14 (E14) was performed with technical support of Tatiana Simon-Ebert. Wild type embryos were isolated from the uterus of a pregnant mouse at the 14th gestation day and collected in ice-cold Dissection Solution. Following decapitation, the skin and the skull of the embryos was carefully cut to expose the brain, which was then extracted avoiding causing any damage to the tissue. After separating the two hemispheres, the meninges, hippocampus, ganglionic eminences and olfactory bulbs were removed using fine forceps and spring scissors and the isolated cerebral cortices were collected in a tube with Expansion Medium. Gentle trituration of the tissues was then achieved with the pipette, before centrifuging the cell suspension at 1400 rpm for 5 minutes

Materials and Methods

at room temperature. After discarding the medium, the pellet was re-suspended in pre-warmed Expansion Medium and the suspension was transferred into PDL-coated flasks.

Poly-D-lysine (PDL) stock (50x)

Poly-D-lysine powder 1 mg/ml in bi-distilled water
Filter-sterilize, then aliquot and store at – 20 °C for up to 6 months.
Dilute to 1x in bi-distilled water before use.

Dissection Solution

1x HBSS	500 ml
1M HEPES	5 ml (10 mM)

Expansion Medium

50x B27 Supplement	1X
10 µg/ml EGF	10 ng/ml
10 µg/ml FGF-2	10 ng/ml
Penicillin/Streptomycin	100 units/ml
DMEM + GlutaMAX	To volume

4.4. Passaging of NSCs from the embryonic cerebral cortex

Following expansion of the culture, cells were passaged at approximately 70% of confluence to avoid block in proliferation and onset of differentiation.

After rinsing with 1x PBS, the cells were treated with Trypsin Solution for 5 minutes at 37°C and checked for successful detachment. Collecting the cell suspension in a tube containing 1 ml of foetal bovine serum (FBS) antagonised trypsin enzymatic activity at the end of the incubation time. Following a gentle mix with the pipette, the cells were centrifuged at 1300 rpm for 5 minutes at 4°C and the medium was discarded. The cell pellet was then re-suspended in Expansion Medium and $1-1.5 \times 10^6$ cells were seeded in PDL-coated flasks (25 cm²).

For differentiation experiments, cells were plated in 24-well plates with PDL-coated glass coverslips. One day after seeding, Differentiation Medium was added in a 1:1 ratio to the old Expansion Medium in order to halve the concentration of growth factors (5 ng/ml for both EGF and FGF-2). The medium was replaced by fresh Differentiation Medium 24 hours later and changed every second day.

Poly-D-lysine (PDL) stock (50x)

Poly-D-lysine powder 1 mg/ml in bi-distilled water
Filter-sterilize, then aliquot and store at – 20 °C for up to 6 months.
Dilute to 1x in bi-distilled water before use.

Trypsin Solution

0.25% Trypsin-EDTA 0.08 - 0.1%
1x PBS To volume

Expansion Medium

50x B27 Supplement 1X
10 µg/ml EGF 10 ng/ml
10 µg/ml FGF-2 10 ng/ml
Penicillin/Streptomycin 100 units/ml
DMEM + GlutaMAX To volume

Differentiation Medium

50x B27 Supplement 1X
Penicillin/Streptomycin 100 units/ml
DMEM + GlutaMAX To volume

4.5. Dissection of the adult sub-ependymal zone (SEZ)

Sub-ependymal zone dissection and culture preparation were performed with technical support of Tatiana Simon-Ebert and Carmen Meyer, as described in Ortega et al., 2011.

Briefly, young adult C57BL/6J mice (8-11 weeks old) were sacrificed by means of a carbon-dioxide chamber and further cervical dislocation. Upon isolation of the head, the brain was carefully extracted from the skull and placed in a Petri dish filled with Dissection Solution.

After orienting the brain with the ventral side up, a coronal cut was performed approximately at the level of the optic chiasm by means of a scalpel and the caudal half was discarded. Turning the rostral half with the dorsal side up, the scalpel was used again to carefully separate the 2 hemispheres.

To expose the surface of the lateral ventricle, a pair of fine spring scissors (Fine Science Tools) was used to cut along the callosal white matter in the medial part of the brain. Then, the hippocampus and part of the thalamus were gently removed with fine forceps (Fine Science

Materials and Methods

Tools). Keeping the fine spring scissors as tangential as possible to avoid the underlying striatum, a small squared tissue corresponding to the lateral and dorsal walls of the SEZ is dissected and collected in a tube with ice-cold Dissection Solution.

Dissection Solution

1x HBSS	500 ml
1M HEPES	5 ml (10 mM)

4.6. Primary SEZ culture in adherent conditions

After collecting the tissue samples in a tube, Dissection Solution was discarded and replaced with pre-warmed Dissociation Solution, which was left for 15 minutes at 37°C. The tissue pieces were gently triturated with a pipette and incubated additionally for 15 minutes at 37°C. Dissociation was stopped by adding an equal volume of ice-cold Solution 3 and gently mixing the suspension. After passing the suspension through a 70µm-strainer, cells were centrifuged at 200 g (1300 rpm) for 5 min at 4°C and re-suspended in ice-cold Solution 2. Subsequently, cells were centrifuged at 450 g for 10 min at 4°C and the cell pellet was re-suspended in a small volume of ice-cold Solution 3, which was then added on 12 ml of the same medium and centrifuged at 250 g for 7 min at 4°C. The cell pellet was finally re-suspended in Expansion Medium and cells were plated on PDL-coated flasks.

Differently from previous publications (Ortega et al., 2011), we promoted proliferation and expansion of the culture by adding EGF and FGF-2 factors to the medium.

Poly-D-lysine (PDL) stock (50x)

Poly-D-lysine powder 1 mg/ml in bi-distilled water
Filter-sterilize, then aliquot and store at – 20 °C for up to 6 months.
Dilute to 1x in bi-distilled water before use.

Solution 1 (HBSS-Glucose)

10× HBSS	50 ml
45% D-(+)-glucose	6 ml
1M HEPES	7.5 ml
Bi-distilled water	To volume (500 ml)

Final pH=7.5

Filter-sterilize the solution, aliquot and store at – 20 °C for up to 6 months.

Solution 2 (Sucrose-HBSS)

10× HBSS	25 ml
D-(+)-sucrose	154 g
Bi-distilled water	To volume (500 ml)

Final pH=7.5

Filter-sterilize the solution, aliquot and store at – 20 °C for up to 6 months.

Solution 3 (BSA-EBSS-HEPES)

1 M HEPES	10 ml
BSA	20 g (4%)
1x EBSS	To volume (500 ml)

Final pH=7.5

Filter-sterilize the solution, aliquot and store at – 20 °C for up to 6 months.

Dissociation Solution

Trypsin powder	3.4 mg
Hyaluronidase powder	3.5 mg
Solution 1	5 ml

Expansion Medium

50x B27 Supplement	1X
10 mg/ml EGF	10 ng/ml
10 mg/ml FGF-2	10 ng/ml
Penicillin/Streptomycin	100 units/ml
DMEM + GlutaMAX	To volume

4.7. Passaging of NSCs from the adult SEZ

SEZ neural stem cells reaching 70% of confluence were passaged as described for NSCs from the embryonic cerebral cortex. Briefly, after removing the medium and rinsing in tissue-culture 1x PBS, cells were allowed to detach at 37°C for 5 minutes in presence of Trypsin Solution, which was inactivated by adding 1 ml of foetal bovine serum (FBS). Cells were subsequently collected in a tube and centrifuged at 1300 rpm for 5 minutes at 4°C. The medium was carefully discarded and the pellet was re-suspended in Expansion Medium prior to seeding in new PDL-coated flasks.

For terminal differentiation, neural stem cells were plated in 24-well plates with PDL-coated

Materials and Methods

plastic coverslips. As differentiation must be induced gradually to minimise cell death, one day after seeding Differentiation Medium was added in a 1:1 ratio to the old Expansion Medium in order to halve the concentration of growth factors (5 ng/ml for both EGF and FGF-2). The medium was replaced by fresh Differentiation Medium 24 hours later and changed every second day.

Poly-D-lysine (PDL) stock (50x)

Poly-D-lysine powder 1 mg/ml in bi-distilled water
Filter-sterilize, then aliquot and store at – 20 °C for up to 6 months.
Dilute to 1x in bi-distilled water before use.

Trypsin Solution

0.25% Trypsin-EDTA	0.08 - 0.1%
1x PBS	To volume

Expansion Medium

50x B27 Supplement	1X
10 mg/ml EGF	10 ng/ml
10 mg/ml FGF-2	10 ng/ml
Penicillin/Streptomycin	100 units/ml
DMEM + GlutaMAX	To volume

Differentiation Medium

50x B27 Supplement	1X
Penicillin/Streptomycin	100 units/ml
DMEM + GlutaMAX	To volume

4.8. Transfection

Transient transfection of cultures, both embryonic and adult, was performed using Lipofectamine2000 (Thermo Fisher Scientific) and following the instructions provided by the manufacturer. Cells were usually seeded two days before transfection at 40-50% of confluence. One hour before transfection, the medium was collected and cells were incubated with pre-warmed OptiMEM + GlutaMAX.

For cells seeded in 24-well plates, a scheme summarising the procedure is shown in the next page.

MIX A

50 µl OptiMEM + GlutaMAX
+ 0.2 µg DNA plasmid (neurogenic gene)
+ 0.3 µg DNA plasmid (miRNA)

MIX B

50 µl OptiMEM + GlutaMAX
+ Lipofectamine2000
(1:100)

5 min

5 min

Mix together

25 min incubation

Add 100 µl/well, drop by drop.

Incubate for 3-4 hours.

At the end of incubation time, the transfection medium was replaced with the old collected medium, mixed in a 1:1 ratio with fresh medium.

For NSCs cultures from both embryonic cerebral cortex and adult SEZ, the concentration of EGF and FGF-2 in the medium was halved (5 ng/ml for both factors) 24 hours after transfection. The factors were then completely removed 48 hours after transfection to promote differentiation. Cells were fixed in 4% paraformaldehyde (PFA) for 15 minutes at room temperature 6 days after transfection and were rinsed twice in 1x PBS prior to processing by immunocytochemistry.

20% Paraformaldehyde (PFA) in PBS

Na ₂ HPO ₄	134 g
Paraformaldehyde (PFA)	400 g
Bi-distilled water	To volume (2 L)
32% NaOH	To better dissolve PFA
Final pH=7.4	

Filter and aliquot, then freeze at -20°C. Dilute to 4% in 1x PBS and measure pH again prior to use.

4.9. Retroviral constructs used

Viral production was performed with technical support of Ines Mühlhahn, Dr. Alexandra Lepier and Detlef Franzen. All viral constructs were purified using a caesium chloride density gradient centrifugation, allowing for separation of DNA based on conformation (supercoiled, circular or linear).

Vesicular stomatitis virus-glycoprotein (VSV-G) pseudotyped retroviruses were used for this work and include the following

pCAG-*Neurog2*-IRES-*RFP*

pCAG-*Dlx2*-IRES-*RFP*

pCAG-IRES-*RFP*

pCAG-*Bcl-2*-IRES-*GFP*

These retroviruses were produced from the human 293-derived retroviral packaging cell line (293GPG; Ory et al., 1996) as previously described (Heinrich et al., 2011; Tashiro et al., 2006). The retroviral suspensions used were collected 6 days (second harvest) and 8 days (third harvest) after transfection of the packaging cell line.

4.10. Animal Surgery

All operations were performed in accordance with the policies of the state of Bavaria under license number 55.2-1-54-2532-171-2011 and 55.2-1-54-2532-150-2011, as well as the policies of use of Animals and Humans in Neuroscience Research, revised and approved by the Society of Neuroscience. Prior to every surgery, mice were anaesthetised with an intra-peritoneal injection of Sleep Solution (10 µl/g body-weight) and their hair was removed at the area to operate. The shaved animals were then fixed in a stereotaxic frame and Bepanthen (Bayer) was administered to prevent eye dryness and damage.

With the completion of the surgery, the wound was closed with Vicryl sutures and the anaesthesia was terminated with an intra-peritoneal injection of Awake Solution (10 µl/g body-weight). To facilitate the awakening of the mice, the cages were kept with one extremity on a pre-warmed pad for at least one hour. The operated mice were eventually maintained in a 12-hour light/dark cycle and monitored daily.

Sleep Solution

Fentanylcitrat	0.0025 mg/ml
Midazolam	0.5 mg/ml
Medetomidin	0.05 mg/ml
NaCl	To volume

Awake Solution

Buprenorphine	0.01 mg/ml
Flumazenil	0.05 mg/ml
Atipamezol	0.25 mg/ml
NaCl	To volume

4.10.1. Stab-wound injury

After fixing the mouse in the stereotaxic frame, the skin of the head was cut with a scalpel and the thin layer of muscles gently spread away to display the skull surface. A small circular cranial window was then drilled into the right parietal bone by means of a high-speed rotary micromotor (Foredom) and the bone flap collected in saline physiological solution (NaCl). Setting the bregma as 0, a 1 mm long stab-wound was performed with a V-lance knife (19 gauge, Alcon) at the following coordinates:

Medio-lateral (x): -1.8

Rostro-caudal (y): -1.6 to -2.5

Dorso-ventral (z): -0.6 from the meninges

In particular, the depth of the cut ensured sparing the deep grey matter layers and the white matter, therefore minimising the risk of neuroblasts recruitment following the injury.

At the end of the procedure, the bone flap was put back in place to protect the wounded area.

4.10.2. Injection of retroviral suspension in the lesion

Three days after performing the stab-wound injury in the cortical grey matter, the mice were anaesthetised and fixed in the stereotaxic frame to undergo retroviral injection.

The skin was cut open in correspondence of the previous incision and the bone flap delicately removed and collected after abundant rinsing with saline solution. Subsequently, 0.5-1 μ l of retroviral suspension for *Neurog2-IRES-RFP* alone or in a 1:1 ratio with *Bcl-2-IRES-GFP* was

injected into the site of the lesion with a glass capillary connected to a microinjector (Nanoliter2000 + Sys-Micro4 Console, World Precision Instrument). The infusion speed was set to a rate of 30 nl/min and gradually increased to a maximum of 50 nl/min, resulting in the absence of any retroviral leakiness on the brain surface.

The capillary was then retracted 5 minutes after completing the procedure to avoid reflux along the injection tract and the bone flap was put back in place to cover the injured area.

4.10.3. Injection of retroviral suspension into the SEZ and RMS

Prior to the surgery, the mice were anaesthetised and shaved as described above. Following their immobilisation in the stereotactic frame, the skin of the head was cut to expose the skull. A small hole was then performed with a drill in correspondence of the injection area.

In particular, the following coordinates were used with regards to the bregma:

SEZ Medio-lateral (x): ± 1.2
 Rostro-caudal (y): $+0.7$
 Dorso-ventral (z): $-1.9/-2.1$ from the meninges

RMS Medio-lateral (x): ± 0.8
 Rostro-caudal (y): $+2.5/+2.6$
 Dorso-ventral (z): $-3.1/-3.2$ from the meninges

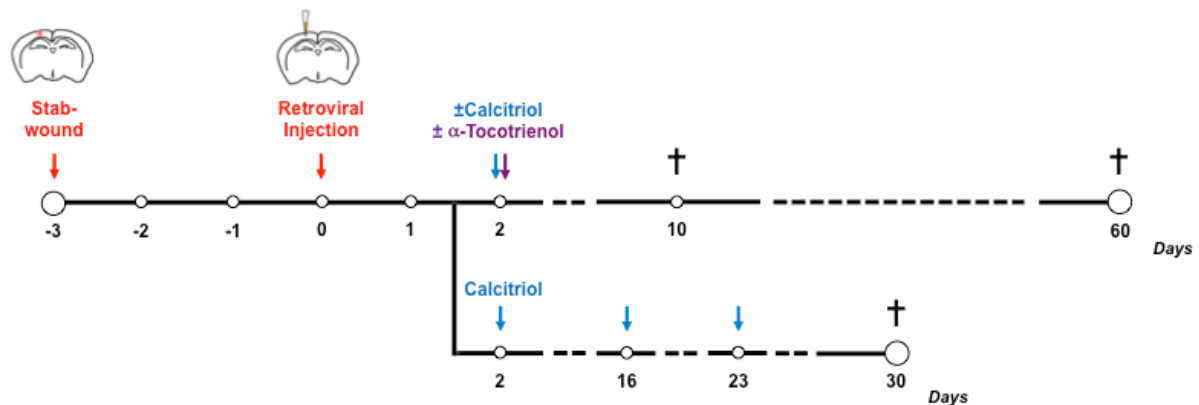
The retroviral suspension (0.5-1 μ l) was infused at a speed of 30-60 nl/min and the capillary was finally withdrawn 5 minutes after completion of the injection. The skin was then closed with Vicryl sutures and anaesthesia was terminated as described.

4.11. Compound administration to animals

4.11.1. Vitamins

In the context of the reprogramming experiments, 2 days after retroviral injection in the injured cortical grey matter vitamins were administered to adult C57Bl/6J mice by gavage (reusable needles, Fine Science Tools).

For Vitamin D receptor pathway stimulation, 200 ng Calcitriol (Tocris) dissolved in 0.2 ml of corn oil (Sigma Aldrich) were administered to each mouse 2 days after retroviral injection. In long-term reprogramming experiments (30 and 60 days post-injection), when indicated in the text, Calcitriol was administered according to the following administration scheme.



For Vitamin E, 3 mg α -Tocotrienol (Fluka, Sigma Aldrich) dissolved in 0.2 ml of corn oil were administered to each mouse 2 days after injection (see scheme).

The dosage of both Calcitriol and α -Tocotrienol was determined and adjusted according to previous publications (Nashold et al., 2013; Park et al., 2011).

4.11.2. Tamoxifen

For the induction of recombination in transgenic mouse lines expressing CreERT2, a solution of 40 mg/ml Tamoxifen (Sigma Aldrich) in 10% EtOH and corn oil was freshly prepared at need and mixed by sonication for 15 minutes. 8-10 week-old mice (body-weight ~25g) were administered 0.25 ml of solution by gavage every other day for a total of 3 times (400 mg/kg body-weight, final dosage of 30 mg).

After the treatment, mice were kept in the same condition as described above.

4.12. Perfusion

Prior to perfusion, mice received an intra-peritoneal injection of Ketamin-Rompun anaesthetic and their limbs were immobilised to expose the abdomen.

At the same time, an isotonic solution of Phosphate-Buffered Saline (PBS) was continuously

Materials and Methods

loaded by a pump system and released through a thin cannula.

After opening skin and muscles of the mouse to reveal the abdominal cavity, the cut was extended more rostrally through the diaphragm until the heart was fully visible, taking care not to injure other organs in the process. The cannula connected to the pump was then inserted in the left ventricle and a resection was performed at the right atrium. This operation allowed for continuous circulation of PBS in the mouse and thus for complete removal of the blood in the whole circulatory system prior to fixative introduction.

Following clearance from blood, the pump was connected to a 4% solution of PFA in PBS, which was ultimately left to circulate in the organism for 30 minutes.

The brain was then carefully removed from the skull and post-fixed in 4% PFA at 4°C for 2 hours (Ring1B experiments) or over-night (reprogramming experiments). The shorter fixation time was necessary for immunohistochemical staining of sensitive proteins (e.g. NG2), while longer fixation times improved immunohistochemistry of nuclear proteins.

Ketamin-Rompun Anaesthetic

100 mg/ml Ketamin	4.4 ml
2% Rompun	1.08 ml
NaCl	To volume (12 ml)

Phosphate-Buffered Saline (PBS) 10x

NaCl	400 g
KCl	10 g
KH ₂ PO ₄	10 g
Na ₂ HPO ₄	58.75 g
Bi-distilled water	To volume (5 L)

Final pH=7.4

Autoclave prior to use; dilute in water to obtain 1x.

20% Paraformaldehyde (PFA) in PBS

Na ₂ HPO ₄	134 g
Paraformaldehyde (PFA)	400 g
Bi-distilled water	To volume (2 L)
32% NaOH	To better dissolve PFA

Final pH=7.4

Filter and aliquot, then freeze at -20°C. Dilute to 4% in 1x PBS and measure pH again prior to use.

4.13. Vibrating microtome (free-floating sections)

PFA-fixed brains were washed twice for 5 minutes in PBS and allowed to dry. For reprogramming experiments, both cerebellum and olfactory bulbs were removed and the brain was placed vertically in a plastic embedding mold. A mix of 4% Agarose/water was then poured in the mould and left to polymerize at room temperature. The block of agarose was subsequently fixed in the vibrating microtome and 60 µm-thick coronal sections were sequentially collected in a 24-well plate filled with 1x PBS.

For Ring1B experiments, the brains were washed in PBS and allowed to dry, but in this case the olfactory bulbs were always maintained. For coronal sections, the brains were placed vertically in the embedding mould and further processed as described above. For sagittal sections, the cerebellum was not removed, but the two brain hemispheres were separated and placed in the embedding mould with the medial side touching the bottom. The thickness of the sections was always 60 µm, except for the experiments of retroviral delivery in the RMS (60-70 µm), which were followed by dendrite tracing of recombined neurons in the olfactory bulbs.

For long-term preservation, the tissue samples were transferred in tubes with Storing Solution and maintained at -20°C.

Phosphate-Buffered Saline (PBS) 10x

NaCl	400 g
KCl	10 g
KH ₂ PO ₄	10 g
Na ₂ HPO ₄	58.75 g
Bi-distilled water	To volume (5 L)

Final pH=7.4

Autoclave prior to use; dilute in water to obtain 1x.

Storing Solution (free-floating sections)

Glycerol	150 ml
Ethylenglycol	150 ml
PO ₄ buffer 10x	50 ml
Bi-distilled water	To volume (500 ml)

Materials and Methods

PO₄ buffer 10x

NaH ₂ PO ₄ x 2H ₂ O	65 g
NaOH	15 g
Final pH=7.2-7.4	
Bi-distilled water	To volume (400 ml)

4.14. Immunocytochemistry

Cells were fixed in 4% PFA in 1x PBS for 15 min at room temperature (RT), washed twice in PBS and incubated in Blocking Solution for 30 min at RT. The following primary antibodies were diluted in Blocking Solution as indicated and left over-night at 4°C on the specimens:

Antigen	Host	Isotype	Company		Dilution
Green Fluorescent Protein (GFP)	Chicken		Aves Labs	GFP-1020	1:1000
Red Fluorescent Protein (RFP)	Rat		Chromotek	5F8	1:500
Glial Fibrillary Acidic Protein (GFAP)	Rabbit		Dako Cytomation	Z0334	1:1000
β-III-Tubulin	Mouse	IgG2b	Sigma	T8660	1:500

After washing twice in PBS, cells were incubated in Blocking Solution with appropriate species- and/or subclass-specific secondary antibodies conjugated to CyTM3, CyTM5 (1:500, Jackson ImmunoResearch) or Alexa Fluor 488, 647 (1:500, Invitrogen) for 2h in the dark at RT, followed by extensive washing in PBS. After treatment with DAPI (1:1000 in PBS, Sigma, *D9564*) for 5 minutes, the coverslips were mounted with Aqua Poly/Mount (Polysciences, Warrington, PA).

Phosphate-Buffered Saline (PBS) 10x

NaCl	400 g
KCl	10 g
KH ₂ PO ₄	10 g
Na ₂ HPO ₄	58.75 g
Bi-distilled water	To volume (5 L)
Final pH=7.4	
Autoclave prior to use; dilute in water to obtain 1x.	

20% Paraformaldehyde (PFA) in PBS

Na ₂ HPO ₄	134 g
Paraformaldehyde (PFA)	400 g
Bi-distilled water	To volume (2 L)
32% NaOH	To better dissolve PFA
Final pH=7.4	

Filter and aliquot, then freeze at -20°C. Dilute to 4% in 1x PBS and measure pH again prior to use.

Blocking Solution (immunocytochemistry)

Bovine Serum Albumin (BSA)	2% in water
Triton X-100	0.1%
PBS	1x
Bi-distilled water	To volume

4.15. Immunohistochemistry

Free-floating sections cut at the vibrating microtome were rinsed twice in PBS and pre-incubated for 30-60 min in Blocking Solution at RT. The following primary antibodies were diluted in Blocking Solution and incubated with the sections for 48 hours at 4°C.

Antigen	Host	Isotype	Company	Dilution
Green Fluorescent Protein (GFP)	Chicken		Aves Labs GFP-1020	1:1000
Red Fluorescent Protein (RFP)	Rabbit		Rockland 600-401-379	1:500
mCherry	Goat		Acris AB0081-200	1:250
Doublecortin (DCX)	Guinea Pig		Millipore AB5910	1:100
NeuN	Mouse	IgG1	Chemicon MAB377	1:250
Myt1L	Rabbit		Courtesy of M. Wernig	1:200
MAP2	Mouse		Synaptic Systems 188011	1:200
Glial Fibrillary Acidic Protein (GFAP)	Mouse	IgG1	Sigma G3893	1:500
Glial Fibrillary Acidic Protein (GFAP)	Rabbit		Dako Cytomation Z0334	1:500
NG2	Rabbit		Millipore AB5320	1:500

Materials and Methods

Antigen	Host	Isotype	Company		Dilution
Ring1B	Mouse	IgG2b	MBL	D139-3	1:250
Tyrosine Hydroxylase (TH)	Mouse	IgG1	Millipore	MAB318	1:250
Calbindin D-28K	Rabbit		Millipore	AB1778	1:500
Calretinin	Mouse		Swant	6B3	1:1000
Parvalbumin	Mouse	IgG1	Sigma	P3088	1:500
GABA	Rabbit		Sigma	A2052	1:1000
Ctip2	Rat		Abcam	Ab18465	1:250
Cux1	Rabbit		Santa Cruz	sc-13024	1:250
Satb2	Mouse	IgG1	Abcam	Ab51502	1:250
FoxP2	Goat		Santa Cruz	sc-21069	1:250
Ki67	Rabbit		Thermo Fisher	RM-9106-S	1:100
Reelin	Mouse	IgG1	Millipore	MAB5364	1:500

Red label: heat-mediated antigen retrieval required.

After washing twice in PBS, secondary antibodies were diluted in blocking solution and incubated at RT for 2 hours. They were chosen according to the primary antibodies and were coupled to Alexa Fluor 488 or FITC, CyTM3, Alexa Fluor 647, CyTM5. For anti-mouse secondary immunostainings in the context of a lesion, isotype-specific antibodies were used.

Sections were then counterstained with DAPI (1:500 in 1x PBS) prior to mounting, as described above.

Blocking Solution (immunohistochemistry)

Bovine Serum Albumin (BSA)	2% in water
Triton X-100	0.5%
PBS	1x
Bi-distilled water	To volume

4.16. Heat-mediated antigen retrieval: Citrate Buffer

For some nuclear immunostaining (e.g. Ring1B), antigen retrieval procedures are required before the incubation step with the primary antibody.

To perform heat-mediated antigen retrieval, free-floating tissue samples were transferred into small tubes with pre-warmed Citrate Buffer and incubated for 20 minutes at 95°C in a dry bath, while kept in mild agitation to prevent folding of the sections.

Following the treatment, the sections were rinsed twice in PBS and incubated in Blocking

Solution with the primary antibody as described in the Immunohistochemistry section.

Citrate Buffer

Sodium citrate	0.384 g
Tween 20	0.05%
Bi-distilled water	To volume (200 ml)
Final pH=6.0	
Dissolved at 65-70°C	

4.17. MicroRNA (miRNA) design and cloning

To promote the knockdown of *Ring1B* expression levels, miRNAs were previously designed and tested by Dr. Sergio Gascón. The sequence of *Mus musculus* Ring1B/Rnf2 transcript (accession number NM_011277.2) was inserted in the BLOCK-iT™ RNAi Designer web tool (Thermo Fisher Scientific) and the default parameters were used (open reading frame as target, G/C percentage 35-55%). Three highly ranked miRNAs were chosen according to the targeted position on the mRNA in order to be sufficiently spaced.

Select	No.	Start	Oligo Type	Oligo Sequence
✓	1	199	Top Strand	5'- TGCTGTTTCCAAGCCATCTGTTATTGGTTTTGGCCACTGACTGACCAATAACATGGCTTGGAAA -3'
			Bottom Strand	5'- CCTGTTTCCAAGCCATGTTATTGGTCAGTCAGTGGCCAAAACCAATAACAGATGGCTTGGAAAC -3'
			ds Oligo	5'- TGCTGTTTCCAAGCCATCTGTTATTGGTTTTGGCCACTGACTGACCAATAACATGGCTTGGAAA -3'
				3'- CAAAGGTTCCGTAGACAATAACCAAAACCGGTGACTGACTGGTTATTGTACCGAACCTTGTCC -5'
✓	2	441	Top Strand	5'- TGCTGATCACGACTGGGATAAATCTTGTGTTTTGGCCACTGACTGACAAAGATTACCACTCGTGAT -3'
			Bottom Strand	5'- CCTGATCACGACTGGTAAATCTTGTGTCAGTCAGTGGCCAAAACAGATTATCCAGTCGTGATC -3'
			ds Oligo	5'- TGCTGATCACGACTGGGATAAATCTTGTGTTTTGGCCACTGACTGACAAAGATTACCACTCGTGAT -3'
				3'- CTAGTGCTGACCTATTAGAACAAAACCGGTGACTGACTGTTCTAAATGGTCAGCACTAGTCC -5'
✓	3	746	Top Strand	5'- TGCTGATGACTGGATCAATCGCCACTGTTTTGGCCACTGACTGACAGTGGCGAGATCCAGTCAT -3'
			Bottom Strand	5'- CCTGATGACTGGATCTCGCCACTGTCAGTCAGTGGCCAAAACAGTGGCGATTGATCCAGTCATC -3'
			ds Oligo	5'- TGCTGATGACTGGATCAATCGCCACTGTTTTGGCCACTGACTGACAGTGGCGAGATCCAGTCAT -3'
				3'- CTACTGACCTAGTTAGCGGTGACAAAACCGGTGACTGACTGTCAACCGCTCTAGTCAGTAGTCC -5'

Following annealing of the complementary sequences, the miRNAs were individually cloned in the pcDNA™ 6.2-GW vector. The resulting construct was transfected in HEK293 cells together with a plasmid encoding for GFP (to visualise the targeted cells) and another encoding for Ring1B. The reduction in Ring1B protein levels was assessed by Western Blot using a commercially available antibody (MBL, D139-3).

The three miRNAs were then chain-cloned in the same pcDNA™ 6.2-GW vector using the

BLOCK-iT™ Pol II miR RNAi Expression Vector Kits (Thermo Fisher Scientific). The efficacy of the knockdown was assessed by lipofection of the construct in a postnatal (P5) primary astrocyte culture, followed by immunostaining for Ring1B (see Immunohistochemistry section).

4.18. Image acquisition and elaboration

Immunostainings were analyzed with a LSM710 laser-scanning confocal microscope or Axio Observer Z1 epifluorescence microscope (Carl Zeiss) and all digital images were acquired using the ZEN software (Carl Zeiss) with a 25x or 40x objective.

The generated files were opened and initially processed with the open-source software Fiji (Schindelin et al., 2012).

4.19. Quantifications and statistics

For *in vitro* experiments, all transfected cells (3-4 different culture passages from 1 experimental batch used for the transfections, 2 coverslips per condition) were counted directly at the epifluorescence microscope on the basis of the reporter (RFP) and β -III-tubulin immunostainings.

For *in vivo* experiments, 3-9 mouse sections per animal were used for immunostaining and pictures of the areas of interest were acquired with the laser-scanning confocal microscope (Carl Zeiss) at 25x or 40x magnification and further processed with Fiji software. In particular, all cell counts were performed with the Cell Counter built-in plugin. Soma volume was semi-automatically estimated with the Volumest plugin (Merzin, 2008) based on Cavalieri method. For this analysis, NeuN immunostaining was preferred over RFP or GFP, whose intensity of the signal could bias the actual measurement of the soma. For semi-automatic dendrite tracing in both olfactory bulbs and hippocampi of Ring1B^{+/+} and Ring1B ^{Δ/Δ} mice, sufficiently isolated recombined cells were selected and analysed with the Simple Neurite Tracer plugin.

The data were tested for significance using unpaired t test or one-/two-way ANOVA analysis (no repeated measurements) with Tukey's correction for multiple comparisons (Prism 6, GraphPad). In the latter case, asterisks in the plots represent multiplicity adjusted P-values.

All error bars indicate \pm standard deviation.

5. References

- Agoston, Z., Heine, P., Brill, M.S., Grebbin, B.M., Hau, A.-C., Kallenborn-Gerhardt, W., Schramm, J., Götz, M., and Schulte, D. (2014). Meis2 is a Pax6 co-factor in neurogenesis and dopaminergic periglomerular fate specification in the adult olfactory bulb. *Development* 141, 28–38.
- Akhtar, A.A., and Breunig, J.J. (2015). Lost highway(s): barriers to postnatal cortical neurogenesis and implications for brain repair. *Front. Cell. Neurosci.* 9, 216.
- Akhtar, R.S., Ness, J.M., and Roth, K.A. (2004). Bcl-2 family regulation of neuronal development and neurodegeneration. *Biochim. Biophys. Acta - Mol. Cell Res.* 1644, 189–203.
- Alcamo, E.A., Chirivella, L., Dautzenberg, M., Dobрева, G., Fariñas, I., Grosschedl, R., and McConnell, S.K. (2008). Satb2 regulates callosal projection neuron identity in the developing cerebral cortex. *Neuron* 57, 364–377.
- Allen, Z.J., Waclaw, R.R., Colbert, M.C., and Campbell, K. (2007). Molecular identity of olfactory bulb interneurons: Transcriptional codes of periglomerular neuron subtypes. *J. Mol. Histol.* 38, 517–525.
- Alvarez-Buylla, A., and Ihrie, R.A. (2014). Sonic hedgehog signaling in the postnatal brain. *Semin. Cell Dev. Biol.*
- Alvarez-Buylla, a., Merkle, F., and Fuentealba, L. (2013). Neurogenesis in the Postnatal VZ-SVZ and the Origin of Interneuron Diversity (Elsevier Inc.).
- Amamoto, R., and Arlotta, P. (2014). Development-inspired reprogramming of the mammalian central nervous system. *Science* 343, 1239882.
- Arlotta, P., and Berninger, B. (2014). Brains in metamorphosis: reprogramming cell identity within the central nervous system. *Curr. Opin. Neurobiol.* 27, 208–214.
- Arlotta, P., Molyneaux, B.J., Chen, J., Inoue, J., Kominami, R., and Macklis, J.D. (2005). Neuronal subtype-specific genes that control corticospinal motor neuron development in vivo. *Neuron* 45, 207–221.
- Arnold, S.J., Huang, G.-J., Cheung, A.F.P., Era, T., Nishikawa, S.-I., Bikoff, E.K., Molnár, Z., Robertson, E.J., and Groszer, M. (2008). The T-box transcription factor Eomes/Tbr2 regulates neurogenesis in the cortical subventricular zone. *Genes Dev.* 22, 2479–2484.
- Azim, K., Rivera, A., Raineteau, O., and Butt, A.M. (2014a). GSK3 β regulates oligodendrogenesis in the dorsal microdomain of the subventricular zone via Wnt- β -catenin signaling. *Glia* 62, 778–779.

References

- Azim, K., Fischer, B., Hurtado-Chong, A., Draganova, K., Cantù, C., Zemke, M., Sommer, L., Butt, A., Raineteau, O., Cantù, C., et al. (2014b). Persistent wnt/ β -catenin signaling determines dorsalization of the postnatal subventricular zone and neural stem cell specification into oligodendrocytes and glutamatergic neurons. *Stem Cells* 32, 1301–1312.
- Azim, K., Hurtado-Chong, A., Fischer, B., Kumar, N., Zweifel, S., Taylor, V., and Raineteau, O. (2015). Transcriptional Hallmarks of Heterogeneous Neural Stem Cell Niches of the Subventricular Zone. *Stem Cells* 33, 2232–2242.
- Bagley, J., LaRocca, G., Jimenez, D.A., and Urban, N.N. (2007). Adult neurogenesis and specific replacement of interneuron subtypes in the mouse main olfactory bulb. *BMC Neurosci.* 8, 92.
- Bao, B.-Y., Ting, H.-J., Hsu, J.-W., and Lee, Y.-F. (2008). Protective role of 1 α , 25-dihydroxyvitamin D3 against oxidative stress in nonmalignant human prostate epithelial cells. *Int. J. Cancer* 122, 2699–2706.
- Batista-Brito, R., Close, J., Machold, R., and Fishell, G. (2008). The Distinct Temporal Origins of Olfactory Bulb Interneuron Subtypes. *J. Neurosci.* 28, 3966–3975.
- Beckervordersandforth, R., Zhang, C., and Lie, D.C. (2015). Transcription-Factor-Dependent Control of Adult Hippocampal Neurogenesis. *Cold Spring Harb. Perspect. Biol.* 7, a018879.
- Bélanger, M., Allaman, I., and Magistretti, P.J. (2011). Brain energy metabolism: focus on astrocyte-neuron metabolic cooperation. *Cell Metab.* 14, 724–738.
- Berninger, B., Costa, M.R., Koch, U., Schroeder, T., Sutor, B., Grothe, B., and Götz, M. (2007). Functional properties of neurons derived from in vitro reprogrammed postnatal astroglia. *J. Neurosci.* 27, 8654–8664.
- Blackledge, N.P., Farcas, A.M., Kondo, T., King, H.W., McGouran, J.F., Hanssen, L.L.P., Ito, S., Cooper, S., Kondo, K., Koseki, Y., et al. (2014). Variant PRC1 complex-dependent H2A ubiquitylation drives PRC2 recruitment and polycomb domain formation. *Cell* 157, 1445–1459.
- Blackledge, N.P., Rose, N.R., and Klose, R.J. (2015). Targeting Polycomb systems to regulate gene expression: modifications to a complex story. *Nat. Rev. Mol. Cell Biol.*
- Blanchart, A., De Carlos, J.A., and López-Mascaraque, L. (2006). Time frame of mitral cell development in the mice olfactory bulb. *J. Comp. Neurol.* 496, 529–543.
- Blum, R., Heinrich, C., Sánchez, R., Lepier, A., Gundelfinger, E.D., Berninger, B., and Götz, M. (2011). Neuronal network formation from reprogrammed early postnatal rat cortical glial

- cells. *Cereb. Cortex* *21*, 413–424.
- Bond, A.M., Ming, G.-L., and Song, H. (2015). Adult Mammalian Neural Stem Cells and Neurogenesis: Five Decades Later. *Cell Stem Cell* *17*, 385–395.
- Borrell, V., and Götz, M. (2014). Role of radial glial cells in cerebral cortex folding. *Curr. Opin. Neurobiol.* *27*, 39–46.
- Bovetti, S., Hsieh, Y.-C., Bovolin, P., Perroteau, I., Kazunori, T., and Puche, A.C. (2007). Blood vessels form a scaffold for neuroblast migration in the adult olfactory bulb. *J. Neurosci.* *27*, 5976–5980.
- Boyer, L.A., Plath, K., Zeitlinger, J., Brambrink, T., Medeiros, L.A., Lee, T.I., Levine, S.S., Wernig, M., Tajonar, A., Ray, M.K., et al. (2006). Polycomb complexes repress developmental regulators in murine embryonic stem cells. *Nature* *441*, 349–353.
- Brandão, J.A., and Romcy-Pereira, R.N. (2015). Interplay of environmental signals and progenitor diversity on fate specification of cortical GABAergic neurons. *Front. Cell. Neurosci.* *9*, 149.
- Brill, M.S., Snappyan, M., Wohlfrom, H., Ninkovic, J., Jawerka, M., Mastick, G.S., Ashery-Padan, R., Saghatelian, A., Berninger, B., and Götz, M. (2008). A *dlx2*- and *pax6*-dependent transcriptional code for periglomerular neuron specification in the adult olfactory bulb. *J. Neurosci.* *28*, 6439–6452.
- Brill, M.S., Ninkovic, J., Winpenny, E., Hodge, R.D., Ozen, I., Yang, R., Lepier, A., Gascón, S., Erdelyi, F., Szabo, G., et al. (2009). Adult generation of glutamatergic olfactory bulb interneurons. *Nat. Neurosci.* *12*, 1524–1533.
- Britanova, O., de Juan Romero, C., Cheung, A., Kwan, K.Y., Schwark, M., Gyorgy, A., Vogel, T., Akopov, S., Mitkovski, M., Agoston, D., et al. (2008). *Satb2* is a postmitotic determinant for upper-layer neuron specification in the neocortex. *Neuron* *57*, 378–392.
- Buettner, G.R. (1993). The pecking order of free radicals and antioxidants: lipid peroxidation, alpha-tocopherol, and ascorbate. *Arch. Biochem. Biophys.* *300*, 535–543.
- Buffo, A., Vosko, M.R., Ertürk, D., Hamann, G.F., Jucker, M., Rowitch, D., and Götz, M. (2005). Expression pattern of the transcription factor *Olig2* in response to brain injuries: implications for neuronal repair. *Proc. Natl. Acad. Sci. U. S. A.* *102*, 18183–18188.
- Caiazzo, M., Dell’Anno, M.T., Dvoretzkova, E., Lazarevic, D., Taverna, S., Leo, D., Sotnikova, T.D., Menegon, A., Roncaglia, P., Colciago, G., et al. (2011). Direct generation of functional dopaminergic neurons from mouse and human fibroblasts. *Nature* *476*, 224–

References

227.

- Calés, C., Román-Trufero, M., Pavón, L., Serrano, I., Melgar, T., Endoh, M., Pérez, C., Koseki, H., and Vidal, M. (2008). Inactivation of the polycomb group protein Ring1B unveils an antiproliferative role in hematopoietic cell expansion and cooperation with tumorigenesis associated with Ink4a deletion. *Mol. Cell. Biol.* 28, 1018–1028.
- Calzolari, F., Michel, J., Baumgart, E.V., Theis, F., Götz, M., and Ninkovic, J. (2015). Fast clonal expansion and limited neural stem cell self-renewal in the adult subependymal zone. *Nat. Neurosci.* 18, 490–492.
- Cao, G., Gu, M., Zhu, M., Gao, J., Yin, Y., Marshall, C., Xiao, M., Ding, J., and Miao, D. (2012). Bmi-1 absence causes premature brain degeneration. *PLoS One* 7, e32015.
- Caubit, X., Tiveron, M.-C., Cremer, H., and Fasano, L. (2005). Expression patterns of the three Teashirt-related genes define specific boundaries in the developing and postnatal mouse forebrain. *J. Comp. Neurol.* 486, 76–88.
- Cave, J.W., Akiba, Y., Banerjee, K., Bhosle, S., Berlin, R., and Baker, H. (2010). Differential regulation of dopaminergic gene expression by Er81. *J. Neurosci.* 30, 4717–4724.
- Ceizar, M., Dhaliwal, J., Xi, Y., Smallwood, M., Kumar, K.L., and Lagace, D.C. (2016). Bcl-2 is required for the survival of doublecortin-expressing immature neurons. *Hippocampus* 26, 211–219.
- Chanda, S., Ang, C.E., Davila, J., Pak, C., Mall, M., Lee, Q.Y., Ahlenius, H., Jung, S.W., Südhof, T.C., and Wernig, M. (2014). Generation of Induced Neuronal Cells by the Single Reprogramming Factor ASCL1. *Stem Cell Reports* 3, 282–296.
- Chang, M.-Y., Sun, W., Ochiai, W., Nakashima, K., Kim, S.-Y., Park, C.-H., Kang, J.S., Shim, J.-W., Jo, A.-Y., Kang, C.-S., et al. (2007). Bcl-XL/Bax proteins direct the fate of embryonic cortical precursor cells. *Mol. Cell. Biol.* 27, 4293–4305.
- Chen, B., Schaeviz, L.R., and McConnell, S.K. (2005a). Fezl regulates the differentiation and axon targeting of layer 5 subcortical projection neurons in cerebral cortex. *Proc. Natl. Acad. Sci. U. S. A.* 102, 17184–17189.
- Chen, B., Wang, S.S., Hattox, A.M., Rayburn, H., Nelson, S.B., and McConnell, S.K. (2008). The Fezf2-Ctip2 genetic pathway regulates the fate choice of subcortical projection neurons in the developing cerebral cortex. *Proc. Natl. Acad. Sci. U. S. A.* 105, 11382–11387.
- Chen, J., Guo, L., Zhang, L., Wu, H., Yang, J., Liu, H., Wang, X., Hu, X., Gu, T., Zhou, Z., et al. (2013). Vitamin C modulates TET1 function during somatic cell reprogramming. *Nat.*

- Genet. *45*, 1504–1509.
- Chen, J., Xu, H., Zou, X., Wang, J., Zhu, Y., Chen, H., Shen, B., Deng, X., Zhou, A., Chin, Y.E., et al. (2014). Snail recruits Ring1B to mediate transcriptional repression and cell migration in pancreatic cancer cells. *Cancer Res.* *74*, 4353–4363.
- Chen, J.-G., Rasin, M.-R., Kwan, K.Y., and Sestan, N. (2005b). Zfp312 is required for subcortical axonal projections and dendritic morphology of deep-layer pyramidal neurons of the cerebral cortex. *Proc. Natl. Acad. Sci. U. S. A.* *102*, 17792–17797.
- Chen, R., Valencia, I., Zhong, F., McColl, K.S., Roderick, H.L., Bootman, M.D., Berridge, M.J., Conway, S.J., Holmes, A.B., Mignery, G.A., et al. (2004). Bcl-2 functionally interacts with inositol 1,4,5-trisphosphate receptors to regulate calcium release from the ER in response to inositol 1,4,5-trisphosphate. *J. Cell Biol.* *166*, 193–203.
- Chen, R., Lin, C., You, Y., and Liu, F. (2012). Characterization of immature and mature 5-hydroxytryptamine 3A receptor-expressing cells within the adult SVZ-RMS-OB system. *Neuroscience* *227*, 180–190.
- de Chevigny, A., Coré, N., Follert, P., Gaudin, M., Barbry, P., Béclin, C., and Cremer, H. (2012a). miR-7a regulation of Pax6 controls spatial origin of forebrain dopaminergic neurons. *Nat. Neurosci.* *15*, 1120–1126.
- de Chevigny, A., Core, N., Follert, P., Wild, S., Bosio, A., Yoshikawa, K., Cremer, H., and Beclin, C. (2012b). Dynamic expression of the pro-dopaminergic transcription factors Pax6 and Dlx2 during postnatal olfactory bulb neurogenesis. *Front. Cell. Neurosci.* *6*, 6.
- Colasante, G., Lignani, G., Rubio, A., Medrihan, L., Yekhlief, L., Sessa, A., Massimino, L., Giannelli, S.G., Sacchetti, S., Caiazzo, M., et al. (2015). Rapid Conversion of Fibroblasts into Functional Forebrain GABAergic Interneurons by Direct Genetic Reprogramming. *Cell Stem Cell*.
- Corbin, J.G., and Butt, S.J.B. (2011). Developmental mechanisms for the generation of telencephalic interneurons. *Dev. Neurobiol.* *71*, 710–732.
- Corley, M., and Kroll, K.L. (2014). The roles and regulation of Polycomb complexes in neural development. *Cell Tissue Res.*
- Di Croce, L., and Helin, K. (2013). Transcriptional regulation by Polycomb group proteins. *Nat. Struct. Mol. Biol.* *20*, 1147–1155.
- Czabotar, P.E., Lessene, G., Strasser, A., and Adams, J.M. (2014). Control of apoptosis by the BCL-2 protein family: implications for physiology and therapy. *Nat. Rev. Mol. Cell Biol.*

References

15, 49–63.

- Dametti, S., Faravelli, I., Ruggieri, M., Ramirez, A., Nizzardo, M., and Corti, S. (2016). Experimental Advances Towards Neural Regeneration from Induced Stem Cells to Direct In Vivo Reprogramming. *Mol. Neurobiol.* 53, 2124–2131.
- Davenne, M. (2005). In Vivo Imaging of Migrating Neurons in the Mammalian Forebrain. *Chem. Senses* 30, i115–i116.
- Díaz-Guerra, E., Pignatelli, J., Nieto-Estévez, V., and Vicario-Abejón, C. (2013). Transcriptional regulation of olfactory bulb neurogenesis. *Anat. Rec. (Hoboken)*. 296, 1364–1382.
- Ding, N., Yu, R.T., Subramaniam, N., Sherman, M.H., Wilson, C., Rao, R., Leblanc, M., Coulter, S., He, M., Scott, C., et al. (2013). A vitamin D receptor/SMAD genomic circuit gates hepatic fibrotic response. *Cell* 153, 601–613.
- Dong, J., Wong, S.L., Lau, C.W., Lee, H.K., Ng, C.F., Zhang, L., Yao, X., Chen, Z.Y., Vanhoutte, P.M., and Huang, Y. (2012). Calcitriol protects renovascular function in hypertension by down-regulating angiotensin II type 1 receptors and reducing oxidative stress. *Eur. Heart J.* 33, 2980–2990.
- Endoh, M., Endo, T. a, Endoh, T., Fujimura, Y., Ohara, O., Toyoda, T., Otte, A.P., Okano, M., Brockdorff, N., Vidal, M., et al. (2008). Polycomb group proteins Ring1A/B are functionally linked to the core transcriptional regulatory circuitry to maintain ES cell identity. *Development* 135, 1513–1524.
- Endoh, M., Endo, T. a, Endoh, T., Isono, K., Sharif, J., Ohara, O., Toyoda, T., Ito, T., Eskeland, R., Bickmore, W. a, et al. (2012). Histone H2A mono-ubiquitination is a crucial step to mediate PRC1-dependent repression of developmental genes to maintain ES cell identity. *PLoS Genet.* 8, e1002774.
- Englund, C., Fink, A., Lau, C., Pham, D., Daza, R. a M., Bulfone, A., Kowalczyk, T., and Hevner, R.F. (2005). Pax6, Tbr2, and Tbr1 are expressed sequentially by radial glia, intermediate progenitor cells, and postmitotic neurons in developing neocortex. *J. Neurosci.* 25, 247–251.
- Eskeland, R., Leeb, M., Grimes, G.R., Kress, C., Boyle, S., Sproul, D., Gilbert, N., Fan, Y., Skoultschi, A.I., Wutz, A., et al. (2010). Ring1B compacts chromatin structure and represses gene expression independent of histone ubiquitination. *Mol. Cell* 38, 452–464.
- Esteban, M.A., Wang, T., Qin, B., Yang, J., Qin, D., Cai, J., Li, W., Weng, Z., Chen, J., Ni, S., et al. (2010). Vitamin C enhances the generation of mouse and human induced pluripotent stem cells. *Cell Stem Cell* 6, 71–79.

- Fasano, C.A., Dimos, J.T., Ivanova, N.B., Lowry, N., Lemischka, I.R., and Temple, S. (2007). shRNA knockdown of Bmi-1 reveals a critical role for p21-Rb pathway in NSC self-renewal during development. *Cell Stem Cell* 1, 87–99.
- Fasano, C.A., Phoenix, T.N., Kokovay, E., Lowry, N., Elkabetz, Y., Dimos, J.T., Lemischka, I.R., Studer, L., and Temple, S. (2009). Bmi-1 cooperates with Foxg1 to maintain neural stem cell self-renewal in the forebrain. *Genes Dev.* 23, 561–574.
- Feliciano, D.M., and Bordey, A. (2013). Newborn cortical neurons: only for neonates? *Trends Neurosci.* 36, 51–61.
- Ferland, R.J., Cherry, T.J., Preware, P.O., Morrissey, E.E., and Walsh, C.A. (2003). Characterization of Foxp2 and Foxp1 mRNA and protein in the developing and mature brain. *J. Comp. Neurol.* 460, 266–279.
- Fernández, M.E., Croce, S., Boutin, C., Cremer, H., and Raineteau, O. (2011). Targeted electroporation of defined lateral ventricular walls: a novel and rapid method to study fate specification during postnatal forebrain neurogenesis. *Neural Dev.* 6, 13.
- Fiorelli, R., Azim, K., Fischer, B., and Raineteau, O. (2015). Adding a spatial dimension to postnatal ventricular-subventricular zone neurogenesis. *Development* 142, 2109–2120.
- Flames, N., Pla, R., Gelman, D.M., Rubenstein, J.L.R., Puellas, L., and Marín, O. (2007). Delineation of multiple subpallial progenitor domains by the combinatorial expression of transcriptional codes. *J. Neurosci.* 27, 9682–9695.
- Fode, C., Ma, Q., Casarosa, S., Ang, S.-L., Anderson, D.J., and Guillemot, F. (2000). A role for neural determination genes in specifying the dorsoventral identity of telencephalic neurons. *Genes & Dev.* 14, 67–80.
- Fuentealba, L.C., Rompani, S.B., Parraguez, J.I., Obernier, K., Romero, R., Cepko, C.L., and Alvarez-Buylla, A. (2015). Embryonic Origin of Postnatal Neural Stem Cells. *Cell* 161, 1644–1655.
- Gascón, S., Murenu, E., Masserdotti, G., Ortega, F., Russo, G.L., Petrik, D., Deshpande, A., Heinrich, C., Karow, M., Robertson, S.P., et al. (2016). Identification and Successful Negotiation of a Metabolic Checkpoint in Direct Neuronal Reprogramming. *Cell Stem Cell* 18, 396–409.
- Gebara, E., Bonaguidi, M.A., Beckervordersandforth, R., Sultan, S., Udry, F., Gijs, P.-J., Lie, D.C., Ming, G.-L., Song, H., and Toni, N. (2016). Heterogeneity of Radial Glia-Like Cells in the Adult Hippocampus. *Stem Cells*.

References

- Ghashghaei, H.T., Lai, C., and Anton, E.S. (2007). Neuronal migration in the adult brain: are we there yet? *Nat. Rev. Neurosci.* 8, 141–151.
- Gil, J., and O’Loghlen, A. (2014). PRC1 complex diversity: where is it taking us? *Trends Cell Biol.*
- Goldman, S.A. (2016). Stem and Progenitor Cell-Based Therapy of the Central Nervous System: Hopes, Hype, and Wishful Thinking. *Cell Stem Cell* 18, 174–188.
- Götz, M., and Huttner, W.B. (2005). The cell biology of neurogenesis. *Nat. Rev. Mol. Cell Biol.* 6, 777–788.
- Grande, A., Sumiyoshi, K., López-Juárez, A., Howard, J., Sakthivel, B., Aronow, B., Campbell, K., and Nakafuku, M. (2013). Environmental impact on direct neuronal reprogramming in vivo in the adult brain. *Nat. Commun.* 4, 2373.
- Greig, L.C., Woodworth, M.B., Galazo, M.J., Padmanabhan, H., and Macklis, J.D. (2013). Molecular logic of neocortical projection neuron specification, development and diversity. *Nat. Rev. Neurosci.* 14, 755–769.
- Guo, F., Maeda, Y., Ma, J., Xu, J., Horiuchi, M., Miers, L., Vaccarino, F., and Pleasure, D. (2010). Pyramidal neurons are generated from oligodendroglial progenitor cells in adult piriform cortex. *J. Neurosci.* 30, 12036–12049.
- Guo, Z., Zhang, L., Wu, Z., Chen, Y., Wang, F., and Chen, G. (2014a). In Vivo direct reprogramming of reactive glial cells into functional neurons after brain injury and in an Alzheimer’s disease model. *Cell Stem Cell* 14, 188–202.
- Guo, Z., Zhang, L., Wu, Z., Chen, Y., Wang, F., and Chen, G. (2014b). In Vivo direct reprogramming of reactive glial cells into functional neurons after brain injury and in an Alzheimer’s disease model. *Cell Stem Cell* 14, 188–202.
- Haba, H., Nomura, T., Suto, F., and Osumi, N. (2009). Subtype-specific reduction of olfactory bulb interneurons in Pax6 heterozygous mutant mice. *Neurosci. Res.* 65, 116–121.
- Hack, I., Bancila, M., Loulier, K., Carroll, P., and Cremer, H. (2002). Reelin is a detachment signal in tangential chain-migration during postnatal neurogenesis. *Nat. Neurosci.* 5, 939–945.
- Hack, M.A., Saghatelian, A., de Chevigny, A., Pfeifer, A., Ashery-Padan, R., Lledo, P.-M., and Götz, M. (2005). Neuronal fate determinants of adult olfactory bulb neurogenesis. *Nat. Neurosci.* 8, 865–872.
- Hand, R., and Polleux, F. (2011). Neurogenin2 regulates the initial axon guidance of cortical pyramidal neurons projecting medially to the corpus callosum. *Neural Dev.* 6, 30.

- Harrington, M.J., Hong, E., and Brewster, R. (2009). Comparative analysis of neurulation: first impressions do not count. *Mol. Reprod. Dev.* 76, 954–965.
- Hawkins, K.E., Joy, S., Delhove, J.M.K.M., Kotiadis, V.N., Fernandez, E., Fitzpatrick, L.M., Whiteford, J.R., King, P.J., Bolanos, J.P., Duchen, M.R., et al. (2016). NRF2 Orchestrates the Metabolic Shift during Induced Pluripotent Stem Cell Reprogramming. *Cell Rep.*
- He, S., Guo, Y., Zhang, Y., Li, Y., Feng, C., Li, X., Lin, L., Guo, L., Wang, H., Liu, C., et al. (2015). Reprogramming somatic cells to cells with neuronal characteristics by defined medium both in vitro and in vivo. *Cell Regen. (London, England)* 4, 12.
- Heinbockel, T., Laaris, N., and Ennis, M. (2007). Metabotropic glutamate receptors in the main olfactory bulb drive granule cell-mediated inhibition. *J. Neurophysiol.* 97, 858–870.
- Heinrich, C., Blum, R., Gascón, S., Masserdotti, G., Tripathi, P., Sánchez, R., Tiedt, S., Schroeder, T., Götz, M., and Berninger, B. (2010). Directing astroglia from the cerebral cortex into subtype specific functional neurons. *PLoS Biol.* 8, e1000373.
- Heinrich, C., Gascón, S., Masserdotti, G., Lepier, A., Sanchez, R., Simon-Ebert, T., Schroeder, T., Götz, M., and Berninger, B. (2011). Generation of subtype-specific neurons from postnatal astroglia of the mouse cerebral cortex. *Nat. Protoc.* 6, 214–228.
- Heinrich, C., Bergami, M., Gascón, S., Lepier, A., Viganò, F., Dimou, L., Sutor, B., Berninger, B., and Götz, M. (2014). Sox2-Mediated Conversion of NG2 Glia into Induced Neurons in the Injured Adult Cerebral Cortex. *Stem Cell Reports* 3, 1000–1014.
- Heins, N., Malatesta, P., Cecconi, F., Nakafuku, M., Tucker, K.L., Hack, M. a, Chapouton, P., Barde, Y.-A., and Götz, M. (2002). Glial cells generate neurons: the role of the transcription factor Pax6. *Nat. Neurosci.* 5, 308–315.
- Hirabayashi, Y., and Gotoh, Y. (2010a). Epigenetic control of neural precursor cell fate during development. *Nat. Rev. Neurosci.* 11, 377–388.
- Hirabayashi, Y., and Gotoh, Y. (2010b). Epigenetic control of neural precursor cell fate during development. *Nat. Rev. Neurosci.* 11, 377–388.
- Hirabayashi, Y., Suzuki, N., Tsuboi, M., Endo, T.A., Toyoda, T., Shinga, J., Koseki, H., Vidal, M., and Gotoh, Y. (2009). Polycomb limits the neurogenic competence of neural precursor cells to promote astrogenic fate transition. *Neuron* 63, 600–613.
- Hsieh, J. (2012). Orchestrating transcriptional control of adult neurogenesis. *Genes Dev.* 26, 1010–1021.
- Ichida, J.K., and Kiskinis, E. (2015). Probing disorders of the nervous system using

References

- reprogramming approaches. *EMBO J.* 34, 1456–1477.
- Ihrie, R.A., Shah, J.K., Harwell, C.C., Levine, J.H., Guinto, C.D., Lezameta, M., Kriegstein, A.R., and Alvarez-Buylla, A. (2011). Persistent sonic hedgehog signaling in adult brain determines neural stem cell positional identity. *Neuron* 71, 250–262.
- Illingworth, R.S., Moffat, M., Mann, A.R., Read, D., Hunter, C.J., Pradeepa, M.M., Adams, I.R., and Bickmore, W. a (2015). The E3 ubiquitin ligase activity of RING1B is not essential for early mouse development. *Genes Dev.* 1897–1902.
- Imamura, F., and Greer, C.A. (2013). Pax6 regulates Tbr1 and Tbr2 expressions in olfactory bulb mitral cells. *Mol. Cell. Neurosci.* 54, 58–70.
- Imamura, F., Nagao, H., Naritsuka, H., Murata, Y., Taniguchi, H., and Mori, K. (2006). A leucine-rich repeat membrane protein, 5T4, is expressed by a subtype of granule cells with dendritic arbors in specific strata of the mouse olfactory bulb. *J. Comp. Neurol.* 495, 754–768.
- Imamura, F., Ayoub, A.E., Rakic, P., and Greer, C. a (2011). Timing of neurogenesis is a determinant of olfactory circuitry. *Nat. Neurosci.* 14, 331–337.
- Imayoshi, I., and Kageyama, R. (2014). bHLH factors in self-renewal, multipotency, and fate choice of neural progenitor cells. *Neuron* 82, 9–23.
- Inoue, T., Ota, M., Ogawa, M., Mikoshiba, K., and Aruga, J. (2007). Zic1 and Zic3 regulate medial forebrain development through expansion of neuronal progenitors. *J. Neurosci.* 27, 5461–5473.
- Jiao, J., Huang, X., Feit-Leithman, R.A., Neve, R.L., Snider, W., Dartt, D.A., and Chen, D.F. (2005). Bcl-2 enhances Ca(2+) signaling to support the intrinsic regenerative capacity of CNS axons. *EMBO J.* 24, 1068–1078.
- Karakuzu, O., Wang, D.P., and Cameron, S. (2009). MIG-32 and SPAT-3A are PRC1 homologs that control neuronal migration in *Caenorhabditis elegans*. *Development* 136, 943–953.
- Karow, M., Sánchez, R., Schichor, C., Masserdotti, G., Ortega, F., Heinrich, C., Gascón, S., Khan, M.A., Lie, D.C., Dellavalle, A., et al. (2012). Reprogramming of pericyte-derived cells of the adult human brain into induced neuronal cells. *Cell Stem Cell* 11, 471–476.
- Kelsch, W., Mosley, C.P., Lin, C.-W., and Lois, C. (2007). Distinct mammalian precursors are committed to generate neurons with defined dendritic projection patterns. *PLoS Biol.* 5, e300.
- Kempermann, G., Song, H., and Gage, F.H. (2015). Neurogenesis in the Adult Hippocampus. *Cold Spring Harb. Perspect. Biol.* 7, a018812 – .

- Khan, A.A., Lee, A.J., and Roh, T.-Y. (2015). Polycomb group protein-mediated histone modifications during cell differentiation.
- Kida, Y.S., Kawamura, T., Wei, Z., Sogo, T., Jacinto, S., Shigeno, A., Kushige, H., Yoshihara, E., Liddle, C., Ecker, J.R., et al. (2015). ERRs Mediate a Metabolic Switch Required for Somatic Cell Reprogramming to Pluripotency. *Cell Stem Cell* 16, 547–555.
- Kohwi, M., Osumi, N., Rubenstein, J.L.R., and Alvarez-Buylla, A. (2005). Pax6 is required for making specific subpopulations of granule and periglomerular neurons in the olfactory bulb. *J. Neurosci.* 25, 6997–7003.
- Kohwi, M., Petryniak, M.A., Long, J.E., Ekker, M., Obata, K., Yanagawa, Y., Rubenstein, J.L.R., and Alvarez-Buylla, A. (2007). A subpopulation of olfactory bulb GABAergic interneurons is derived from Emx1- and Dlx5/6-expressing progenitors. *J. Neurosci.* 27, 6878–6891.
- Kondo, T., Ito, S., and Koseki, H. (2015). Polycomb in Transcriptional Phase Transition of Developmental Genes. *Trends Biochem. Sci.* 41, 9–19.
- Kosaka, T., and Kosaka, K. (2012). Further characterization of the juxtglomerular neurons in the mouse main olfactory bulb by transcription factors, Sp8 and Tbx21. *Neurosci. Res.* 73, 24–31.
- Kriegstein, A., and Alvarez-Buylla, A. (2009). The glial nature of embryonic and adult neural stem cells. *Annu. Rev. Neurosci.* 32, 149–184.
- Kronenberg, G., Gertz, K., Cheung, G., Buffo, A., Kettenmann, H., Götz, M., and Endres, M. (2010). Modulation of fate determinants Olig2 and Pax6 in resident glia evokes spiking neuroblasts in a model of mild brain ischemia. *Stroke.* 41, 2944–2949.
- Laugesen, A., and Helin, K. (2014). Chromatin repressive complexes in stem cells, development, and cancer. *Cell Stem Cell* 14, 735–751.
- Leeb, M., and Wutz, A. (2007). Ring1B is crucial for the regulation of developmental control genes and PRC1 proteins but not X inactivation in embryonic cells. *J. Cell Biol.* 178, 219–229.
- Lemasson, M., Saghatelian, A., Olivo-Marin, J.-C., and Lledo, P.-M. (2005). Neonatal and adult neurogenesis provide two distinct populations of newborn neurons to the mouse olfactory bulb. *J. Neurosci.* 25, 6816–6825.
- Li, X., Sun, C., Lin, C., Ma, T., Madhavan, M.C., Campbell, K., and Yang, Z. (2011). The transcription factor Sp8 is required for the production of parvalbumin-expressing

References

- interneurons in the olfactory bulb. *J. Neurosci.* *31*, 8450–8455.
- Lim, D.A., and Alvarez-Buylla, A. (2014). Adult neural stem cells stake their ground. *Trends Neurosci.* *37*, 563–571.
- Lim, D.A., and Alvarez-Buylla, A. (2016). The Adult Ventricular–Subventricular Zone (V–SVZ) and Olfactory Bulb (OB) Neurogenesis. *Cold Spring Harb. Perspect. Biol.* a018820.
- Liu, M.-L., Zang, T., Zou, Y., Chang, J.C., Gibson, J.R., Huber, K.M., and Zhang, C.-L. (2013). Small molecules enable neurogenin 2 to efficiently convert human fibroblasts into cholinergic neurons. *Nat. Commun.* *4*, 2183.
- Lledo, P.-M., and Saghatelian, A. (2005). Integrating new neurons into the adult olfactory bulb: joining the network, life-death decisions, and the effects of sensory experience. *Trends Neurosci.* *28*, 248–254.
- Lodato, S., and Arlotta, P. (2014). Generating Neuronal Diversity in the Mammalian Cerebral Cortex. *Annu. Rev. Cell Dev. Biol.* *31*, annurev – cellbio – 100814–125353.
- Lodato, S., Molyneaux, B.J., Zuccaro, E., Goff, L.A., Chen, H.-H., Yuan, W., Meleski, A., Takahashi, E., Mahony, S., Rinn, J.L., et al. (2014). Gene co-regulation by Fezf2 selects neurotransmitter identity and connectivity of corticospinal neurons. *Nat. Neurosci.* *17*, 1046–1054.
- Lois, C., García-Verdugo, J.-M., and Alvarez-Buylla, A. (1996). Chain Migration of Neuronal Precursors. *Science* (80-.). *271*, 978–981.
- López-Juárez, A., Howard, J., Ullom, K., Howard, L., Grande, A., Pardo, A., Waclaw, R., Sun, Y.-Y., Yang, D., Kuan, C.-Y., et al. (2013). Gsx2 controls region-specific activation of neural stem cells and injury-induced neurogenesis in the adult subventricular zone. *Genes Dev.* *27*, 1272–1287.
- De Marchis, S., Bovetti, S., Carletti, B., Hsieh, Y.-C., Garzotto, D., Peretto, P., Fasolo, A., Puche, A.C., and Rossi, F. (2007). Generation of distinct types of periglomerular olfactory bulb interneurons during development and in adult mice: implication for intrinsic properties of the subventricular zone progenitor population. *J. Neurosci.* *27*, 657–664.
- Masserdotti, G., Gillotin, S., Sutor, B., Drechsel, D., Irmeler, M., Jørgensen, H.F., Sass, S., Theis, F.J., Beckers, J., Berninger, B., et al. (2015). Transcriptional Mechanisms of Proneural Factors and REST in Regulating Neuronal Reprogramming of Astrocytes. *Cell Stem Cell* *17*, 74–88.
- Merkle, F.T., Tramontin, A.D., García-Verdugo, J.M., and Alvarez-Buylla, A. (2004). Radial glia give rise to adult neural stem cells in the subventricular zone. *Proc. Natl. Acad. Sci. U.*

- S. A. *101*, 17528–17532.
- Merkle, F.T., Mirzadeh, Z., and Alvarez-Buylla, A. (2007). Mosaic organization of neural stem cells in the adult brain. *Science* *317*, 381–384.
- Merkle, F.T., Fuentealba, L.C., Sanders, T.A., Magno, L., Kessaris, N., and Alvarez-Buylla, A. (2014). Adult neural stem cells in distinct microdomains generate previously unknown interneuron types. *Nat. Neurosci.* *17*, 207–214.
- Mirzadeh, Z., Merkle, F.T., Soriano-Navarro, M., Garcia-Verdugo, J.M., and Alvarez-Buylla, A. (2008). Neural stem cells confer unique pinwheel architecture to the ventricular surface in neurogenic regions of the adult brain. *Cell Stem Cell* *3*, 265–278.
- Mlody, B., Lorenz, C., Inak, G., and Prigione, A. (2016). Energy metabolism in neuronal/glia induction and in iPSC models of brain disorders. *Semin. Cell Dev. Biol.* *52*, 102–109.
- Molofsky, A. V, He, S., Bydon, M., Morrison, S.J., and Pardal, R. (2005). Bmi-1 promotes neural stem cell self-renewal and neural development but not mouse growth and survival by repressing the p16Ink4a and p19Arf senescence pathways. *Genes Dev.* *19*, 1432–1437.
- Molyneaux, B.J., Arlotta, P., Hirata, T., Hibi, M., and Macklis, J.D. (2005). Fezl is required for the birth and specification of corticospinal motor neurons. *Neuron* *47*, 817–831.
- Molyneaux, B.J., Arlotta, P., Menezes, J.R.L., and Macklis, J.D. (2007). Neuronal subtype specification in the cerebral cortex. *Nat. Rev. Neurosci.* *8*, 427–437.
- Moon, J.-H., Heo, J.S., Kim, J.S., Jun, E.K., Lee, J.H., Kim, A., Kim, J., Whang, K.Y., Kang, Y.-K., Yeo, S., et al. (2011). Reprogramming fibroblasts into induced pluripotent stem cells with Bmi1. *Cell Res.* *21*, 1305–1315.
- Morey, L., Santanach, A., and Di Croce, L. (2015). Pluripotency and Epigenetic Factors in Mouse Embryonic Stem Cell Fate Regulation. *Mol. Cell. Biol.* *35*, 2716–2728.
- Mori, K., Kishi, K., and Ojima, H. (1983). Distribution of dendrites of mitral, displaced mitral, tufted, and granule cells in the rabbit olfactory bulb. *J. Comp. Neurol.* *219*, 339–355.
- Mori, K., Takahashi, Y.K., Igarashi, K.M., and Yamaguchi, M. (2006a). Maps of odorant molecular features in the Mammalian olfactory bulb. *Physiol. Rev.* *86*, 409–433.
- Mori, T., Tanaka, K., Buffo, A., Wurst, W., Kühn, R., and Götz, M. (2006b). Inducible gene deletion in astroglia and radial glia--a valuable tool for functional and lineage analysis. *Glia* *54*, 21–34.
- Morimoto-Suzuki, N., Hirabayashi, Y., Tyssowski, K., Shinga, J., Vidal, M., Koseki, H., and Gotoh, Y. (2014). The polycomb component Ring1B regulates the timed termination of

References

- subcerebral projection neuron production during mouse neocortical development. *Development* 141, 4343–4353.
- Mullen, R.J., Buck, C.R., and Smith, A.M. (1992). NeuN, a neuronal specific nuclear protein in vertebrates. *Development* 116, 201–211.
- Nagayama, S., Homma, R., and Imamura, F. (2014). Neuronal organization of olfactory bulb circuits. *Front. Neural Circuits* 8, 98.
- Nakamura, H., and Watanabe, Y. (2005). Isthmus organizer and regionalization of the mesencephalon and metencephalon. *Int. J. Dev. Biol.* 49, 231–235.
- Nakamura, A., Swahari, V., Plestant, C., Smith, I., McCoy, E., Smith, S., Moy, S.S., Anton, E.S., and Deshmukh, M. (2016). Bcl-xL Is Essential for the Survival and Function of Differentiated Neurons in the Cortex That Control Complex Behaviors. *J. Neurosci.* 36, 5448–5461.
- Nakamura, T., Colbert, M.C., and Robbins, J. (2006). Neural crest cells retain multipotential characteristics in the developing valves and label the cardiac conduction system. *Circ. Res.* 98, 1547–1554.
- de Napoles, M., Mermoud, J.E., Wakao, R., Tang, Y.A., Endoh, M., Appanah, R., Nesterova, T.B., Silva, J., Otte, A.P., Vidal, M., et al. (2004). Polycomb group proteins Ring1A/B link ubiquitylation of histone H2A to heritable gene silencing and X inactivation. *Dev. Cell* 7, 663–676.
- Naritsuka, H., Sakai, K., Hashikawa, T., Mori, K., and Yamaguchi, M. (2009). Perisomatic-targeting granule cells in the mouse olfactory bulb. *J. Comp. Neurol.* 515, 409–426.
- Nashold, F.E., Nelson, C.D., Brown, L.M., and Hayes, C.E. (2013). One calcitriol dose transiently increases Helios⁺ FoxP3⁺ T cells and ameliorates autoimmune demyelinating disease. *J. Neuroimmunol.* 263, 64–74.
- Nieto, M., Monuki, E.S., Tang, H., Imitola, J., Haubst, N., Khoury, S.J., Cunningham, J., Gotz, M., and Walsh, C.A. (2004). Expression of Cux-1 and Cux-2 in the subventricular zone and upper layers II-IV of the cerebral cortex. *J. Comp. Neurol.* 479, 168–180.
- Obernier, K., Tong, C.K., and Alvarez-Buylla, A. (2014). Restricted nature of adult neural stem cells: re-evaluation of their potential for brain repair. *Front. Neurosci.* 8, 162.
- Onder, T.T., Kara, N., Cherry, A., Sinha, A.U., Zhu, N., Bernt, K.M., Cahan, P., Marcarci, B.O., Unternaehrer, J., Gupta, P.B., et al. (2012). Chromatin-modifying enzymes as modulators of reprogramming. *Nature* 483, 598–602.
- Orona, E., Scott, J.W., and Rainer, E.C. (1983). Different granule cell populations innervate

- superficial and deep regions of the external plexiform layer in rat olfactory bulb. *J. Comp. Neurol.* *217*, 227–237.
- Ortega, F., Costa, M.R., Simon-Ebert, T., Schroeder, T., Götz, M., and Berninger, B. (2011). Using an adherent cell culture of the mouse subependymal zone to study the behavior of adult neural stem cells on a single-cell level. *Nat. Protoc.* *6*, 1847–1859.
- Ortega, F., Gascón, S., Masserdotti, G., Deshpande, A., Simon, C., Fischer, J., Dimou, L., Chichung Lie, D., Schroeder, T., and Berninger, B. (2013). Oligodendroglial and neurogenic adult subependymal zone neural stem cells constitute distinct lineages and exhibit differential responsiveness to Wnt signalling. *Nat. Cell Biol.* *15*, 602–613.
- Ory, D.S., Neugeboren, B.A., and Mulligan, R.C. (1996). A stable human-derived packaging cell line for production of high titer retrovirus/vesicular stomatitis virus G pseudotypes. *Proc. Natl. Acad. Sci. U. S. A.* *93*, 11400–11406.
- Pang, Z.P., Yang, N., Vierbuchen, T., Ostermeier, A., Fuentes, D.R., Yang, T.Q., Citri, A., Sebastiano, V., Marro, S., Südhof, T.C., et al. (2011). Induction of human neuronal cells by defined transcription factors. *Nature* *476*, 220–223.
- Paridaen, J.T.M.L., and Huttner, W.B. (2014). Neurogenesis during development of the vertebrate central nervous system. *EMBO Rep.* *15*, 351–364.
- Park, H.-A., Kubicki, N., Gnyawali, S., Chan, Y.C., Roy, S., Khanna, S., and Sen, C.K. (2011). Natural vitamin E α -tocotrienol protects against ischemic stroke by induction of multidrug resistance-associated protein 1. *Stroke* *42*, 2308–2314.
- Pencea, V., and Luskin, M.B. (2003). Prenatal development of the rodent rostral migratory stream. *J. Comp. Neurol.* *463*, 402–418.
- Petreaanu, L., and Alvarez-Buylla, A. (2002). Maturation and death of adult-born olfactory bulb granule neurons: role of olfaction. *J. Neurosci.* *22*, 6106–6113.
- Petryniak, M.A., Potter, G.B., Rowitch, D.H., and Rubenstein, J.L.R. (2007). *Dlx1* and *Dlx2* control neuronal versus oligodendroglial cell fate acquisition in the developing forebrain. *Neuron* *55*, 417–433.
- Pfisterer, U., Kirkeby, A., Torper, O., Wood, J., Nelander, J., Dufour, A., Björklund, A., Lindvall, O., Jakobsson, J., and Parmar, M. (2011). Direct conversion of human fibroblasts to dopaminergic neurons. *Proc. Natl. Acad. Sci. U. S. A.* *108*, 10343–10348.
- Pilz, G.-A., Shitamukai, A., Reillo, I., Pacary, E., Schwausch, J., Stahl, R., Ninkovic, J., Snippert, H.J., Clevers, H., Godinho, L., et al. (2013). Amplification of progenitors in the

References

- mammalian telencephalon includes a new radial glial cell type. *Nat. Commun.* **4**, 2125.
- Puche, A.C., and Shipley, M.T. (2001). Radial glia development in the mouse olfactory bulb. *J. Comp. Neurol.* **434**, 1–12.
- Puelles, L., Kuwana, E., Puelles, E., Bulfone, A., Shimamura, K., Keleher, J., Smiga, S., and Rubenstein, J.L. (2000). Pallial and subpallial derivatives in the embryonic chick and mouse telencephalon, traced by the expression of the genes *Dlx-2*, *Emx-1*, *Nkx-2.1*, *Pax-6*, and *Tbr-1*. *J. Comp. Neurol.* **424**, 409–438.
- Puelles, L., Harrison, M., Paxinos, G., and Watson, C. (2013). A developmental ontology for the mammalian brain based on the prosomeric model. *Trends Neurosci.* **36**, 570–578.
- Qi, L., Cao, J.-L., Hu, Y., Yang, J.-G., Ji, Y., Huang, J., Zhang, Y., Sun, D.-G., Xia, H.-F., and Ma, X. (2013). The dynamics of polycomb group proteins in early embryonic nervous system in mouse and human. *Int. J. Dev. Neurosci.* **31**, 487–495.
- Qi, S., Fang, Z., Wang, D., Menendez, P., Yao, K., and Ji, J. (2015). Concise review: induced pluripotency by defined factors: prey of oxidative stress. *Stem Cells* **33**, 1371–1376.
- Rallu, M., Corbin, J.G., and Fishell, G. (2002). Parsing the prosencephalon. *Nat. Rev. Neurosci.* **3**, 943–951.
- Richly, H., Aloia, L., and Di Croce, L. (2011). Roles of the Polycomb group proteins in stem cells and cancer. *Cell Death Dis.* **2**, e204.
- Robel, S., and Sontheimer, H. (2015). Glia as drivers of abnormal neuronal activity. *Nat. Neurosci.* **19**, 28–33.
- Rojczyk-Gołębiewska, E., Pałasz, A., and Wiaderkiewicz, R. (2014). Hypothalamic subependymal niche: a novel site of the adult neurogenesis. *Cell. Mol. Neurobiol.* **34**, 631–642.
- Román-Trufero, M., Méndez-Gómez, H.R., Pérez, C., Hijikata, A., Fujimura, Y., Endo, T., Koseki, H., Vicario-Abejón, C., and Vidal, M. (2009). Maintenance of undifferentiated state and self-renewal of embryonic neural stem cells by Polycomb protein Ring1B. *Stem Cells* **27**, 1559–1570.
- Rowitch, D.H., and Kriegstein, A.R. (2010). Developmental genetics of vertebrate glial-cell specification. *Nature* **468**, 214–222.
- Rubenstein, J.L.R., and Campbell, K. (2013). Neurogenesis in the Basal Ganglia. In *Patterning and Cell Type Specification in the Developing CNS and PNS*, (Elsevier), pp. 455–473.
- Saino-Saito, S., Cave, J.W., Akiba, Y., Sasaki, H., Goto, K., Kobayashi, K., Berlin, R., and Baker, H. (2007). ER81 and CaMKIV identify anatomically and phenotypically defined

- subsets of mouse olfactory bulb interneurons. *J. Comp. Neurol.* 502, 485–496.
- Sakamoto, M., Kageyama, R., and Imayoshi, I. (2014). The functional significance of newly born neurons integrated into olfactory bulb circuits. *Front. Neurosci.* 8, 121.
- Sasaki, T., Kitagawa, K., Yagita, Y., Sugiura, S., Omura-Matsuoka, E., Tanaka, S., Matsushita, K., Okano, H., Tsujimoto, Y., and Hori, M. (2006). Bcl2 enhances survival of newborn neurons in the normal and ischemic hippocampus. *J. Neurosci. Res.* 84, 1187–1196.
- Sawamoto, K. (2006). New Neurons Follow the Flow of Cerebrospinal Fluid in the Adult Brain. *Science* (80-.). 311, 629–632.
- Schindelin, J., Arganda-Carreras, I., Frise, E., Kaynig, V., Longair, M., Pietzsch, T., Preibisch, S., Rueden, C., Saalfeld, S., Schmid, B., et al. (2012). Fiji: an open-source platform for biological-image analysis. *Nat. Methods* 9, 676–682.
- Schuurmans, C., Armant, O., Nieto, M., Stenman, J.M., Britz, O., Klenin, N., Brown, C., Langevin, L.-M., Seibt, J., Tang, H., et al. (2004). Sequential phases of cortical specification involve Neurogenin-dependent and -independent pathways. *EMBO J.* 23, 2892–2902.
- Shaker, T., Dennis, D., Kurrasch, D.M., and Schuurmans, C. (2012). Neurog1 and Neurog2 coordinately regulate development of the olfactory system. *Neural Dev.* 7, 28.
- Shen, Q., Wang, Y., Kokovay, E., Lin, G., Chuang, S.-M., Goderie, S.K., Roysam, B., and Temple, S. (2008). Adult SVZ stem cells lie in a vascular niche: a quantitative analysis of niche cell-cell interactions. *Cell Stem Cell* 3, 289–300.
- Sherman, M.H., Yu, R.T., Engle, D.D., Ding, N., Atkins, A.R., Tiriach, H., Collisson, E.A., Connor, F., Van Dyke, T., Kozlov, S., et al. (2014). Vitamin D Receptor-Mediated Stromal Reprogramming Suppresses Pancreatitis and Enhances Pancreatic Cancer Therapy. *Cell* 159, 80–93.
- Singh, V.K., Kalsan, M., Kumar, N., Saini, A., and Chandra, R. (2015). Induced pluripotent stem cells: applications in regenerative medicine, disease modeling, and drug discovery. *Front. Cell Dev. Biol.* 3.
- Smith, D.K., and Zhang, C.-L. (2015). Regeneration through reprogramming adult cell identity in vivo. *Am. J. Pathol.* 185, 2619–2628.
- Snayyan, M., Lemasson, M., Brill, M.S., Blais, M., Massouh, M., Ninkovic, J., Gravel, C., Berthod, F., Götz, M., Barker, P.A., et al. (2009). Vasculature guides migrating neuronal precursors in the adult mammalian forebrain via brain-derived neurotrophic factor

References

- signaling. *J. Neurosci.* 29, 4172–4188.
- Srinivasan, K., Leone, D.P., Bateson, R.K., Dobрева, G., Kohwi, Y., Kohwi-Shigematsu, T., Grosschedl, R., and McConnell, S.K. (2012). A network of genetic repression and derepression specifies projection fates in the developing neocortex. *Proc. Natl. Acad. Sci. U. S. A.* 109, 19071–19078.
- Stenman, J., Toresson, H., and Campbell, K. (2003). Identification of Two Distinct Progenitor Populations in the Lateral Ganglionic Eminence: Implications for Striatal and Olfactory Bulb Neurogenesis. *J. Neurosci.* 23, 167–174.
- van der Stoop, P., Boutsma, E.A., Hulsman, D., Noback, S., Heimerikx, M., Kerkhoven, R.M., Voncken, J.W., Wessels, L.F.A., and van Lohuizen, M. (2008). Ubiquitin E3 ligase Ring1b/Rnf2 of polycomb repressive complex 1 contributes to stable maintenance of mouse embryonic stem cells. *PLoS One* 3, e2235.
- Sultan, K.T., Brown, K.N., and Shi, S.-H. (2013). Production and organization of neocortical interneurons. *Front. Cell. Neurosci.* 7, 221.
- Sun, T., and Hevner, R.F. (2014). Growth and folding of the mammalian cerebral cortex: from molecules to malformations. *Nat. Rev. Neurosci.* 15, 217–232.
- Sun, W., Kim, H., and Moon, Y. (2010). Control of neuronal migration through rostral migration stream in mice. *Anat. Cell Biol.* 43, 269–279.
- Tam, P.P., and Quinlan, G.A. (1996). Mapping vertebrate embryos. *Curr. Biol.* 6, 104–106.
- Tashiro, A., Zhao, C., and Gage, F.H. (2006). Retrovirus-mediated single-cell gene knockout technique in adult newborn neurons in vivo. *Nat. Protoc.* 1, 3049–3055.
- Tavares, L., Dimitrova, E., Oxley, D., Webster, J., Poot, R., Demmers, J., Bezstarosti, K., Taylor, S., Ura, H., Koide, H., et al. (2012). RYBP-PRC1 complexes mediate H2A ubiquitylation at polycomb target sites independently of PRC2 and H3K27me3. *Cell* 148, 664–678.
- Tavazoie, M., Van der Veken, L., Silva-Vargas, V., Louissaint, M., Colonna, L., Zaidi, B., Garcia-Verdugo, J.M., and Doetsch, F. (2008). A specialized vascular niche for adult neural stem cells. *Cell Stem Cell* 3, 279–288.
- Taverna, E., Götz, M., and Huttner, W.B. (2014). The cell biology of neurogenesis: toward an understanding of the development and evolution of the neocortex. *Annu. Rev. Cell Dev. Biol.* 30, 465–502.
- Tian, C., Liu, Q., Ma, K., Wang, Y., Chen, Q., Ambroz, R., Klinkebiel, D.L., Li, Y., Huang, Y., Ding, J., et al. (2013). Characterization of induced neural progenitors from skin fibroblasts

- by a novel combination of defined factors. *Sci. Rep.* 3, 1345.
- Tole, S., and Hébert, J. (2013). *Telencephalon patterning* (Elsevier).
- Toni, N., and Schinder, A.F. (2016). Maturation and Functional Integration of New Granule Cells into the Adult Hippocampus. *Cold Spring Harb. Perspect. Biol.* 8, a018903.
- Treloar, H.B., Miller, A.M., Ray, A., and Greer, C.A. (2010). Development of the Olfactory System. In *The Neurobiology of Olfaction*, A. Menini, ed. (CRC Press/Taylor & Francis),.
- Tsunemoto, R.K., Eade, K.T., Blanchard, J.W., and Baldwin, K.K. (2015). Forward engineering neuronal diversity using direct reprogramming. *EMBO J.* 34, 1445–1455.
- Tucker, E.S., Polleux, F., and LaMantia, A.-S. (2006). Position and time specify the migration of a pioneering population of olfactory bulb interneurons. *Dev. Biol.* 297, 387–401.
- Vergaño-Vera, E., Yusta-Boyo, M.J., de Castro, F., Bernad, A., de Pablo, F., and Vicario-Abejón, C. (2006). Generation of GABAergic and dopaminergic interneurons from endogenous embryonic olfactory bulb precursor cells. *Development* 133, 4367–4379.
- Victor, M.B., Richner, M., Hermansteyne, T.O., Ransdell, J.L., Sobieski, C., Deng, P.-Y., Klyachko, V.A., Nerbonne, J.M., and Yoo, A.S. (2014). Generation of Human Striatal Neurons by MicroRNA-Dependent Direct Conversion of Fibroblasts. *Neuron* 84, 311–323.
- Vierbuchen, T., and Wernig, M. (2012). Molecular roadblocks for cellular reprogramming. *Mol. Cell* 47, 827–838.
- Vierbuchen, T., Ostermeier, A., Pang, Z.P., Kokubu, Y., Südhof, T.C., and Wernig, M. (2010). Direct conversion of fibroblasts to functional neurons by defined factors. *Nature* 463, 1035–1041.
- Voehringer, D.W., McConkey, D.J., McDonnell, T.J., Brisbay, S., and Meyn, R.E. (1998). Bcl-2 expression causes redistribution of glutathione to the nucleus. *Proc. Natl. Acad. Sci. U. S. A.* 95, 2956–2960.
- Vogel, T., Stoykova, A., and Gruss, P. (2006). Differential expression of polycomb repression complex 1 (PRC1) members in the developing mouse brain reveals multiple complexes. *Dev. Dyn.* 235, 2574–2585.
- Waclaw, R.R., Allen, Z.J., Bell, S.M., Erdélyi, F., Szabó, G., Potter, S.S., and Campbell, K. (2006). The Zinc Finger Transcription Factor Sp8 Regulates the Generation and Diversity of Olfactory Bulb Interneurons. *Neuron* 49, 503–516.
- Wapinski, O.L., Vierbuchen, T., Qu, K., Lee, Q.Y., Chanda, S., Fuentes, D.R., Giresi, P.G., Ng, Y.H., Marro, S., Neff, N.F., et al. (2013). Hierarchical mechanisms for direct

References

- reprogramming of fibroblasts to neurons. *Cell* 155, 621–635.
- Whitman, M.C., and Greer, C.A. (2009). Adult neurogenesis and the olfactory system. *Prog. Neurobiol.* 89, 162–175.
- Whitman, M.C., Fan, W., Rela, L., Rodriguez-Gil, D.J., and Greer, C.A. (2009). Blood vessels form a migratory scaffold in the rostral migratory stream. *J. Comp. Neurol.* 516, 94–104.
- Winpenny, E., Lebel-Potter, M., Fernandez, M.E., Brill, M.S., Götz, M., Guillemot, F., and Raineteau, O. (2011). Sequential generation of olfactory bulb glutamatergic neurons by Neurog2-expressing precursor cells. *Neural Dev.* 6, 12.
- Yiu, G., and He, Z. (2006). Glial inhibition of CNS axon regeneration. *Nat. Rev. Neurosci.* 7, 617–627.
- Young, K.M., Fogarty, M., Kessaris, N., and Richardson, W.D. (2007). Subventricular zone stem cells are heterogeneous with respect to their embryonic origins and neurogenic fates in the adult olfactory bulb. *J. Neurosci.* 27, 8286–8296.
- Zaret, K.S., and Carroll, J.S. (2011). Pioneer transcription factors: Establishing competence for gene expression. *Genes Dev.* 25, 2227–2241.
- Zimmermann, A.K., Loucks, F.A., Schroeder, E.K., Bouchard, R.J., Tyler, K.L., and Linseman, D.A. (2007). Glutathione Binding to the Bcl-2 Homology-3 Domain Groove: A MOLECULAR BASIS FOR BCL-2 ANTIOXIDANT FUNCTION AT MITOCHONDRIA. *J. Biol. Chem.* 282, 29296–29304.

Acknowledgements

First of all, I would like to thank **Magdalena** for giving me the chance to perform the PhD in her lab and for her great supervision. It has been a long journey from the first moment I stepped into your group and I can only be happy of what I managed to learn since then.

Along the same line, a very special “thank you” goes to **Sergio**. You gave me trust, you taught me everything day by day, you encouraged me along the way. If I am here in this important day it is also thanks to you. You are an amazing colleague and a dear friend!

Big thanks also to **Steffi** and **Jesi**, my super office mates... I had (and still have) so much fun with you! We helped each other, confronted experiences, shared hopes and expectations... I couldn't really ask for more :)

A particular thank you also to **Sofia**, not only for every day scientific help/discussions, but also for genuine and whole-hearted support. You were always there, always ready to make me smile and offer help. This is invaluable for me. And thanks also to **Andromachi** (with whom I shared probably the craziest moments ever!) and **David** (for our collaboration... and a good amount of laughter).

Of course, many thanks to all the technical staff... what would we do without you? And particularly, thanks to my friends **Ines**, **Carmen** and **Manja**. You are all so very dear to me...!

Very warm thanks also to all my lab colleagues, you all gave me something in the every day life and made my PhD really enjoyable :) Above all, thanks to the people I had the chance to get to know better: **Daisy**, **Ania**, **Chiara**, **Luisa**, **Laura**, **Nicole**, **Nicola**, **Gianluca**, **Belen**... thank you all so much guys!

A big “thank you” also to you, **Lana** and **Leda**... you gave me trust and support from the beginning.

Thanks also to the **GSN** and the **IMPRS** coordinators, as well as to my TAC members (**Wolfgang Wurst** and **Gunnar Schotta**) for all the help along this journey.

Grazie anche alla vecchia guardia di Amici con la A maiuscola per tutto il supporto durante questi anni! Grazie **Gilda**, sempre al mio fianco nei momenti più significativi della mia vita; e grazie a te **Cinzia**, perché da anni mi rendi una persona migliore. Grazie anche a **Mari** e **Ale**, con cui ho condiviso davvero tanto... E grazie a **Tania**, **Simona**, **Andre**, **Giusy** e **Paola** che mi hanno visto partire armata di paure e sogni e mi hanno sempre incoraggiato. Un grazie speciale a te **Adri**, per avermi supportato (e sopportato) come pochi e per esserci sempre.

Un grazie molto, molto sentito ai miei amati **genitori**. Siete la mia roccia, sempre. Questa piccola grande vittoria non è soltanto mia... è un nostro traguardo.

Un pensiero anche ai miei parenti, che sono sempre nel mio cuore. E un altro dolce pensiero a persone che sognavo di avere qui con me in questo momento così importante e che invece ho perso lungo il cammino. Dedico tutto questo a voi, nonni... e a te caro cugino.

Infine un grazie a me... perché la mia testa dura e la mia grinta a volte fanno qualcosa di buono :)

Curriculum vitae

Name	Elisa Murenu
Nationality	Italian
Date of birth	27 th March 1985, Pisa (Italy)

Professional and educational history

PhD Thesis

Dates	2011 - 2016
Research projects	Metabolic barriers in direct neuronal reprogramming <i>in vivo</i> . Role of Ring1B in adult neurogenesis.
Institute	Institute of Physiological Genomics, Ludwig-Maximilians University, Munich, Germany
Supervisor	Prof. Dr. Magdalena Götz, Helmholtz Zentrum München, Neuherberg (Germany)

Pre-doctoral fellowship

Dates	2009 - 2011
Research projects	Generation of a retinal fate in mouse embryonic stem cells (ES) by induction with the secreted factor Noggin.
Institute	National Research Council, Pisa (Italy) Centre for Integrative Biology (CIBIO), Trento (Italy)
Supervisor	Dr. Federico Cremisi, Scuola Normale Superiore, Pisa (Italy) Dr. Simona Casarosa, Centre for Integrative Biology (CIBIO), Trento (Italy)

Master's Thesis in Molecular Neurobiology, final score 110/110 *cum laude*

Dates	2007 - 2009
Thesis title	"Generation of a retinal fate in mouse embryonic stem cells (ES) by induction with the secreted factor Noggin".
Institute	Department of Cell Biology, University of Pisa, Pisa (Italy)
Supervisors	Dr. Simona Casarosa, Centre for Integrative Biology (CIBIO), Trento (Italy) Prof. Robert Vignali, University of Pisa, Department of Cell Biology, Pisa (Italy)

Bachelor's Thesis in Biodiversity and Ecology, final score 110/110 *cum laude*

Dates	2004 - 2007
Thesis title	"Analysis of genes regulated by the thyroid hormone in <i>Xenopus laevis</i> retina".
Institute	Department of Cell Biology, University of Pisa
Supervisor	Dr. Simona Casarosa, Centre for Integrative Biology (CIBIO), Trento (Italy)

Scholarships and fellowships

- Scholarship for GSN graduate school, Ludwig-Maximilian University, Munich, Germany (2011)
- Scholarship for IMPRS-LS graduate school, Max Planck Institute, Martinsried, Germany (2010)
- Fellowship for "Progetto Impresa" from Consorzio Impat, Italy (2010)

Poster presentation at scientific conferences

- Driving Stem Cell Research Towards Therapy. Edinburgh (Scotland), 2012. Poster presentation.
- 5th LMU-Harvard Young Scientists' Forum. Munich (Germany), 2013. Poster presentation.
- 106th Annual Meeting of the German Zoological Society. Munich (Germany), 2013. Poster presentation.

General methods and specialised techniques

Methods

<i>Molecular biology</i>	Standard cloning methods; dot blot assay; PCR, semi-quantitative real time PCR; immunocytochemistry, immunohistochemistry, <i>in situ</i> hybridisation; TUNEL
<i>Cell culture techniques</i>	Mouse embryonic stem cells (ES) culture and differentiation (neurons, cardiomyocytes), Chinese Hamster Ovary (CHO) cells culture; mouse postnatal astrocytes culture, mouse neural stem cells culture (from E14 embryos or adult sub-ependymal zone), mouse adult reactive glia culture
<i>In vivo techniques</i>	<i>Xenopus laevis</i> : breeding and embryo fertilization; embryo collection and staging; embryo microdissection and microinjection Mouse: brain extraction and microdissection; cerebral cortex stab-wound injury; retroviral injection in different brain areas; intracardial perfusion; forced-feeding (oral gavage)
<i>Laboratory instruments</i>	Surgery: stereotactic frame for brain surgery, microinjection apparatus Sectioning: cryostat, vibrating microtome Microscopes: stereo, epifluorescent, laser confocal

Computer packages

General	Microsoft Office (Word, Excel, PowerPoint)
Specialised	Mendeley, Adobe Photoshop, Fiji (ImageJ), GraphPad Prism, Zen software (Carl Zeiss), Primer3

Languages

Italian	Native-speaker
English	Fluent
French	Elementary
German	Elementary
Russian	Basic

Workshops and training events

Methods learning	Scientific image processing, Genomatix course, cell transplantation and mini-pumps implantation, <i>in vitro</i> time-lapse imaging
Scientific soft skills	Grant writing, scientific writing, poster design, using and evaluating learning and memory paradigms
Laboratory management	Intercultural communication

List of publications

- Gascón, S.* , **Murenu, E.***, Masserdotti, G., Ortega, F., Russo, G.L., Petrik, D., Deshpande, A., Heinrich, C., Karow, M., Robertson, S.P., Schroeder, T., Beckers, J., Irmeler, M., Berndt, C., Angeli, J.P.F., Conrad, M., Berninger, B., Götz, M., 2016. Identification and Successful Negotiation of a Metabolic Checkpoint in Direct Neuronal Reprogramming. *Cell Stem Cell* 18, 396–409. doi:10.1016/j.stem.2015.12.003
- Bertacchi, M., Pandolfini, L., **Murenu, E.**, Viegi, A., Capsoni, S., Cellerino, A., Messina, A., Casarosa, S., Cremisi, F., 2013. The positional identity of mouse ES cell-generated neurons is affected by BMP signaling. *Cell. Mol. Life Sci.* 70, 1095–111. doi:10.1007/s00018-012-1182-3
- Sgadò, P., Genovesi, S., Kalinovsky, A., Zunino, G., Macchi, F., Allegra, M., **Murenu, E.**, Provenzano, G., Tripathi, P.P., Casarosa, S., Joyner, A.L., Bozzi, Y., 2013. Loss of GABAergic neurons in the hippocampus and cerebral cortex of Engrailed-2 null mutant mice: implications for autism spectrum disorders. *Exp. Neurol.* 247, 496–505. doi:10.1016/j.expneurol.2013.01.021
- Messina, A., Casarosa, S. and **Murenu, E.**, 2011. Stem Cells and the Retina – Challenges for Regenerative Medicine, Embryonic Stem Cells - Recent Advances in Pluripotent Stem Cell-Based Regenerative Medicine, Prof. Craig Atwood (Ed.), ISBN: 978-953-307-198-5, InTech, DOI: 10.5772/14780. Available from: <http://www.intechopen.com/books/embryonic-stem-cells-recent-advances-in-pluripotent-stem-cell-based-regenerative-medicine/stem-cells-and-the-retina-challenges-for-regenerative-medicine>

*: equal contribution

Eidesstattliche Versicherung/Affidavit

Hiermit versichere ich an Eides statt, dass ich die vorliegende Dissertation “Role of metabolism and epigenetics in forced and endogenous neurogenesis *in vivo*” elbstständig angefertigt habe, mich außer der angegebenen keiner weiteren Hilfsmittel bedient und alle Erkenntnisse, die aus dem Schrifttum ganz oder annähernd übernommen sind, als solche kenntlich gemacht und nach ihrer Herkunft unter Bezeichnung der Fundstelle einzeln nachgewiesen habe.

I hereby confirm that the dissertation “Role of metabolism and epigenetics in forced and endogenous neurogenesis *in vivo*” is the result of my own work and that I have only used sources or materials listed and specified in the dissertation.

München, den

Munich, date

26/01/2017

Murenu Elisa

Declaration of author contributions

The semi-automatic tracing and the quantifications described in Figure 27 as well as in paragraph 2.22 of the results were performed in collaboration with Dr. David Petrik and presented upon his consent.

Munich, 3.06.16

Signature of head of the lab

Signature